INVESTIGATION OF CATALYTIC IGNITION OF OXYGEN / HYDROGEN SYSTEMS

BY

R. C. ROBERTS

PREPARED FOR

NATIONAL AERONAUTICS AND SPACE ADMINISTRATION

CONTRACT NAS 3-2565

ROCKETDYNE RESEARCH DEPARTMENT

NORTH AMERICAN AVIATION, INC.

6633 CANOGA AVENUE, CANOGA PARK, CALIFORNIA

NASA CR-54086
ROCKETDYNE R-5709

FINAL REPORT

INVESTIGATION OF CATALYTIC IGNITION OF OXYGEN/HYDROGEN SYSTEMS

By
R. W. Roberts

Prepared for
National Aeronautics and Space Administration

August 1964

Contract NAS 3-2565

Technical Management
NASA Lewis Research Center
Cleveland, Ohio
Advanced Rocket Technology Branch
John W. Gregory

Rocketdyne Research Department
North American Aviation, Inc.
6633 Canoga Avenue, Canoga Park, California

FOREWORD

This research program was conducted by the Research Department of Rocketdyne, a Division of North American Aviation, Inc., under NASA Contract NAS3-2565, sponsored by the Office of Advanced Research and Technology and managed by the Advanced Rocket Technology Branch of Lewis Research Center. This report covers research accomplished during the period 19 June 1963 through 19 April 1964.

ACKNOWLEDGMENT

The author gratefully acknowledges the assistance of Dr. M. Ladacki, Physical Chemistry Group, Rocketdyne Research, who conducted the Task I laboratory effort in support of this program and, in addition, contributed with his translations from the Russian literature.

ABSTRACT

The results of an investigation of catalytic ignition of the oxygen/hydrogen system are presented. Included in this report are the results of preliminary laboratory screening for catalyst surface characterization and relative activity measurements at various temperatures for several commercially available catalysts as recommended by catalyst vendors, and for a single research catalyst. Also included are ignition evaluations of selected catalysts at environmental temperatures of -250 F for both catalyst and propellants, and of evaluations with liquid propellants and catalyst environmental temperatures equivalent to those of liquid hydrogen. Ignition lag measurements are presented for reaction systems with both liquid and gaseous propellants. The ability of a catalytic system to promote ignition with the liquid oxygen/liquid hydrogen propellant combination is clearly demonstrated. Author

CONTENTS

Foreword iii

Abstract v

Summary 1

Introduction 3

Experimental Program Plan 9

Catalysts 9

Propellants 15

Apparatus 16

Experimental Procedures 25

Catalyst Selection 25

Experimental Evaluation 29

Results and Discussion 33

Catalyst Selection Results 34

Experimental Evaluation Results 46

Liquid Oxygen/Liquid Hydrogen Ignition Investigations . . . 55

Conclusions 63

Concluding Remarks 65

References 67

Appendix A

Theory of Catalysis 69

Appendix B

Summary Translations from Russian Literature 91

Nomenclature 94

LIST OF ILLUSTRATIONS

A-1. Potential Energy Diagram Illustrating Relative Location of Activated Complex in Comparison to Initial and Final States of Reactants and Products 89

1. Schematic of Reactor Illustrating 4-on-1 Injection System and Component Parts of the Reaction Chamber 112
2. Photograph of 1-inch-Diameter Combustor Disassembled to Show Major Components--5-inch Catalyst Bed Configuration 113
3. Illustration of 4-on-1 Injector Showing Relative Positions of Fuel and Oxidizer Injection Ports 114
4. Schematic of Assembled Reactor 115
5. Injector Design Illustrating 7-element, 4-on-1 (H_2on O_2) Impinging Stream Injector Pattern 116
6. Injector Retainer Plate and Hydrogen Propellant Manifold 117
7. Catalyst Chamber Coolant Inlet Manifold 118
8. Adapter Plate for Temperature and Pressure Measurement Sensors 119
9. Catalyst Chamber Illustrating Coolant Jacket and Temperature Measurement Ports 120
10. Exit Nozzle and Housing, and Temperature and Pressure Measurement Adapter 121
11. Schematic of Apparatus for Catalyst Activity Measurement 122
12. Schematic of Gaseous Oxygen Supply System 123
13. Plumbing Schematic of Modified Gaseous Hydrogen/ Liquid Nitrogen Heat Exchanger System 124

14. Schematic Representation of Liquid Oxygen System for Small Catalytic Igniter Studies 125
15. Schematic Representation of Liquid Hydrogen System for Small Igniter Evaluations 126
16. Approximate Time Constants for Exposed Junction Thermocouple in Moving Air 127
17. Theoretical Oxygen/Hydrogen Mixture Temperatures as a Function of Mixture Ratio and Hydrogen Inlet Temperature. . 128
18. Comparative Pore Size Distribution for Engelhard MFSA, MFSS, and Used MFSS Catalysts Illustrating the Effect of Use on Catalyst Pore Size Distribution 129
19. Comparative Pore Size Distribution Curves for the Engelhard MFSA Catalyst Illustrating the Effects of Drying and Calcining on Pore Size Distribution 130
20. Pore Size Distribution Curves for Engelhard MFSA, Houdry A-200SR, and Shell 8240-168 Catalysts 131
21. Pore Size Distribution Curves for Girdler G-68 Catalyst Illustrating the Effect of Calcining on Pore Size Distribution 132
22. Representative Curves Depicting the Rate of Approach to Steady State Chamber Pressure for the Engelhard MFSA Catalyst With Gaseous Propellants. Illustrated are the Effects of Chamber Pressure Spiking Relative to Stable Ignition 133
23. Typical Curves for the Rate of Approach to Steady State Chamber Temperature for the Engelhard MFSA Catalyst Illustrating the Effects of Chamber Temperature Spikes Relative to Stable Ignition with Gaseous Propellants . . 134

24. Typical Reponse Curves for the Engelhard MFSS Catalyst. Illustrated are the Effects of Chamber Pressure Spikes Relative to Stable Ignition with Gaseous Propellants . . 135
25. Typical Curves Presenting the Rate of Approach to Steady State Chamber Temperature for the Engelhard MFSS Catalyst with the Gaseous O_2/H_2 System Illustrating the Effects of Flowrate on Rate of Approach to Equilibrium 136
26. Typical Curves for the Relative Rates of Approach to Equilibrium Chamber Temperature and Pressure for the Engelhard DSS Catalyst Using Gaseous Propellants 137
27. A Correlation of the Effect of Catalyst/Propellant Residence Time on the Rate of Approach to Steady State Chamber Pressure for the Engelhard MFSA Catalyst Using Gaseous Propellants 138
28. Correlation of the Effect of Propellant Residence Time in the Catalyst Bed on Rate of Approach to Steady-State Chamber Temperature for the Engelhard MFSA Catalyst Using Gaseous Propellants 139
29. A Correlation of the Effect of Propellant Residence Time in the Catalyst Bed on the Rate of Approach to Steady-State Chamber Pressure for the Engelhard MFSS Catalyst Using Gaseous Propellants 140
30. Correlation of the Effect of Catalyst/Propellant Contact Time on the Rate of Approach to Steady-State Chamber Temperature for the Engelhard MFSS Catalyst Using Gaseous Propellants 141
31. Typical Curves for the Rate of Approach to Steady-State Chamber Pressure for the Engelhard MFSA Catalyst Using Liquid Propellants. Illustrated are Comparative Effects of Spiking and Stable Ignition 142
32. Typical Curves for the Rate of Approach to Equilibrium Chamber Pressure for the Engelhard MFSS Catalyst with Liquid Propellants Illustrating the Relative Effects of Spiking and Stable Ignition 143

TABLES

1. Investigation of Catalytic Ignition of Oxygen/Hydrogen Systems 95
2. Spectrographic Analysis of Catalysts 97
3. Catalyst Surface Characteristics 98
4. Results of Catalytic Activity Tests 99
5. Catalyst Crush Strength 103
6. Thermal Shock Resistance 105
7. Effect of the Thermal Shock Treatment on Catalytic Activity 106
8. Effect of the Thermal Shock Treatment on Surface Characteristics 107
9. Summary of Results with Gaseous Propellants 108
10. Summary of Results with Liquid Propellants 110

SUMMARY

The objectives of this program were the selection and evaluation of commercially available catalysts for promoting the oxygen/hydrogen reaction, demonstration of the feasibility of catalytic ignition of liquid oxygen/liquid hydrogen propellants at liquid hydrogen environmental temperature, and generation of information appropriate to the preliminary design of catalytically ignited oxygen/hydrogen systems.

Physical properties measured in evaluating the catalysts were surface area, pore volume, average pore diameter, and pore size distribution, as measured in the Engelhard "Isorpta" analyzer, relative catalyst activity at environmental temperatures down to -300 F, resistance to thermal shock, and crush strength. In addition, catalyst comparisons were made in 1-inch-diameter hardware at environmental temperatures for both propellant and hardware of -250 F. The results of these comparisons showed the Engelhard DSS, MFSS, MFSA, Houdry A-200SR, and Girdler G-68 catalysts to be the best of the available catalysts.

Following selection of the above five catalysts, the Engelhard DSS, MFSS, and MFSA catalysts were subjected to evaluations in 3-inch-diameter engine hardware with liquid oxygen and liquid hydrogen propellants at catalyst environmental temperatures equal to that of liquid hydrogen. Both the Engelhard MFSS and MFSA catalysts proved capable of inducing the liquid oxygen/liquid hydrogen reaction. In the course of these evaluations, problems of igniter pressure spiking were encountered. The experimental results and analytical interpretations indicate that these problems can be resolved by maintaining the combined propellant flowrate above some threshold level. For the 3-inch-diameter reactor, this

threshold level of flowrate is approximately 0.3 lb/sec, and provides for a propellant velocity through the reactor of nearly 5 ft/sec under typical operating conditions. In any event, the velocity mass throughput must exceed the rate of flame propagation for the specific flow condition and mixture of oxygen and hydrogen concerned.

The results of this research program demonstrate the feasibility of the catalytic ignition concept for liquid oxygen/liquid hydrogen propellants in rocket engine systems.

INTRODUCTION

The oxygen/hydrogen propellant combination for use in rocket engine systems has received considerable attention in recent years because of certain advantages. Among these are high specific impulse, low combustion temperature, fast burning rate, lack of toxicity, and excellent regenerative cooling capability. The combination is not without disadvantages, however. Its inherent lack of hypergolicity requires some type of ignition system. Since ignition and reignition capability under conditions of space environment are of utmost importance in upper-stage engine systems, it is essential that this ignition system be highly reliable and capable of multiple reignition. A study contract (Ref. 1) recently completed at Rocketdyne lists several potential systems:

1. Hypergolic cartridges
2. Solid propellant cartridges
3. Hypergol additives
4. Spark igniters
   a. Direct
   b. Augmented
5. Catalytic igniters

Solid propellant and hypergolic cartridges are unsatisfactory for missions requiring more than one or two starts because of complexity. The use of hypergolic additives which could be mixed with either the fuel or oxidizer in reservoir storage presents an interesting possibility, but this is not part of the state of the art for rocket engine systems. At this time, direct- and augmented-spark ignition systems are not completely satisfactory for repeated ignition, and they pose problems of electrical

interference to electronic measurements and communication associated with mission requirements. An additional disadvantage of spark ignition is the requirement for facilities for electrical power generation.

The remaining potential ignition technique is catalytic ignition. This ignition concept incorporates simplicity and reliability in a single system, and also presents a technique which has demonstrated durability (gas purification, hydrogenation of oxygenated hydrocarbons, etc.). Additional advantages of this concept are the lack of requirements for electrical ignition equipment or auxiliary power units.

Potential areas of application for the catalytic ignition concept are primary ignition of large oxygen/hydrogen engine systems, hot-gas generation for propellant expulsion or turbine drive, attitude-control, and/or primary space engines, and midcourse maneuvering systems.

Primary ignition of larger upper-stage oxygen/hydrogen engines, of which the J-2, M-1, and RL-10 are examples, would require installation of a catalyst chamber and propellant system such that the hot exhaust gases from the catalytic reactor are injected into the main thrust chamber in sufficient quantity and energy levels to induce ignition of the main propellants. Hot-gas generation is accomplished in a similar manner; the difference consists of directing the exhaust gases to a different end application. For attitude-control applications, the requirement is to deliver small and repeatable impulse bits. On this basis, the previously demonstrated (Ref. 2 and 3) capability and reliability of the catalytic technique for ignition and repeated reignition of hydrogen/oxygen propellant combinations shows this concept to be ideally suited for attitude-control systems. For primary space engine systems, the thrust chamber would include a catalyst bed, with propellants fed to the chamber in conventional fashion.

For midcourse maneuvering, the principal requirement is for large thrust-time products, not for large thrusts. Consequently, the relatively low-thrust mainstage igniter could be turned on and allowed to run for an extended time to generate required small-force midcourse corrections. An obvious advantage of this approach is its superior controllability relative to short-duration, high-impulse, main-engine bursts.

Each of this applications (ignition, gas generation, attitude control, midcourse maneuvering) is equally suited for operation on main-engine propellants. In fact, each application lends itself to direct use of boiloff gas from main fuel and oxidizer tanks, assuming that the rate of gas (hydrogen, oxygen) generation from these tanks is sufficient for specific application energy requirements. In a liquid oxygen/liquid hydrogen missile state at the end of burning, significant quantities of both fuel and oxidizer gases are present in the ullage after tank emptying. These propellant gases mixed with the very light pressurant (helium) would serve as an excellent, reasonably high pressure ($>$100 psia) propellant source for attitude control, docking, etc., propulsive requirement utilizing a catalyst energized thrust chamber. The use of the catalytic ignition concept as a means of main-engine ignition offers the added advantage of providing a force for settling propellants prior to starting the main engine. This is accomplished by passing propellants, regardless of phase condition, through the catalyst bed. The resulting ignition will generate sufficient thrust to settle the propellants as well as provide high-enthalpy gases for main-engine ignition.

With these advantages in mind, this program was established to investigate the range of commercially available catalysts of the noble-metal type which offer promise of promoting the oxygen/hydrogen reaction, and to evaluate their disadvantages and limitations. Specifically, the objectives of this research program were:

1. Conduct a survey of the range of commercially available noble-metal type catalysts (as recommended by leading catalyst vendors) for promoting the oxygen/hydrogen reaction, and select not more than four of these catalysts for further evaluation; the basis of selection to be the results of such laboratory tests as catalyst surface area, pore size, resistance to thermal shock, and relative activity.
2. Perform an evaluation of selected catalysts in test hardware at propellant and hardware preignition environmental temperatures of -250 and -400 F, and final selection of not more than two of these catalysts for parametric combustion evaluations at environmental conditions approximating liquid hydrogen temperature.
3. Carry out a parametric combustion evaluation at both hardware and propellant preignition environmental temperatures approximating liquid hydrogen temperatures, to evaluate the effects of propellant residence time and catalyst bed preignition environmental temperature on ignition delay time.
4. Prepare the results of this program in a form suitable for execution of preliminary design for specific applications.

Because of the wide range of noble metal and nickel catalysts available from the various vendors, it was necessary to place heavy reliance on the experience and recommendations of the catalyst manufacturers in

selecting candidates for this study. Personal and/or telephone contacts were made with representatives of the following companies:

1. Engelhard Industries, Inc.
2. Houdry Process Corporation
3. Catalysts and Chemicals, Inc.
4. Catalytic Combustion Co.
5. Girdler Chemical Co.
6. Universal Oil Products
7. Davison Chemical Co.
8. Shell Oil Co.

The companies contacted recommended various catalysts as having potential for promoting the oxygen/hydrogen reaction, and of these, 22 catalysts were obtained for evaluation in this program.

In addition to presenting the results of this program, this report includes a generalized discussion of catalyst theory, presented to aid understanding of the catalytic reaction concept and to clarify the reasons for choosing certain catalysts for oxygen/hydrogen ignition. Included as appendixes are summary translations from the Russian literature of certain hitherto untranslated papers pertinent to the subject.

EXPERIMENTAL PROGRAM PLAN

The experimental program was conducted with high-purity propellants, and centered around 22 basic catalyst formulations. The selected catalysts were chosen on the basis of vendor recommendations and of past experience with noble-metal type catalysts. In most instances, the catalysts differed in type of substrate, noble-metal content, and manner of preparation. It was not the purpose of this program to prepare catalysts, and no such effort was conducted. The manner of catalyst preparation is considered proprietary by the vendors and is not described herein.

CATALYSTS

With two exceptions, the catalysts used in this program were of the noble-metal type. The exceptions were catalysts recommended by Universal Oil Products and Houdry Process Corporation, and were designated C-IV (nickel-on-"mineral support") and A-25Z (chromia-alumina), respectively. A list of the catalysts used in this program is shown in Table 1 and described in the following paragraphs.

Engelhard Industries, Inc. Catalysts

Engelhard provided four different catalysts for evaluation in this program. These were all noble metals impregnated on a spherically shaped alumina substrate.

DS Catalyst. The DS catalyst consists essentially of a high surface-area alumina pellet, nominally 1/8-inch in diameter, impregnated with palladium equal to about 0.5 weight percent. The analysis of this catalyst, as performed by emission spectrographic techniques, is presented in Table 2. Physical characteristics of the DS 1/8 formulation are shown in Table 3. Surface area, pore volume, and average pore diameter were obtained by use of an Engelhard "Isorpta" analyzer. For a description of the theory and operation of this device, refer to the vendor's instruction manual (Ref. 4).

DSS Catalyst. This catalyst was recommended by the vendor as a possible substitute for the DS formulation because the DSS pellet has better resistance to thermal shock without an appreciable decrease in catalytic activity. Like the DS, the DSS catalyst consists of a palladium-impregnated alumina pellet, and is nominally a 1/8-inch-diameter sphere. Properties of the DSS catalyst are shown in Tables 2 and 3.

MFSS Catalyst. The MFSS catalyst, while similar in physical appearance to the previous samples, has a somewhat different formulation. The MFSS was found by chemical analysis to be a platinum-rhodium-on-alumina material rather than a palladium-on-alumina-type catalyst. Of interest here is that, according to the vendor, the purpose of the platinum is to enable impregnation of the alumina substrate with rhodium, because the rhodium otherwise tends to slough off rather than adhere to the alumina. Prior impregnation of substrate with platinum serves to provide a base on which the rhodium will adhere. Properties of the MFSS catalyst are shown in Tables 2 and 3.

MFSA Catalyst. The MFSA catalyst is a later version of the MFSS configuration, and is very similar in physical appearance and type of substrate to the other three Engelhard catalysts. The primary differences are the surface characteristics and chemical composition, shown in Tables 2 and 3.

The manner of preparation may be significantly different, as indicated by the relatively large surface area, pore volume, and average pore diameter but this information is proprietary with the vendor.

The MFSA catalyst has essentially the same total noble-metal content as the MFSS, but includes lead as a third constituent. The specific effect of lead is not known, nor is the specific reason for its addition.

Girdler Chemical Company Catalysts

Girdler provided five catalysts for this program; all were the platinum or palladium type on an alumina substrate. The samples provided were nominally 1/8-inch-thick tablets varying in diameter from 1/8- to 1/4-inch.

G-43B Catalyst. The G-43B catalyst is a simple platinum-on-alumina configuration made up into a 1/4-inch-diameter by 1/8-inch-thick tablet. This catalyst is typical of those used for conversion of hydrocarbons.

G-46 Catalyst. The G-46 catalyst is basically a palladium composition impregnated on alumina and pressed into 3/16-inch-diameter by 1/8-inch-thick tablets.

G-55 Catalyst. The G-55 catalyst is a promoted palladium catalyst having the physical dimensions of a 1/8-inch-diameter by 1/8-inch-thick cylinder. The specific nature of the promoting agent is unknown, but this catalyst, as the two previous Girdler catalysts, has an alumina substrate.

G-58 Catalyst. This catalyst is identical in appearance with the G-46 catalyst, and is similarly a palladium-on-alumina formulation. The specific difference between the two is unknown, but is presumed to be the manner of preparation and chemical composition.

G-68 Catalyst. The G-68 catalyst is a promoted palladium catalyst identical in appearance to the G-55 catalyst. Presumably, the only difference is the nature of the promoting agent. As with the G-55 catalyst, the G-68 formulation is impregnated on an alumina carrier.

Universal Oil Products Catalyst

Universal Oil Products supplied only one catalyst for evaluation in this program. The particular sample provided was designated C-IV and consisted of nickel impregnated on a mineral support. The catalyst, as provided, was in the form of 1/8-inch-diameter by 1/8-inch-long tablets.

Catalytic Combustion Company Catalyst

Catalytic Combustion Company, a division of Universal Oil Products, provided a unique sample. This consisted of a ribbon matt-plug approximately 1-inch in diameter by 1-inch long, consisting of a continuous ribbon

(similar to steel wool) of nickel-alloy coated with platinum. The ribbon was no more than 1 to 2 mils thick by 6 to 8 mils wide, and was "bunched" into a screen container of the dimensions indicated.

Houdry Process Corporation Catalysts

Houdry recommended five catalyst samples having potential for promoting the O_2/H_2 reaction. With one exception, all the catalysts were impregnated on alumina; the exception being a palladium catalyst on kaolin, a diatomacious earth.

A-100S Catalyst. This catalyst is a platinum-on-alumina formulation and physically appears as a 1/8-inch-diameter by random length (~ 3/8-inch maximum) extruded cylinder. This sample is of relatively low surface area and is typical of catalysts used in moderate hydrogenation service in the petroleum industry.

A-200SR Catalyst. The A-200SR formulation is similar to the A-100S catalyst in all respects except two. This catalyst has a moderate surface area (nominally 200 square meters per gram) and is prepared to be resistant to catalyst poisoning by sulfur. The physical dimensions are 3/16-inch diameter by random length, not exceeding 3/8-inch.

A-25Z Catalyst. The A-25Z catalyst represents the second departure from noble-metal formulations evaluated in this program. This catalyst sample consisted of chromia (Cr_2O_3) impregnated on alumina, and was prepared in the form of a 1/8-inch-diameter extrudate not greater than 3/8-inch long.

B-100S Catalyst. This material was identical to the A-100S except that palladium was used as the catalytic agent in place of platinum.

Pd-K Catalyst. The Pd-K catalyst was Houdry's final recommendation. This catalyst consists of palladium impregnated on 0.15-inch spheres of kaolin.

Davison Chemical Company Catalysts

Four samples were provided by Davison for evaluation in this program.

SMR 55-1097-1 Catalyst. This catalyst consisted of a granular material (silica gel) having an extremely high surface area and nominally 6 weight percent platinum.

SMR 55-1097-2 Catalyst. The second Davison catalyst was a 1/8-inch-diameter by 1/8-inch-long tableted alumina substrate impregnated with nominally 0.6 weight percent platinum. This material was also stated to have very high surface area.

SMR 55-1097-3 Catalyst. Davison's third selection was identical to the SMR 55-1097-2 catalyst in all respects, except method of substrate preparation. The relative techniques for preparation are proprietary, and consequently are not presented herein.

SMR 55-1097-4 Catalyst. The final Davison catalyst appeared to be identical to the Engelhard samples, but differed in type of substrate and manner of preparation. As with the SMR 55-1097-1 catalyst, this catalyst consisted of platinum impregnated on silica gel and contained approximately 0.6 weight percent platinum.

Shell 8240-168 Catalyst

This catalyst was supplied by Shell Development Company, and represents a formulation developed in their studies on hydrazine decomposition catalysts. The formulation is basically a noble metal-on-alumina material with moderate surface area, but high in noble-metal content.

PROPELLANTS

In this program, both gaseous and liquid propellants were used. The gaseous propellants used in this study were typical of commercial bottle gases with a single exception; each gas was passed through a "molecular sieve" drier (calcium-aluminum-silicate) for removal of moisture prior to use. Liquid propellants corresponded to military specifications for liquid hydrogen and liquid oxygen, respectively.

Gaseous Hydrogen

The hydrogen was obtained as an ambient-temperature gas from high-pressure storage bottles located in the Propulsion Research Area. These gases contained oxygen, nitrogen, and water in the parts-per-million range as impurities. As supplied to the reactor, the hydrogen contained less than 15-ppm water, with an over-all impurity level of less than 60 ppm.

Gaseous Oxygen

The oxygen was obtained from 2.13-cu ft K bottles. The particular gas used (typical) was found by analysis to contain appreciable quantities of carbon dioxide (~ 2500 ppm) and water (~ 200 ppm), both of which are known to deactivate noble-metal catalysts. Therefore, the oxygen, as in the case of the hydrogen, was passed through a molecular sieve drier for removal of these impurities. The high removal efficiency of the molecular sieve drier is indicated by the fact that the carbon dioxide content of the gas leaving the drier was less than 50 ppm, while the water content was less than 0.5 ppm.

Liquid Hydrogen

Liquid hydrogen was obtained as a saturated liquid from primary liquid hydrogen storage at the Santa Susana Field Laboratory, and complied with appropriate military specifications for propellant purity.

Liquid Oxygen

The liquid oxygen was supplied from GFP storage as a saturated liquid, and complied with the appropriate military specifications for propellant purity.

APPARATUS

Two reaction systems were used in this program: a 1-inch-diameter reactor for the phase conducted with gaseous propellants, and a 3-inch-diameter reactor for the phase conducted with liquid propellants. Both

systems are described in the following paragraphs. The 1-inch-diameter reactor represented an available system appropriate for use in the screening operation; however, this reactor was considered to be only marginally scalable. Scalability considerations dictate that a minimum reactor diameter/pellet diameter of 8 is necessary for catalytic reaction systems. To ensure scalability, a 3-inch-diameter reactor was used with liquid propellants.

One-Inch-Diameter Hardware

Reactor. The reactor used in the gaseous phase of the program consisted essentially of a 1-inch-diameter (ID) stainless steel tube jacketed to provide for prechilling both the reactor and catalyst with liquid nitrogen prior to use. The reactor internal geometry was adapted to provide flexibility in the location and length of the catalyst bed. The downstream end of the reactor was threaded to provide for insertion of an exhaust nozzle, and to provide flexibility in the selection of an appropriate throat diameter. A schematic of the reactor and a photograph of the disassembled reaction assembly is presented in Fig. 1 and 2, respectively.

Catalyst pellets are randomly packed in a 4-inch-long sleeve, and held in place by perforated end plates or screens. Two types of catalyst pellet retainers were used in this study: 70-percent open-area stainless steel screens, and 31-percent open-area perforated plates. Most of the tests were conducted with the screen upstream and perforated plate downstream of the catalyst bed.

The downstream end of the combustor was threaded as indicated in Fig. 1 to accommodate a stainless steel insert. The insert was drilled and machined to a convergent contour and served as the exit nozzle. Various inserts with different throat diameters were used to control the combustion pressure and velocity distribution through the combustor. A 0.221-inch-diameter nozzle was used almost exclusively throughout this program, however, primarily because this seemed to give good combustion characteristics.

Injector. A basic 4-on-1 impinging-stream injector was used exclusively in this program. The injector had been proven in a previous program, and since injector optimization was not an objective of this study, no further consideration was given to the injection system. The injector was made of stainless steel and consisted of five elements of four hydrogen jets impinging on a central oxygen stream at an impingement angle of 30 degrees. Impingement distance from the injector face was 1/4 inch. The basic design called for a balanced momentum impingement at a mixture ratio of 1.0, but the injector has been found to operate satisfactorily over a range of ratios from approximately 0.6 to 1.6. The 4-on-1 impinging-stream injector is as shown in Fig. 3.

Three-Inch-Diameter Hardware

Reactor. The 3-inch-diameter reactor used in the phase of this program concerned with liquid propellants was constructed of stainless steel, and designed as shown in Fig. 4 through 10. A 3-1/8-inch-ID cylinder, flanged on each end and jacketed to enable precooling of the hardware and catalyst, comprised the main body of the reactor. A 4-inch-long sleeve, closed on

one end by a 31-percent, open-area drilled plate and a 70-percent, open-area screen on the other end, served as a catalyst chamber. This cylinder was randomly packed with catalyst and inserted appropriately in the main reactor body prior to firing.

A nozzle assembly, designed and fabricated as shown in Fig. 10 was bolted to the main reactor body and served jointly as a part of the thrust chamber and as a nozzle adapter. The downstream end of this assembly was threaded as indicated to accept various nozzles. These nozzles were contoured and drilled to various sizes to enable variation in chamber pressure independent of flowrate.

Injector. The injector used with the 3-inch-diameter reactor was basically the same as that used with the 1-inch reactor. The primary difference, other than physical size, was the fact that the 3-inch-diameter injector was comprised of seven elements. Impingement angle and impingement distance from the injector face were the same as with the smaller injector previously described.

A schematic of the assembled reactor and injector is shown in Fig. 4.

Crush Strength Test Device

The apparatus used in evaluating crush strength of the various catalysts was similar to devices used in the catalyst industry and consisted of a hydraulic jack of the dead-weight tester type arranged to exert pressure on a catalyst pellet placed between the tester plate and a rigid plate. Force measurements to the nearest 0.1 pound were made by a calibrated pressure gage and a known-diameter tester-plate piston.

Preliminary Catalyst Evaluation Apparatus

The apparatus used in the preliminary catalyst screening operation was as shown schematically in Fig. 11. This apparatus consists essentially of a flow-metering (and proportioning) system for providing reactant gases to the catalyst bed in controlled fashion, a catalyst bed for effecting reaction, and a water absorbent material for selectively removing the reaction product (water) from the effluent gas stream. Provision is also made for environmental cooling (to -300 F) of the catalyst and reactants prior to use. The catalyst bed is mounted in a detachable "U-tube" fitted with a thermocouple for measuring environmental as well as reaction temperature. The adsorbent material (indicator "Drierite") is similarly mounted in a detachable U-tube to facilitate weighing before and after the run. A back-pressure regulator is provided for maintaining constant pressure in the reaction chamber.

Test Facility

Gaseous Oxygen System. The oxygen system consists simply of three manifolded K bottles which supply gaseous oxygen to the reactor through an appropriately instrumented flow loop. The gaseous oxygen flows first through a metering orifice for flowrate measurement, then through a sonic orifice, and then to the injector. The sonic orifice serves to isolate the GOX supply system from pressure perturbations when ignition occurs and reaction chamber pressure increases, thus maintaining a constant GOX flowrate. Typical Marotta valves are used to initiate flow. The system is provided with sufficient valving to allow for initiation of oxygen flow through a vent system prior to the actual ignition test. As the test is initiated, the oxygen stream is diverted into the reactor, and the system does not suffer the time lags associated with

line filling, nor is the metering orifice system over-ranged at the beginning of a run. Figure 12 is a schematic of the oxygen supply system. The oxygen was provided as an ambient-temperature gas.

Gaseous Hydrogen System. The hydrogen supply system is shown schematically in Fig. 13. Hydrogen is supplied to the test stand from high-pressure storage bottles. The flow loop is the same as that described for oxygen, with one exception: hydrogen is prechilled to some appropriate temperature before entering the reactor. The chilling is done by means of heat exchange with liquid nitrogen in a double-wall heat exchanger. Hydrogen flows from the double-orifice arrangement through the inner tube of the heat exchanger. Liquid nitrogen flows through the annulus from a double-wall dewar pressurized as necessary with gaseous nitrogen to deliver the desired flowrate. The chilled hydrogen flows overboard to the atmosphere during the transient phase. When the exit temperature of the hydrogen reaches a steady-state value, flow is diverted to the reactor, and the test is initiated.

Liquid Oxygen System. The liquid oxygen system consists of a liquid nitrogen-jacketed dewar which provides liquid oxygen to the reactor through a system of valves, flowmeters, and pressure and temperature measuring instruments as shown in Fig. 14. Gaseous boiloff is dumped overboard through a vent valve during the hardware chilldown cycle. Once the hardware is at essentially liquid oxygen temperature, the liquid oxygen main valve is activated and the liquid flows through the injector to the catalyst bed. Temperature and pressure measurements, as well as flowrate measurements, are made as appropriate.

Liquid Hydrogen System. The liquid hydrogen system is as shown schematically in Fig. 15. The hydrogen dewar consists of a triple-wall vessel containing liquid hydrogen in the inner sphere. The surrounding annulus is evacuated to reduce heat leaks to the inner vessel, and the outer vessel is filled with liquid nitrogen. The outer shell is further covered with 9 inches of insulation to reduce liquid nitrogen boiloff. The liquid hydrogen dewar is provided with a nominally 25-foot-high vent stack to dissipate gaseous hydrogen boiloff; it is equipped with appropriate safety disks, check valves, and pressure-relief valves as indicated.

The liquid hydrogen flow loop is entirely vacuum jacketed, with the exception of flowmeters and valves, to reduce boiling in the transfer lines and thereby permit accurate flowrate measurements and delivery of liquid hydrogen to the injector. Liquid hydrogen temperatures are measured with a gold-cobalt thermocouple using liquid nitrogen as a cold junction.

Instrumentation

The instrumentation systems used in this study were typical of those used throughout the industry with one exception; that of the liquid hydrogen temperature measurement system. This system was as described in a following paragraph. No performance measurements were made since performance documentation was not an objective of the program.

Pressure Measurements. Pressure measurements were obtained by use of the usual Taber, Statham, and Wianko-type pickups. Where appropriate, the pickups were close coupled to reduce pneumatic lag in the transmission of the pressure impulse.

Temperature Measurement. Temperature measurements, except for liquid hydrogen temperature, were made through the use of bare-wire thermocouples, either iron-constantan or chromel-alumel, as necessary. The iron-constantan thermocouple was used for all temperature measurements except the combustion chamber temperature. The latter temperature often exceeds the operating range of iron-constantan and for that reason, chromel-alumel was used.

Liquid hydrogen temperatures were measured by use of a gold-cobalt thermocouple arrangement. In this system, a single wire consisting of a gold-cobalt alloy was joined to a hard-drawn copper wire to form a thermocouple junction. This thermocouple was inserted in the liquid hydrogen. A similar thermocouple was inserted in a liquid nitrogen bath, and the differential millivolt output was used to evaluate liquid hydrogen temperature. Use of this liquid nitrogen cold-junction compensated thermocouple permitted more accurate temperature measurements than would otherwise be available.

All propellant temperatures, the temperature of the liquid nitrogen supplied to the gaseous hydrogen heat exchanger, catalyst bed temperatures, and the chamber temperature were recorded. The catalyst bed thermocouples were inserted to the centerline of the bed. The combustion chamber temperature was recorded both on a dynalog and on the oscillograph. For the oscillographic record, a 36-gauge bare-wire chromel-alumel thermocouple was used because of the superior response of fine-wire thermocouples. For all other measurements, 20-gauge thermocouples were used. The 36-gauge thermocouple is said to respond in 5 percent of the time required for the 20-gauge thermocouple (Fig. 16). The temperatures presented in this report are as read and are subject to the normal corrections for thermocouple lag.

Flowrate Measurements. Flowrates of both propellant gases were measured by a dual technique. A calibrated metering orifice immediately downstream of the propellant reservoir indicated a differential pressure which was converted into a flow measurement. Concurrently, a sonic orifice downstream of the metering orifice served to enable calculation of the flowrate by the nozzle equation for sonic flow. Orifice coefficient and expansion factors were obtained from the literature (Ref. 5 and 6). Each system presented a reliable check on the other. The two systems agreed within the range of limitations appropriate to the techniques.

Liquid propellant flowrate measurements were made by means of Fisher-Porter turbine flowmeters. Volumetric flows were corrected for temperature and pressure as appropriate.

EXPERIMENTAL PROCEDURES

CATALYST SELECTION

The catalyst selection phase of this program was divided into two major areas: Chemical activity measurement, as indicated by degree of conversion of oxygen and hydrogen to water; and physical characterization, as determined by various physical tests.

Chemical Activity

For the purpose of this study, a dynamic, or flow method of analysis was selected as the means of measuring catalytic activity. The apparatus is shown schematically in Fig. 11. The specific method of analysis consisted of passing a mixture of oxygen and hydrogen at a pre-established mixture ratio and flowrate through a reactor containing a constant weight of catalyst (5 grams) and fitted with a thermocouple to indicate the presence of reaction. The reacted mixture then passes through a water absorber (indicator Drierite) for removal of water of reaction. The dry gases were then vented. The change in weight of the water absorber during the run reflects the amount of water formed by reaction. Sample bulbs are provided both upstream and downstream of the reactor for sampling both inlet and exit gases. Sample gas analyses, conducted mass spectrographically, provide control checks on the absorber weight-gain method of activity measurement. All tests are conducted at constant gas mixture ratio, flowrate, reactor backpressure (and hence residence time), and run duration. Therefore, all runs are directly comparable. Since the purpose of these analyses is to compare catalysts rather than to gain absolute performance data, this method of analysis is considered appropriate.

Provision was made for submerging the reactor in a constant-temperature bath to ensure comparability from catalyst to catalyst of the results of the low environmental temperature reactions. In instances where water was seen to freeze on the catalyst pellets or reactor walls, the reactor was also weighed and the gain in weight during the run added to the gain in weight of the absorber to establish the amount of water formed.

Physical Characterization

The physical characterization of the catalysts was generally limited to an elemental analysis (spectrographic), the evaluation of the effects of thermal shock on catalyst structural properties, and analyses of surface area, pore volume, and pore size distribution.

Elemental Analysis. The elemental analyses of the various catalysts were made by Pacific Spectrochemical Laboratories by conventional emission spectroscopy techniques.

Thermal Shock Treatment. The thermal shock tests (modified sauna treatment) were conducted by means of a modified Engelhard procedure. The catalyst pellets were cooled in liquid nitrogen to thermal equilibrium, placed in a muffle furnace operating at 1000 C (1832 F) for 10 minutes, and then plunged into liquid nitrogen. Damage to the catalyst was observed visually and by means of succeeding activity measurement.

Surface Characteristics. The characterization of surfaces for the various catalysts was done by use of an Engelhard Isorpta Analyzer. With this instrument, nitrogen adsorption isotherms may be obtained from which

the surface area, pore volume, average pore diameter, and pore size distribution can be computed. The analytical technique is somewhat lengthy and, for a comprehensive explanation of the procedure, refer to the manufacturer's instruction manual (Ref. 4). From a preliminary analysis, however, it is seen that the measurement of surface characteristics is a function of the amount of nitrogen adsorbed by a catalyst under conditions of given temperature and nitrogen partial pressure. Both the technique of application and manner of calculation are based on classical BET (Brunauer, Emmett, Teller) theory (Ref. 7).

For the purposes of this report, surface area is defined as the total surface area of the catalyst per gram of catalyst, without regard to the relative amount of catalytically active surface. The active surface area of a catalyst is virtually impossible to measure; however, active surface area is known to be proportional to total surface area, and is commonly used as a measure of relative activity for comparable catalysts. It is intuitive that the greater the catalyst surface area, the higher the rate of collision between reactant and catalyst; hence, large surface area in a catalyst is desirable.

Catalyst pore volume is similarly considered to be a criterion of over-all catalyst activity, as is average pore diameter. These catalyst properties are, however, secondary characteristics which are essential if a catalyst is to have high surface area. The pore volume is a general measure of catalyst porosity and indicates the general ease with which reactants may pass into the catalyst interstices and reach the less accessible active metal sites. Average pore size serves as an indicator of the relative availability of catalyst pores for reaction. For example, in a reaction between chemical species having molecular diameters of 5 Å, a catalyst

having an average pore diameter of only 4 Å would not be expected to promote the reaction as well as a similar one having an average pore diameter of 10 Å.

Pore size distribution is another catalyst property which serves as an indicator of activity and of durability. Since catalyst damage generally results from pore closure during the reaction sequence, and since the smaller pores are usually preferentially closed, pore size distribution can be used as an indicator of the extent of catalyst damage and of the ability of a catalyst to continue to promote a reaction. It is not possible to conclude generally that a wide range of pore sizes is preferable to a narrow range or vice versa. In fact, the optimum range would be that which provides the desired reaction in spite of slight pore damage (shrinkage), but does not allow for undesirable side reactions.

In certain instances, a special surface treatment was given the catalyst to evaluate its effects on surface characteristics. This treatment consisted of calcining the catalyst in air at 680 F (360 C), and was done for the purpose of ensuring proper drying of the catalyst prior to analysis. Calcining in this sense is, therefore, defined as the very efficient drying and removal of trace impurities from the catalyst surface.

Crush Strength. Catalyst crush strength was measured with the device previously described. In general, the catalyst samples were placed on the tester plate and compressed by increasing pressure on the hydraulic jack piston. Compression was increased until the pellet was crushed. The pressure at which the catalyst failed was noted, multiplied by the area of the piston (0.1 sq in.), and recorded as the crush strength of the catalyst. Multiple runs (5 to 10) were made to provide representative sampling results.

EXPERIMENTAL EVALUATION

The experimental evaluation task was divided into two primary phases: catalyst screening with chilled gaseous propellants, and catalyst evaluation with liquid propellants.

Catalyst Screening

Catalyst screening with chilled gaseous propellants was conducted in the 1-inch-diameter hardware, and used the gaseous propellant systems previously described. The catalyst to be screened was placed in the reactor and chilled to the target temperature by heat exchange with liquid nitrogen flowing through the reactor jacket. Once the catalyst sample reached the desired temperature, gaseous hydrogen flow was initiated. Gaseous hydrogen was dumped overboard during the propellant chilldown cycle, and diverted through the engine once the desired fuel temperature was reached (normally -270 F). Gaseous oxygen, at ambient temperature, was introduced when it was desired to start the test run. The mixture of ambient oxygen and chilled hydrogen produced the desired propellant environmental temperature (Fig. 17).

The majority of the tests were for a duration of 10 seconds; however, the total range of test duration was from 8 to 24 seconds. All tests were sequenced electrically. In some, a gaseous oxygen lead prevailed, but most of the tests were conducted with a 1-second hydrogen lead. Similarly, a 3- to 5-second hydrogen lag was used to ensure that the catalyst was dry and de-oxidized for the succeeding run. In this regard, it was established that prior reduction of the catalyst from a possible oxidized state to the reduced metal enhanced the catalytic activity. Originally, the procedure was to place the catalyst-filled reactor in

an oven operating at approximately 250 F to remove moisture prior to the actual test. This was not effective in reducing the catalyst, since it was not feasible to introduce a reducing agent (hydrogen) into the hot oven. The next approach was to mount the reactor in place on the test stand and preburn the catalyst at a temperature of about 500 F for about 30 to 60 seconds prior to the initiation of a series of test runs. This proved to be a satisfactory procedure, and was used in the remainder of the catalyst screening tests.

Following the catalyst reduction by preburning in a fuel-rich atmosphere, ignition tests were conducted at environmental temperatures (hardware and propellant) of -250 F. Propellant flowrate and inlet temperature were measured, and mixture ratio (o/f) was computed. Catalyst bed and combustion chamber temperature were evaluated as a function of time, as was combustion chamber temperature. Ignition delay, defined as the time differential between the signal to the oxidizer (lagging propellant) valve and the first indication of ignition as measured by chamber pressure or temperature, was determined from oscillograph charts and used in comparing relative activities of the various catalyst samples at the reduced temperature (-250 F). The over-all ignition delay, as reported, includes a pneumatic response lag of about 20 milliseconds and a thermal lag of approximately 2 milliseconds when the combined mass flowrate is on the order of 0.04 lb/sec. These inherent system time lags must be subtracted from the apparent ignition delay to arrive at a more nearly accurate value for ignition delay.

Low-Temperature Catalyst Evaluation

The catalyst evaluation procedure was conducted with liquid propellants and represented a much more severe test of catalyst activity than the catalyst screening tests. The general procedure used in these tests was

to place a previously reduced sample of catalyst (reduced by purging in a hydrogen atmosphere for approximately 1 hour) in the 3-inch-diameter reactor, to pass liquid hydrogen through the catalyst bed until liquid hydrogen could be seen leaving the nozzle of the engine, and then initiate liquid oxygen flow to the catalyst bed. In each instance, at least a 5-second liquid hydrogen lead through the catalyst bed was used. Liquid oxygen was dumped overboard prior to diverting it through the injector. In this manner, delivery of liquid oxygen to the catalyst bed was ensured almost instantaneously upon demand. A 1-second hydrogen lag followed cessation of oxygen flow.

RESULTS AND DISCUSSION

The homogeneous reaction of oxygen with hydrogen is generally regarded to be a branched-chain mechanism, and can be treated in semi-rigorous fashion under certain circumstances. The addition of a catalyst to promote the reaction complicates the analysis of the O_2/H_2 reaction. Catalysis, per se, is not too well understood, and injection of this concept, with none of the refinements of an analytical reactor, into the oxygen/hydrogen reaction system virtually eliminates any possibility of a precise kinetic analysis of the catalytically promoted oxygen/hydrogen reaction. The absence of an analytical (differential) reactor renders impossible the separation analytically of the interrelated effects of temperature and pressure on the O_2/H_2 reaction; therefore, little theoretical significance can be ascribed to the results of the ignition tests. Since the purpose of this study, however, was the practical applied research task of defining the constraints and limitations of the catalytic oxygen/hydrogen reaction, a precise analysis of the catalytic reaction is not essential. With this in mind, the results of the various phases of this project are presented. Theoretical significance is discussed where possible and appropriate. A discussion of the basic theory of catalysis is presented as Appendix A as an aid in understanding the fundamental aspects of the catalytic phenomenon. This appendix also includes a discussion of the catalyst selection criteria.

CATALYST SELECTION RESULTS

Catalytic Activity

The results of the activity measurements are as shown in Table 4. Each run reported was of 10-minutes duration and was conducted with a 5-gram catalyst charge. A 2-minute hydrogen lead preceded each run. The oxygen/hydrogen weight mixture ratio was 0.33, and the combined gas flow-rate was such that 100-percent conversion of oxygen corresponded to the generation of 0.396 gram of water.

The results of the activity measurements indicated that the only catalysts worthy of further consideration in this task were:

Engelhard	DS
Engelhard	DSS
Engelhard	MFSS
Engelhard	MFSA
Houdry	A-200SR
Girdler	G-68 (treated)
Shell	8240-168
Davison	SMR 55-1097-1

The manner of treatment for the Girdler catalyst is described later in this report.

Neither the Shell 8240-168 nor the Davison SMR 55-1097-1 catalyst was available in sufficient quantity or sufficiently early in the program for serious consideration in this task. Consequently, they were given only limited study. It is interesting to note, however, that the Shell catalyst has a low-temperature (-300 F) activity level exceeded only by the Engelhard MFSA catalyst.

The Davison SMR 55-1097-1 catalyst is only marginally better than the Houdry A-200SR configuration, and would not have been selected for further study in this task even had it been available.

From the remaining six catalysts, the decision was made to evaluate only the following:

Engelhard	MFSA
Engelhard	MFSS
Engelhard	DSS
Houdry	A-200SR

Since the Houdry catalyst does not, by comparison, appear to be better than the Engelhard DS catalyst, some explanation for its selection is appropriate. Past discussions with Engelhard representatives have indicated that the only significant difference between the DS and DSS formulations is the increased resistance to thermal shock of the DSS catalyst. On the basis of this large degree of similarity between the DS and DSS catalysts, it was decided to delete the DS catalyst from future phases of the study and to substitute Houdry A-200SR in its place. Selection of the four catalysts previously indicated also provided four basically different catalyst types for further study; namely, platinum, palladium, platinum-rhodium, and platinum-rhodium-lead, all on alumina bases.

Although no Davison catalyst was selected for study, it is interesting to note the effect of noble-metal concentration on catalyst activity exhibited by these catalysts. The SMR 55-1097-1 configuration contained nominally 6-weight percent platinum on silica gel. The SMR 55-1097-4 was supposedly prepared in the same manner, had the same surface characteristics and type of substrate, but contained only 0.6-weight percent

platinum. The higher platinum-content catalyst was seen to have an activity equivalent to 99.9-percent conversion at an environmental temperature of 77 F. Similarly, the lower platinum-content material converted only 8.8 percent of the propellant combination. The difference in conversion level points up vividly the effect of catalyst metal concentration on catalytic activity.

Surface Characterization

Surface characterization was conducted on a representative sampling of the available catalysts in an effort to correlate catalytic activity with surface condition. Only very general correlations are possible because of the variety of catalytic metals, manners of catalyst preparation, types of substrates, and noble-metal concentrations used. It appears, however, that catalyst activity is strongly influenced by surface area and active metal concentration. The general trend also appears to indicate that catalytic activity increases with pore volume. These are merely indications, however, and definitive correlations can be made only on the basis of a much more intensive study program.

The results of the surface characterization measurements on certain of the catalysts selected for this program are shown in Table 3. The Engelhard DS and DSS catalysts are seen to have moderate surface area, pore volume, and average pore diameter, and on this basis alone would be expected to have average and comparable activity and life.

Two samples of the MFSS catalyst were subjected to analysis by the Isorpta technique. The first, a fresh sample, was seen to have a moderately high surface area with average pore volume and pore diameter. The

second sample, one which had been subjected to extensive use in oxygen/hydrogen reaction promotion service, was similarly analyzed, and the results indicate that MFSS has the property of retaining its surface area, pore volume, average pore diameter, and apparently, activity over an extended period of use. The relative change in pore size distribution resulting from catalyst use is shown in Fig. 18. These results show the smaller pores to be preferentially closed in use.

The final Engelhard catalyst, the MFSA, had a surface area surpassing that of any of the others, and for that matter, surpassing any other known alumina-based catalyst. The pore volume was correspondingly high, as expected from the high surface area. On the basis of surface area alone, the MFSA catalyst should have outstanding activity (as was later demonstrated), and should have reignition capability far surpassing any of the previous catalysts.

A second sample of MFSA catalyst, calcined in a muffle furnace for 2 hours at 1110 F, was also subjected to surface characterization tests, and was found to have lost nearly 50 percent of the original surface area and pore volume. The calcining operation was known to be a rather drastic treatment, however, since the calcining was done in the presence of air, and the duration of the treatment was quite long. It is interesting to note that the smaller-sized pores were preferentially closed or occluded, as demonstrated by the comparative pore size distribution curves shown in Fig. 19. Loss of very small pores is not considered to be a major loss, however, since the smaller pores are less accessible to the reactants than the larger pores and, therefore, do not play a major role in reaction promotion.

The Houdry catalysts had a low (A-100S, Pd-K) to moderate (A-200SR) surface area, pore volume, and average pore diameter. The A-100S and Pd-K catalysts are not recommended for the particular application considered because of the probable rapid loss in activity due to reduction in surface area in the heating and cooling cycles associated with rocket engine service. The A-200SR catalyst, however, compares favorably with the Engelhard DSS catalyst, and would be recommended on the basis of surface characteristics. Pore size distribution characteristics of the Houdry A-200SR catalyst are shown in Fig. 20.

The Girdler G-58 catalyst was immediately discarded when an analysis of its surface indicated a surface area of only 10 square meters/gram. The remaining Girdler catalysts had better than average surface area and associated characteristics. A sample of G-68 was subjected to the same calcining operation conducted on Engelhard MFSA, and was found to have lost only about 25 percent of its surface area. The pore size distribution results presented in Fig. 21 show most of the loss to be due to preferential small pore closure or occlusion.

The Universal Oil Products C-IV nickel-on-alumina catalyst had a relatively low surface area, very low pore volume, and low average pore diameter. For this reason, it is not recommended, and no further study was made on this catalyst.

The Catalytic Combustion Company catalyst was unique in its manner of preparation, but was found to have extremely low surface characteristics. No further work was done with this catalyst.

The two Davison catalysts analyzed were virtually identical in surface area, pore size, and pore volume, indicating a similar method of preparation, and the use of essentially the same substrate. Surface area for these catalysts was the highest of those evaluated, while pore volume was only average, and average pore size quite low. This is typical of silica-gel-based catalysts. On the basis of surface area, the Davison catalysts would be expected to have a long active "life," and should be highly resistant to thermal damage.

The final catalyst, the Shell 8240-168, was quite similar to the Engelhard DSS catalyst in surface area, pore volume, and average pore size. This catalyst was originally thought to be based on kaolin, but subsequently was found to be manufactured from an alumina substrate impregnated with appropriate metals.

In reviewing the catalyst surface characteristics, it is seen that the Engelhard MFSA catalyst is much more cellular in nature than the others evaluated, as evidenced by the larger changes in pore volume with changes in pore diameter. Therefore, more surface would be available for reaction promotion. This fact is confirmed by the large surface area reported.

Chemical Analysis

Only five of the most promising catalysts, based on activity measurements, were submitted for spectrographic analysis in this program. These catalysts were Engelhard's DS, DSS, MFSS, and MFSA; and Houdry's A-200SR. The results of these analyses are shown in Table 2.

Reviewing the data presented in Table 2, it should be noted that the major difference between the DS and DSS catalysts is the amount of sodium present. Since alkali metals are known to promote catalyst sintering with resultant loss in surface area and activity, it is conceivable that the DSS formulation would have greater reignition capability than the DS formulation. The MFSS catalyst is seen to be different from the DS and DSS catalysts in noble-metal content. The catalytic agents in the MFSS formulation are platinum and rhodium. The vendor contends that rhodium is more active in promoting the reaction of oxygen and hydrogen than either platinum or palladium. (This is consistent with theory, as discussed in Appendix A. Rhodium, however, is very difficult to deposit on a substrate; hence, platinum is used as a base on which to deposit rhodium. Some synergistic effects may result from use of a bimetallic catalyst, but such was not the purpose in the original formulation.

The second catalyst shown in Table 2, MFSA, is seen to be similar to MFSS in the use of platinum and rhodium, but the analysis indicates an absence of any appreciable quantity of silicon, reduced platinum and rhodium content, and the presence of lead as a third metal. The virtual absence of sodium should make this catalyst capable of repeated use without appreciable loss in activity.

The fifth catalyst, A-200SR, appears to be simply a platinum-on-alumina formulation, typical of re-forming catalysts used in the petroleum industry. This particular catalyst is one of a series of sulfur-resistant platinum configurations deposited on, nominally, a 200 square meter per gram surface area substrate. The term "sulfur-resistant" refers to resistance to poisoning by the action of sulfur compounds. This property is not important in the present application, but does add to an understanding of the nature of the catalyst.

Catalyst Treatments

Since catalysts provided directly from vendors often contain considerable quantities of moisture and, in some cases, have an oxide mantle covering the active metal, preliminary treatments were given certain of the catalysts. The Girdler G-55 and G-68 promoted palladium-on-alumina catalysts were subjected to a calcining operation in air for 2 hours at 1110 F to volatilize the promoters and expose more catalytic surface. This was done as an afterthought when it was observed that neither of these catalysts exhibited appreciable activity. Such calcining was seen to enhance the activity of the G-68 catalyst, but not to improve the activity of the G-55 catalyst appreciably (Table 4).

The MFSA catalyst was subjected to two such treatments. The first consisted of a simple drying operation in which the catalyst was heated to 250 C (492 F) for approximately 1 hour in a drying oven.

The large weight loss (10.8 percent) of MFSA on heating at 250 C in the drying oven was obviously due to the loss of water of hydration. The following table gives theoretical weight losses and temperatures of transition applicable to the alumina hydrates:

Alumina Hydrate	Formula Weight	Temp. of Trans. to Lower Hydrate	Percent Weight Loss Per Step
$Al_2O_3 \cdot 3H_2O$	156	200 C (392 F)	11.5
$Al_2O_3 \cdot 2H_2O$	138	360 C (680 F)	13.0
$Al_2O_3 \cdot H_2O$	120	> 360 C (> 680 F)	15.0

The observed 10.8 percent weight loss on heating at 250 C shows that MFSA is on an $Al_2O_3 \cdot 3H_2O$ (gibbsite) support. The catalyst weight loss of 10.1 percent in the reactor and approximately the same weight gain in

the water absorber was noted after the run at 77 F. This fact leads to the conclusion that, during the run, the temperature of the solid catalyst must have reached at least 200 C (392 F).

The second treatment of the MFSA catalyst consisted of calcining in a muffle furnace at 1110 F for approximately 2 hours. During this operation, the MFSA catalyst suffered a weight reduction of approximately 22 percent. This corresponds to a loss of two waters of hydration.

Surface characteristics for the Girdler G-68 and Engelhard MFSA catalysts after each treatment are shown in Table 3 and Fig. 19 and 21. The G-68 catalyst suffered only minor loss in surface properties, but showed a marked increase in activity, as presented in Table 4. The relative pore size distribution for the G-68 catalyst before and after calcining is shown in Fig. 21. The reduction in number of small pores is apparently due to sintering, while the increase in number of large pores and catalyst activity is probably due to more efficient drying (moisture removal) and perhaps to volatilization of promoter from the pores.

The MFSA catalyst suffered a large decrease in surface area on calcining, with corresponding decreases in pore volume and average pore size. Figure 19 shows changes in the pore size distribution of MFSA on heating and on calcining. Moderate heating (drying) increase enormously the proportion of large pores by freeing them of water. Calcining (roasting) reduced the number of small pores by sintering. The enhancement of activity observed with calcined MFSA is apparently due to a more efficient drying. All catalysts were treated for 2 hours in a hydrogen atmosphere at 680 F prior to catalyst activity tests.

Catalyst Crush Strength

The various catalysts evaluated in this program were subjected to crush strength tests to determine their relative resistance to physical shock and acceleration loading. The apparatus used in these tests was described previously. In these tests, the cylindrical pellets were tested in two orientations; long axis horizontal and long axis vertical. The results are presented in Table 5. These data indicate that the Catalysts and Chemicals, Incorporated C-54 catalyst had the highest crush strength (52 pounds) of the spherical catalysts. Of the recommended catalysts, the MFSS had the highest crush strength (26.6 pounds).

Of the cylindrical catalysts, the highest resistance to crushing in the vertical position was exhibited by the Girdler catalysts, none of which were crushed at 200-pounds of force. In the horizontal position, the Girdler G-58 catalyst appeared to be the hardest, with a crush strength of 112 pounds.

In general, calcining has the effect of reducing crush strength; the greater the degree of calcining, the greater the reduction.

Thermal Shock Resistance

The resistance of the various catalysts to thermal shock was measured by the sauna treatment previously described, and the results presented in Table 6. In general, only the MFSS 1/4-inch cylinders and 1/4-inch spheres (not otherwise evaluated in this program) were damaged physically (visually). The Girdler G-55 and G-68, both palladium catalysts, changed color as a result of the thermal shock treatment. Because only two of the catalysts to be used in this program were damaged in these tests, and

because this is thought to be due to promoter volatilization rather than actual catalyst damage, a good general resistance to thermal shock is indicated for all of the catalysts seriously considered for use in experimental evaluation.

Following the sauna treatment, the four selected catalysts were subjected to activity tests and measurement of surface characteristics. The results, with comparable results from tests on untreated catalysts, are shown in Tables 7 and 8. Only the DSS and A-200SR catalysts appeared to suffer appreciable loss in activity under ambient conditions. Similarly, these same catalysts were drastically reduced in activity at an environmental temperature of -112 F. Appreciable reduction in activity at this temperature was also noted for the MFSA catalyst, but not as dramatically as the previous two. At an environmental temperature of -300 F, all catalysts suffered loss in activity resulting from the thermal shock test. The A-200 SR catalyst retained about half of its original activity, while the MFSA and MFSS samples retained only one-third of their original activity. The DSS catalyst lost approximately 85 percent of its activity at the -300 F environmental temperature.

Table 8 presents the effects of thermal shock on catalyst surface characteristics. It is noted at this point that thermal shock tests are not analogous to calcination but, in fact, represent destructive testing of the catalyst. Results obtained are indicative only of the catalyst's resistance to thermal shock. The MFSS and DSS catalysts appear to sustain relatively mild damage from thermal shock, and even indicate an increase in pore volume. On this basis, these two catalysts might be expected to perform well after high-temperature shock. Such is not true, however,

for the DSS catalyst (as shown in Table 7). The MFSS catalyst, on the other hand, does appear to retain good activity. This is consistent with information obtained from the vendor relative to the resistance of the MFSS catalyst to thermal shock.

Both the MFSA and A-200SR catalysts are seen to suffer considerable damage from thermal shock. Both suffer large decreases in surface area and pore volume, while showing an increase in average pore diameter. This indicates preferential closure of small catalyst pores.

On the basis of these tests, the MFSS and MFSA catalysts appear to have the greater resistance to thermal shock. The MFSA catalyst suffers more surface damage, and also appears to suffer the greater loss in low temperature activity in terms of absolute magnitude. The MFSA catalyst low-temperature activity remains at a higher level than the MFSS catalyst, however, even after the thermal shock test. On this basis, it appears that the MFSA formulation is superior to that of the MFSS in terms of over-all reaction promotion ability for the liquid oxygen/liquid hydrogen system.

EXPERIMENTAL EVALUATION RESULTS

This task was divided into two general areas of effort; one with gaseous propellants conducted in 1-inch-diameter hardware, and the other with liquid propellants conducted in 3-inch-diameter hardware.

Catalyst Screening in 1-inch Hardware

Following selection of the Engelhard MFSA, MFSS, DSS, and Houdry A-200SR catalysts for further study, the test hardware phase of the program was initiated. The reactor configuration used in these tests is as shown in Fig. 1 and Ref. 3. The injector is of the 4-on-1 impinging stream (hydrogen-on-oxygen) type, consisting of five elements and having an impingement angle (hydrogen-on-oxygen) of 30 degrees. From the injector, the prechilled gaseous mixture passes through a mixing chamber which may vary in length from 1 to 3 inches before entering the catalyst bed. The catalyst bed length was maintained at 2 inches throughout the course of these runs, but may vary up to 5 inches. The combustion (or reaction) products leave the reactor through a combustion chamber designed to provide a characteristic chamber length of 40 inches. On the basis of past experience, this value appears to be adequate for complete combustion.

In the initial runs, the instrumentation system was such that the ignition delay measurements were actually a measure of the time between the opening of the oxidizer main valve and the first indication of ignition. More recently, the system has been modified to eliminate the time lag associated with oxygen flow from the main valve to the catalyst bed. A pitot tube has been installed immediately in front of the catalyst bed to allow recording of the time at which the oxygen reaches the bed, and

thereby to enable a more nearly accurate measurement of ignition delay. By using this method of analysis, apparent "ignition delay" has been decreased from about 40 milliseconds to roughly, 20 milliseconds, depending on the particular catalyst and bed length used.

The initial testing, with the Engelhard MFSA and MFSS catalysts, was conducted almost routinely without difficulty. However, concurrently with the beginning of tests on the other catalysts, a contaminant appeared in the hydrogen supplied to the test area. The contaminant was established by mass spectrographic analysis to be compressor oil, and began to appear in the hydrogen gas stream only after a change in filter medium was made at the gas compressor station. Previously, the filter medium had been activated charcoal. This material performed satisfactorily in all respects except one; the charcoal became saturated quite rapidly in service which necessitated frequent replacement. For this reason, the filter medium was changed to activated alumina, which has a longer service life. In retrospect, undoubtedly the reason for this longer service life is the fact that the alumina is not as efficient a filter material as the charcoal.

With the change in filter material, compressor oil began to pass through and enter the storage bottles used in the test area, and thence into the test system. Compressor oils invariably contain both sulfur and nitrogen organically bound as mercaptans, thiophenes, amines, etc. Both nitrogen and sulfur are known poisons to noble-metal catalysts, and the presence of these materials in the hydrogen gas supplied to the catalyst resulted in poisoning. In practice, the various catalysts tested fired effectively on the first try, but failed in succeeding tests. This mode of catalyst failure is exactly what would be expected if the catalyst were poisoned by some reactant contaminant.

The test failures occurred at such a time initially as to be nonsuspect, since the catalysts in some instances were undergoing their first tests. The conclusion was that the catalyst simply had no reignition capability, and the sample was discarded. As time went by and the number of test failures mounted, samples of catalysts (MFSA) which had previously proved satisfactory, were tested as a control measure. When these catalysts failed to reignite the propellant combination, the search began which finally proved the problem to lie with the oil contaminant in the hydrogen.

The specific manner of catalyst damage from poisoning by sulfur and nitrogen compounds is reasonably well established. In general, sulfur is converted to hydrogen sulfide in the presence of the catalyst. This, in turn, attacks the catalytic metal in such a way as to reduce the ability of the catalyst to promote the O_2/H_2 reaction. It is of interest that sulfur poisoning is reversible, and would be corrected with the introduction of pure hydrogen.

Nitrogen poisoning, on the other hand, is irreversible. Nitrogen tends to deactivate the acidic sites and therefore the ability of a catalyst to generate hydrogen atoms. In this sense, it is much like sulfur as a poison. However, an additional effect of nitrogen is that it tends to promote noble-metal crystal growth. With crystal growth comes crystal annealment and the associated loss in points of catalyst crystal distortion, corresponding to points of high activity. The result is an irreversible catalyst poisoning.

After determining the cause of previous catalyst failure, the storage bottle system for storing high-pressure (3000 psi) hydrogen was disassembled, cleaned thoroughly to remove oil contaminants, and replaced in service. Prior to filling this system, however, a filter system

containing activated charcoal for removal of compressor oil was placed in the fill line from the compressor station. The system then operated in a completely satisfactory manner.

While the storage system was being cleaned and modified, experimental evaluations were continued on a reduced basis with gaseous hydrogen purchased in K bottles.

Results of Catalyst Screening Studies. A total of 118 screening evaluations were made in this phase of the experimental evaluation. Approximately 45 of these runs were discarded because of hydrogen contamination. The general pattern in these discarded runs was for the catalyst to provide one ignition, usually delayed, or at best unstable, and then to fail to reignite. Since the hydrogen was known to be contaminated, all runs associated with contaminated gas were discarded. The results of the remaining 73 runs are presented in Table 9 and Fig. 22 through 30.

The results of ignition lag measurements (defined as the time lag between the arrival time of the second propellant, oxygen, at the front face of the catalyst bed and the first indication of ignition) are presented in Table 9. This lag time, of course, includes the pneumatic fill time for the reactor, as well as the thermal lag associated with the system.

In this phase of the program, it was established that the apparent ignition lag is consistently of the order of 20 milliseconds when measured by pressure transducers, and 20 to 40 milliseconds when measured by thermocouples. Further calculations indicate that the time necessary to heat the catalyst bed sufficiently to induce movement of the oscillograph pen is approximately 20 milliseconds under typical flow conditions. An additional thermal response delay of nearly 2 milliseconds was calculated as thermocouple lag. The sum total of these lags is 22 milliseconds when the combined O_2/H_2 flowrate to the reactor is on the order of 0.04 lb/sec. As propellant flowrate is reduced, the thermal response lag increases proportionally. These calculated values for thermal lag, when compared to the measured apparent ignition lag, indicate that the catalytic reaction of the O_2/H_2 combination, even at the reduced temperatures of these tests, occurs with less than a 1-millisecond lag.

Figures 22 through 26 present curves depicting the rate of approach of the reacting system to a steady-state condition. Figure 22 presents data for typical pressure response rate curves for the Engelhard MFSA catalyst. The curve numbers correspond to test run numbers in Table 9. Run No. 1 is typical of a system having an ignition lag of 20 milliseconds and a chamber pressure spike and flashback. Flashback is defined as the propagation of the flame front out of the catalyst bed back to the point of propellant impingement. Curve 12, in contrast, is representative of a system undergoing a chamber pressure spike without flashback. The rate of approach to steady state is seen to be markedly different for these two runs, in spite of the fact that the propellant flowrate was higher for Run No. 12 than for Run No. 1. This seeming anomaly results from the fact that ignition conditions were grossly different for the two runs. Following Run No. 1, the reactor was disassembled and inspected to establish the cause of flashback. The up-stream

catalyst retainer screen was slightly burned (catalyst apparently not damaged), indicating nonhomogeneous mixing in the mixing zone, maintained at a constant length of 1 inch throughout all of the runs with gaseous propellants. Further investigation revealed that the hydrogen flow was partially obstructing in two injector ports due to an unknown source of foreign material. The result was a relatively high-mixture-ratio oxidizer streak. This provided a likely path for flame front propagation back to the point of propellant impingement (flashback), resulting in a high chamber pressure spike. Run No. 12, in contrast, apparently had a homogeneously mixed propellant combination upstream of the catalyst bed, and did not flash back. It was observed, however, that the propellant combination appeared to ignite outside the reactor (downstream of the nozzle) and to propagate back into the chamber, resulting in a high chamber pressure spike. The likely cause of the failure to ignite within the catalyst bed was partial catalyst surface occlusion by ice formed from moisture (humidity) condensed on the catalyst during the environmental cooling cycle. This accounts for the fact that the rate of approach to steady state is significantly faster for Run No. 1 than for Run No. 12, in spite of the fact that the propellant flowrate for Run No. 1 is less than two-thirds of that for Run No. 12. The remaining curves, 6, 16, and 19, are representative of normal reaction conditions, and illustrate the effect of propellant flowrate on the rate of approach to steady-state conditions. It is observed that the rate of approach to steady state increases with increasing flowrate.

Figure 23 presents similar data for the MFSA catalyst in terms of the rate of approach of chamber temperature to steady state. It is noted in Run No. 1 that temperature spikes are also seen with chamber pressure spikes, though not as severe. The other curves illustrate the effect of

propellant flowrate on the rate of approach of chamber temperature to steady state. It is also seen that, for normal reaction without pressure or temperature spikes, the rate of approach to steady state is faster for chamber temperature than for chamber pressure. This is an anticipated result, since the O_2/H_2 reaction is known to proceed very rapidly. The pressure buildup is a pneumatic effect, and would be expected to reach equilibrium slower than temperature, which is a function of reaction and catalyst bed mass (however, when a pressure and temperature spike occur causing flashback, as in Run No. 1, the chamber pressure reaches equilibrium more rapidly than chamber temperature). Figures 24 and 25 present similar results for the MFSS catalyst. Curve 1, as does Curve 12 in Fig. 22, presents data for a condition wherein the reaction system undergoes a chamber pressure spike. It appeared that no flashback occurred in this run, and the rate of approach to steady state is quite slow after the pressure spike. Curve 23 represents a system that exhibited a tendency to spike, but ignited stably. The remaining curves are typical of normal operation.

Figure 25 is illustrative of the effects of flowrate on the rate of approach to steady-state chamber temperature for the MFSS catalyst. It is interesting that chamber temperature did not exhibit a spike as chamber pressure did in Run No. 1. Curve 7 illustrates a system that showed an unusually long ignition lag, but which propagated uniformly once ignition occurred. Curve 11, in contrast, is representative of a system having a normal ignition lag, but which shows a tendency to quench and not propagate uniformly. This particular system did not quench, but finally became sustained and propagated at an accelerated rate, as indicated by the steep slope of the curve.

Figure 26 presents typical data for a successful run with the Engelhard DSS catalyst. Chamber temperature response was grossly delayed with this catalyst at the reduced (-250 F) environmental temperature, as is the rate of approach to steady state. Chamber pressure also is shown to increase at a slower rate, consistent with the lower rate for temperature buildup.

The information presented in Fig. 27 through 30 illustrates a correlation between a function of propellant catalytic reaction rate and residence time within the catalyst chamber. In considering these correlations, certain considerations must be made. From a continuity standpoint, the time spent (residence time) by the propellant in the catalyst bed is equal to the volume of the catalyst bed divided by the volumetric rate of propellant flow. For a constant density catalyst, fixed catalyst bed geometry, and constant rate of propellant flow, this relationship may be stated in terms of weight. Therefore, residence time can be equated to the ratio of catalyst weight to propellant weight rate of flow. In the processing industries, this ratio is referred to as reciprocal "weight hourly space velocity," or other units of time. In this particular application, the residence time is equal to pounds of catalyst/lb/sec propellant, and has the dimensions of seconds. As residence time increases (propellant flowrate decreases, or catalyst weight is increased), the relative density of active catalyst sites to reactant materials increases, and the reaction is seen to approach completion more rapidly. However, since the oxygen/hydrogen reaction proceeds very rapidly, the approach to completion is almost instantaneous. Consequently, the limiting step in the approach to steady-state conditions is the rate at which propellant is supplied to the chamber. On this basis, Fig. 28 through 31 could have been prepared with propellant flowrate (catalyst mass was held constant in all runs) plotted as the abscissa. However,

to provide a generalized correlation, the figures were prepared as shown. It is seen from these figures that the rate of approach to equilibrium conditions, as measured both by chamber pressure and temperature transients, is a smooth function of propellant flowrate through the constant volume catalyst bed.

The information presented in Fig. 27 through 30 should not be scaled to larger engine systems without due caution. The data shown are thought to be scalable upward over a limited thrust range (perhaps as high as 10:1), and should not be scaled down directly. Smaller engine diameters result in excessive "wall effect" and channeling of reactant through the catalyst bed. The result is incomplete combustion resulting from inadequate contact between catalyst and reactant.

On the basis of the results of catalyst screening tests conducted with the Engelhard MFSA, MFSS, and DSS catalysts, and with the Houdry A-200SR catalyst, it was concluded that only the Engelhard MFSA and MFSS catalysts offered promise of promoting the liquid oxygen/liquid hydrogen reaction. Consequently, only these catalysts were considered for further study with liquid propellants at liquid hydrogen environmental temperatures.

LIQUID OXYGEN/LIQUID HYDROGEN IGNITION INVESTIGATIONS

Apparatus and Procedures

This phase of the study was conducted with stainless steel hardware, patterned largely after the reaction hardware used in the previous phase. The reactor consisted primarily of a spool-like catalyst chamber as shown in Fig. 9. A nozzle adapter was attached to this chamber and threaded to accept nozzle inserts with throat areas appropriate to the specific objectives of the run. A 4-on-1 injector was used as before. An assembled view of the reactor and injector is shown schematically in Fig. 4. Catalyst was loaded into the reactor as described earlier.

The 3-inch-diameter reactor differs from the 1-inch-diameter reactor in a number of respects (Fig. 2, and Fig. 4 through 10). The fundamental difference, however, relates to hydraulic scalability aspects of the two reactors. The 1-inch-diameter reactor is marginally subject to detrimental interactions of third bodies (walls) which quench the reaction by removal of active species from the reactants, as shown in Eq. 19 through 21 of Appendix A. Similarly, the 1-inch reactor is subject to reactant "channeling," in which the hydrogen and oxygen may pass through the catalyst bed without contacting the catalyst. In general, channeling does not appreciably affect a catalytic reaction provided the ratio of reactor diameter to catalyst pellet diameter is greater than 8:1. Since 1/8-inch-diameter catalyst pellets were used in the earlier studies, channeling may have occurred. To avoid this possibility in the studies with liquid-phase reactants, a 3-inch reactor was selected. In this reactor, the wall surface area/volume ratio was decreased by a factor of three relative to the 1-inch-diameter reactor, thereby reducing wall effects.

Increasing the reactor diameter to 3 inches also virtually eliminated the effects of reactant channeling, since the ratio of reactor diameter/catalyst pellet diameter was increased to 36:1, well above the marginal level of 8:1.

On this basis, the results from studies with the 3-inch-diameter reactor are thought to be scalable, whereas those obtained with the 1-inch reactor may not be.

During this investigation, it was found not feasible to prechill the reactor and catalyst bed by liquid hydrogen flow through the annulus surrounding the catalyst chamber. The specific problem was associated with the heat leakage to the reactor outside wall, which was in excess of the heat-absorbing ability of the available liquid hydrogen coolant flow. In addition, leakage of hydrogen from the annulus past the gasket faces was observed. Consequently, it was decided to chill the catalyst bed to liquid hydrogen temperatures by passing liquid hydrogen directly through the catalyst during the chilldown cycle prior to the test runs. It was established that this procedure was entirely adequate, and that the chill time was only a few seconds, depending upon the climatic conditions prevailing at the time of the experiment. This represented the only departure from the procedure originally planned.

While evaluating the ability of the MFSS and MFSA catalysts to promote the liquid oxygen/liquid hydrogen reaction, considerable difficulty was experienced in accurately metering the liquid hydrogen. Turbine meters proved capable of metering the volume of flow, but the accurate determination of liquid temperature, and therefore of liquid density was extremely difficult.

Platinum resistance thermometers were considered, but were unavailable when needed and, in addition, represented a cost item not covered by the contract. The gold-cobalt system, previously described, was considered the best alternate and provided reasonably accurate results.

The second problem associated with metering a constant flow of liquid hydrogen to the injector was that of maintaining constant liquid hydrogen temperature in the delivery line. As chamber pressure built up, the liquid flowrate diminished in a manner consistent with the decrease in driving pressure drop across the injector. This reduction in flowrate resulted in an increase in heat leak to the liquid hydrogen with a resultant warming of the liquid fuel. The result was a progressive decrease in fuel flowrate throughout the course of the run. As a result, the run durations were held to nominally 2 seconds following introduction of the liquid oxygen.

Results

The evaluation of the catalytic ignition characteristics of the oxygen/hydrogen system at liquid hydrogen environmental conditions began as a study quite similar to that conducted at -250 F with gaseous propellants. The objective in these analyses was the correlation of the effects of reactant flowrate and mixture ratio on such characteristics as ignition delay, as measured in the manner described earlier for the 1-inch-diameter hardware studies, and catalyst-reignition capability. However, problems of high chamber pressure spiking and flashback were encountered. These problems were quite severe and the experimental results obtained were such that no correlations were possible. Consequently, effort

was directed toward minimizing the pressure spikes, or eliminating them if possible.

Flashback effects are determined by the presence of extensive catalyst damage by burning. Flashback is usually considered to result from propagation of the flame front back through the catalyst bed toward the injector face along an oxygen-rich streak or zone. This would generally result in a high-temperature streak with corresponding streaky burning of the catalyst bed.

A total of 38 experimental runs were conducted in this phase of the program; however, a number of the runs resulted in unstable ignition, and are not discussed in detail. General comments on these runs are as indicated in Table 10.

The first group of runs (1 through 22, as shown in Table 10) attempted with the liquid propellant system was unsuccessful from a controlled-ignition point of view. High chamber pressure spikes blew out the catalyst bed on a number of tests, and excessive chamber temperatures, caused by low hydrogen flowrates, burned out the catalyst bed in others. In almost every case, however, ignition did occur, indicating the feasibility of liquid propellant ignition.

Following the initial runs (1 through 15), modifications were made in the internal reactor geometry to provide for lower pressure drop through the catalyst bed. Specifically, the catalyst bed retainer plates were replaced with plates and/or screens having a greater fraction of

open area. This resulted in a large decrease in the magnitude of the chamber pressure spikes, and made possible the retention of a catalyst bed in the chamber during all but one of the succeeding runs. This, in turn, permitted later demonstration of catalyst reignition capability.

The test system, as revised, was still largely unsatisfactory because of the pressure spikes generated during each test. Consequently, efforts were directed toward diminishing the extent of the spike and, hopefully, eliminating it. In reviewing the data previously obtained (runs 13, 19, and 23), it was observed that increased propellant flowrate resulted in a decreased pressure spike and thereby allowed for moderately stable runs. In general, it was observed that, at propellant flowrates of approximately 0.30 lb/sec and higher, the chamber pressure spike was reduced to a tolerable level and, in some cases, completely eliminated. The final runs (25 through 38) were conducted at or near this nominal flowrate. Pressure transients typical of the tests conducted are shown in Fig. 31 and 32. (These curves are plots of the oscillographic data.)

Runs 25 through 38, and 34 through 38 are worthy of special comment. Runs 25, and 34 through 36 were made with a single sample of Engelhard MFSA catalyst, and demonstrate the reignition capability of this catalyst in liquid oxygen/liquid hydrogen service. Run 25 was conducted at a mixture ratio of 1.15 o/f, and resulted in a chamber pressure spike and chamber thermocouple burnout. The catalyst bed did not appear to be damaged, however, and was reused in runs 34 through 36. Both runs 34 and 35 resulted in smooth, stable ignition with uniform propagation to a steady-state condition as shown in Fig. 31. Run No. 36, however, exhibited a tendency toward spiking, though not as severe as many previous runs. The catalyst from run 36 appeared undamaged when withdrawn from the reactor.

No precise explanation of the cause of spiking in runs 25 and 36 is given; however, it is believed that propellant accumulation in the mixing zone during the period of ignition lag may have resulted in a chamber pressure spike in run 25. The cause of the long ignition delay (140 ms) could have been the result of inadequate catalyst reduction prior to use. A similar occurrence might have caused the spike observed in run 36; however, the reason for the ignition delay was not the same. A possible explanation for the occurrence of a chamber pressure spike in run 36 is the fact that the propellant flowrate in this run is at a marginal level below which chamber pressure spikes invariably occurred. Although run 35 appears to refute this statement, it should be remembered that liquid hydrogen mass flowrate is extremely difficult to determine, and the steady-state chamber pressure measured in this run tends to indicate that the flowrate in run 35 may have been higher than that for either run 34 or 36. In any event, the flowrate of approximately 0.28 lb/sec for run 36 is believed to be marginally adequate for stable ignition. This opinion is discussed in more detail in a succeeding paragraph.

The reignition capability of the MFSS catalyst in liquid oxygen/liquid hydrogen service is demonstrated by the results of runs 26 through 28 (Fig. 32). These runs were all conducted with a single sample of Engelhard MFSS catalyst, in the same manner as the runs with the MFSA catalyst. The first two runs, 26 and 27, were conducted with relatively high mixture ratios (1.2 o/f) and resulted in thermocouple burnout. The final run of the series was conducted at a moderate mixture ratio (1.0 o/f) and resulted in a chamber pressure spike of 532 psig. It is not implied that the reduced mixture ratio contributed to chamber pressure spiking. It is indicated by the results of measurements of pressure drop through the catalyst bed that catalyst damage may have resulted from the high

temperatures experienced in runs 26 and 27, and caused the ignition delay which, when accompanied by excessive propellant accumulation in the mixing zone, resulted in a chamber pressure spike in run 28.

The results presented as runs 37 and 38 were obtained with the Engelhard DSS catalyst, and demonstrate the inability of this catalyst to promote the liquid-phase reaction of hydrogen and oxygen.

In summary, the results of this phase clearly demonstrate the feasibility of the catalytic ignition concept for the ignition of liquid oxygen/ liquid hydrogen propellants.

Interpretation of Pressure Spiking

The high chamber pressure spiking results are thought to occur because of a higher mass density accumulation in the premix zone, which is ignited with a propagating flashback combustion wave from the catalyst bed. The spiking results are more observable at liquid hydrogen temperatures than they would be at -250 F because of the higher mass densities. The affected accumulated mass in the premix zone at -250 F is only about 0.0046 that of the accumulated mass at liquid hydrogen conditions, and, therefore, the possibility of spiking at -250 F would be considerably less than under liquid hydrogen conditions.

In evaluating the data obtained in runs 26 through 28, and in runs 25, and 34 through 36, it was apparent that operation at higher flowrates tended to ameliorate the chamber pressure spiking problem and, in some instances, to eliminate it completely. An effort was initiated to establish a theoretical basis for this phenomenon. The linear velocity of

the combined reactants in the zone upstream of the catalyst bed for a mass flowrate of 0.3 lb/sec was computed to be approximately 5.0 ft/sec. Consequently, it was considered that, to avoid chamber pressure spiking, the rate of propellant flame propagation must not exceed 5.0 ft/sec. Information presented in Ref. 8 indicated that the flame speed for stoichiometric mixtures of oxygen and hydrogen in the presence of various diluents such as argon, nitrogen, or helium may be as low as 2.25 ft/sec. For the particular mixture ratio used in this program ($\sim$ 1.0 o/f), the reactants may be considered as a stoichiometric mixture of oxygen and hydrogen diluted with 87.5 volume-percent hydrogen. With this as a basis, flame-speed calculations were made by several different available analytical techniques which indicated that, at 60 R and 200 psia, the laminar flame speed is between 3 and 5 ft/sec. Turbulence may increase the flame speed considerably. These results indicate that, to eliminate the tendency toward upstream propagation of the flame front from the catalyst bed and the accompanying chamber pressure spike, the reactant mass flowrate must be in excess of, nominally, 0.28 to 0.3 lb/sec and perhaps higher, for this reactor geometry. For this reason, a flowrate of approximately 0.3 lb/sec is considered a threshold value for satisfactory ignition of liquid oxygen/liquid hydrogen propellants in a 3-inch-diameter reactor.

For the design of other reactors, consideration must be given to the linear throughput velocities in the premix zone and their comparison to propagating flame velocities.

CONCLUSIONS

On the basis of the results presented, the following conclusions are made:

1. The catalytic ignition concept represents an entirely feasible ignition system for liquid oxygen/liquid hydrogen propellant combinations.
2. Both the commercially available Engelhard MFSS and MFSA catalysts are capable of catalytically igniting the liquid oxygen/liquid hydrogen propellant combination.
3. The Shell 8240-128 formulation and the Davison SMR 55-1097-1 formulation offer potential as ignition catalysts for liquid oxygen/liquid hydrogen propellants.
4. None of the other catalysts evaluated in this program appear capable of igniting this liquid propellant combination.
5. Catalytic activity appears to be largely a function of catalyst surface area and noble metal content, as well as manner of catalyst preparation.
6. Ignition lag, as measured in the hardware and by the methods described in this report, is of the order of 20 milliseconds for gaseous propellants and 35 milliseconds for liquid propellants.
7. The liquid hydrogen/liquid oxygen operating condition imposes minimum flowrate design operating conditions for a given reactor volume. The minimum flowrate is determined from a consideration of flame velocities for the premix of H_2/O_2. The throughput velocity must be in excess of the flame velocity.

CONCLUDING REMARKS

The results of this study, obtained with a single basic igniter configuration and only currently available commercial catalyst types, show the catalytic ignition concept as having great potential in liquid oxygen/liquid hydrogen engine systems. Since only one basic engine configuration and only a limited number of catalysts were used in this study, it is likely that these results do not represent an optimum. For this reason, other configurations in both engine and catalyst, should be studied in future applied research programs to increase the flexibility and range of application of the catalytic ignition concept. In addition, various other catalyst metals should be considered.

The most severe limitation exhibited by the catalytic ignition concept is that of the maximum allowable catalyst bed temperature. Before the full potential of the catalytic concept can be realized, this limitation must either be eliminated or circumvented. One means of circumventing the limitation is to modify the propellant injection system to enable injection of supplemental oxygen downstream of the catalyst bed. Such an arrangement would provide for combustion chamber temperatures in excess of 1500 F, but for the most part, would not require catalyst bed temperatures in excess of 1000 to 1200 F.

A future technique which may eliminate the problem of the temperature limitation would be the development of more highly temperature-resistant catalyst substrates, such as thoria or some ceramic. Such an approach to the specific problem at hand, however, presents many difficulties and is not considered to offer any distinct possibility in the near future. Strong recommendation is given, however, to consideration of a

high noble-metal content catalyst formulation, such as the MFSA blend, impregnated on a silica gel substrate. In this manner, the most active formulation can be blended with the highest surface area substrate.

In addition to noble metal-type catalysts, consideration should be given to the possible use of metal oxide catalysts, specifically such oxides as those of cobalt, iron, and nickel. The noble metals are known to suffer loss of activity on oxidation, the noble metal oxide representing an inactive state. The oxides of such metals as cobalt, iron, or nickel are considered to be active for promotion of the oxygen/hydrogen reaction, however, and would not be subject to loss in activity with oxidation. These catalysts would, of course, have greatest application in systems operating with mixture ratios greater than stoichiometric.

REFERENCES

1. NASA Contract NAS7-164, Optimization of Operating Conditions for Manned Spacecraft Engines.
2. RR 63-9, Hydrogen/Oxygen Catalytic Ignition, C. Bendersky, January 1963.
3. RR 64-2, Hydrogen Oxygen Catalytic Ignition Studies for Application to the J-2 Engine, R. Roberts, January 1964.
4. Instruction Manual, Isorpta Analyzer Model 2A, Engelhard Industries, Inc., Newark, New Jersey.
5. ASME Paper No. 50A-45, Orifice Meters With Supercritical Compressible Flow, by R. G. Cunningham, Transactions of the ASME, July 1951, 625-637.
6. ASME, Fluid Meters, Their Theory and Application, Fifth Edition, New York, 1959.
7. Braunauer, Emmett, Teller: JACS 60, 309, 1938.
8. Morgan, G. H., and W. R. Kane: Fourth Symposium on Combustion, 1953, 313.

APPENDIX A

THEORY OF CATALYSIS

INTRODUCTION

The word "catalysis" (Greek: loosen) was first coined by Berzelius in 1835 following a review of a number of apparently diverse observations, including the work of Faraday with hydrogen and oxygen, which had a factor in common: in every case the nature of the reaction was influenced by the presence of a substance that was itself unchanged in the process. Berzelius was of the opinion that a "catalytic" force was manifest, and that certain reactions, including the combination of hydrogen and oxygen on platinum sponge, were brought about under the influence of this force. The concept of the catalytic force has since been discarded, but the term remains to describe all processes in which the rate of reaction is influenced by a substance that remains chemically unaffected. Catalysts may hinder as well as enhance a reaction, but in general, the work is applied to substances that enhance the reaction.

The first catalysts consciously used were the ferments on enzymes reported in 1778. This application was associated with the predecessor of the present-day alcoholic beverage industry. Since that time, and particularly during the period since 1940, the use of catalysts has become widespread in the oil and chemical industries. More recently, research has been initiated toward exploiting catalysts as reaction promotors and burning rate modifiers in the aerospace industry.

CRITERIA OF CATALYSTS

Regardless of the physical or chemical makeup of a catalyst, there are certain characteristics common to all catalytic materials. In general, these characteristics may be stated briefly as follows:

1. The catalyst is unchanged chemically at the end of a reaction.
2. A small amount of catalyst is often sufficient to cause a considerable reaction.
3. The catalyst does not affect the position of equilibrium in a reversible reaction.

While the catalyst is chemically unaltered at the end of a reaction, it may undergo a physical change (e.g., from large crystals to fine powder). Because the catalyst often undergoes a physical alteration, it is evidently involved directly in the mechanism of the reaction, being regenerated in a somewhat different form at the end.

Since the catalyst is not consumed in the course of a chemical reaction, a small amount will often induce large quantities of material to react. In general, however, the rate of a chemical reaction is proportional to the concentration of the catalyst. This is largely a matter of statistics, since the probability of a reaction-producing collision on a catalytic surface increases with the amount of catalytic surface presented.

Furthermore, since the catalyst is unchanged chemically at the end of a reaction, it cannot contribute any energy to the system. Therefore, the second law of thermodynamics requires that the same position of equilibrium should be attained ultimately whether or not a catalyst is used. On this

basis, it is seen that for a reversible reaction, the forward and reverse reactions are enhanced to the same degree. This fact is only of incidental interest in the present program, however, because of the extreme disparity between the rates of the forward and reverse reactions ($2\ H_2 + 0_2 \rightleftharpoons 2\ H_20$). In this instance, the position of equilibrium is shifted so far to the right that the dissociation of water to form hydrogen and oxygen occurs at a negligible rate relative to the forward reaction of H_2 and 0_2 to form water.

In considering the third criterion of catalysis, it is interesting to consider a hypothetical material which is in violation of this third criterion. A gas reaction system that proceeds with a change in volume could be confined in a cylinder fitted with a piston. The catalyst could be placed in a small receptacle within the cylinder in such a fashion that it could be alternately exposed and covered. If the equilibrium position were altered by exposing the catalyst, the volume would change, the piston would move up and down, and a perpetual-motion machine would be available. Such a machine is clearly an impossibility.

REACTION PROMOTION BY CATALYSTS

The ability of a catalyst to promote a reaction is a well-documented phenomenon, and one which has been exploited commercially for many years. The question of the ability of a catalyst to initiate a reaction, however, has been a point of controversy for many years, and it is doubtful that sufficient evidence exists to resolve the question. Reactions are known for which there is no measurable rate in the absence of a catalyst, but there is always some doubt as to whether the reaction is occurring immeasurably slow. The combination of hydrogen and oxygen to form

water is thought to be an example of this type of reaction. On the other hand, there are reactions (e.g., mutarotation of glucose) which, in the absence of a catalyst, appear to have no mechanism by which the reaction can occur; hence, the catalyst is thought to serve both functions of reaction initiation and promotion. This latter argument does not appear to be valid, because for any reaction that can be written there is some mechanism by which it can occur, even if it involves the complete dissociation of the reactant and a reorganization of the atoms. Such a process would involve a very high free energy of activation, and the reaction would therefore take place at a negligible rate. On this basis, the catalyst is a substance which lowers the free energy of activation by allowing the reaction to occur by an alternative mechanism.

While a specific answer to the question of the ability of a catalyst to initiate a chemical reaction is not a purpose of this report, it appears on the basis of information available (Ref.A-1) that in the case of the oxygen/hydrogen reaction, the reaction is merely promoted by the catalyst, not initiated.

Mechanism of Catalysis

To attempt to understand the phenomenon of catalysis, it is necessary to consider the actual mechanisms of heterogeneous catalytic reactions. These reactions can, in general, be broken down into five elementary steps:

1. Diffusion of the reactants to the surface
2. Adsorption of reactants
3. Reaction within the adsorbed layer
4. Desorption of the products of reaction
5. Diffusion of products away from the surface.

Any of these may be the slowest step in the reaction sequence and therefore may determine the over-all reaction velocity. However, the design of reactors is normally such that the diffusion process takes place rapidly and steps 1 and 5 become relatively unimportant. In the event that the catalyst is very highly porous, diffusion to and from the interior surfaces may be such that the reaction appears to be of a complex nature. In general, however, diffusion-controlled reactions are rare, and are generally observed in liquid-phase or mixed-phase reactions involving very high molecular weight compounds (e.g., catalytic hydrogenation of certain polycyclic organic compounds). An observation of the effect of temperature on reaction rate will establish the diffusion-dependence of a reaction. Diffusion is known to have a $T^{1/2}$ temperature dependence, where chemical reaction has a $e^{-\frac{1}{T}}$ dependence. Hence, only reactions having a relatively slight increase in reaction rate with temperature can be considered to be diffusion controlled.

Steps 2 and 4 are generally more rapid than step 3. In fact, step 4 is often indistinguishable from step 3, either because the mechanisms actually are identical, or because the reaction product is weakly adsorbed and is desorbed in the act of its formation. A notable exception to the general rule that steps 2 and 4 occur more rapidly than step 3, is the reaction of hydrogen and nitrogen to form ammonia. In this reaction, the rate of adsorption of nitrogen on the catalytic surface is known (Ref.A-2)to be the rate-determining step. Similarly, in the catalytic decomposition of ammonia over an iron catalyst, the desorption of nitrogen from the surface controls the process.

Since step 4 generally occurs extremely fast or concurrently with step 3, it is only rarely found to be rate controlling. For this reason, steps 2 and 3 are of most interest and will be discussed in detail.

Adsorption of Reactants at the Surface. When two immiscible phases are brought into contact, it is found that the concentration of one phase is greater at the interface than in its bulk. This tendency for accumulation at the surface is called "adsorption." Its occurrence is due to the atoms in any surface being subject to unbalanced forces of attraction, acting perpendicular to the surface plane and therefore possessing a certain unsaturation (unsatisfied valency requirement).

Adsorption always occurs with a decrease in surface free energy, ΔG, and also with a decrease in entropy, ΔS, because by confining a molecule to a thin surface layer, certain degrees of freedom are lost. Hence, use of the equation

$$\Delta G = \Delta H - T\Delta S \qquad (1)$$

shows that ΔH also decreases; i.e., adsorption is always exothermic. An example is the fact that high-surface-area nickel catalysts are seen to be heated when subjected to an atmospheric environment by adsorption of oxygen to the point of ignition, and burn violently.

Although the degree of unsaturation of surfaces may vary widely, and probably continuously, there are only two types of adsorption: physical and chemical. Physical adsorption occurs when the surface is inert in the sense that the valency requirements of the substance are satisfied by bonding with adjacent atoms, and takes place through forces of physical attraction, or van der Waals forces. This type of adsorption is similar to the condensation of a vapor on the surface of its own liquid.

The second type of adsorption, "chemisorption," may occur when the surface is highly unsaturated, having valency requirements not fully satisfied by bonding with nearby atoms. In adsorption, such a surface will

tend to form chemical bonds with the adsorbed substance. Therefore, an essential difference between chemical and physical adsorption is the fact that electron transfer occurs between adsorbent and adsorbate in chemisorption, but not in physical adsorption. Other differences between physical and chemical adsorption are as follows:

1. Heats of adsorption associated with chemisorption may be as high as 100 kcal/mole or higher, where heats of physical adsorption seldom exceed 5 kcal/mole.

2. Physical adsorption generally occurs at temperatures near or below the boiling temperature of the adsorbate, while chemisorption may occur (but not necessarily) at temperatures far above the boiling temperature.

3. Chemisorption, being a chemical reaction, may require an appreciable activation energy, and therefore will proceed at a reasonable rate only above a certain minimum temperature. This is not to say that the temperature is necessarily high, because many surfaces are so unsaturated that chemisorption occurs at extremely low temperatures (Ref. A-3). Physical adsorption, on the other hand, requires no activation energy, and hence should occur quite rapidly at any temperature.

4. Physical adsorption occurs on all surfaces under the correct conditions of temperature and pressure, whereas chemisorption possesses a certain specificity. This is because chemisorption will occur only on an unsaturated surface free of surface contamination.

5. Chemisorption occurs only as a monomolecular layer, whereas physical adsorption has no such limitation.

In considering the relative importance of physical and chemical adsorption, it can be stated virtually unequivocably that no catalytic reactions ever occur on surfaces where neither reactant is chemisorbed. In support of this view is the fact that many catalytic reactions occur at temperatures higher by far than those at which physical adsorption of the reactants occur (e.g., catalytic dehydrogenation of hydrocarbons). Furthermore, even when a reaction occurs at temperatures in the region where physical adsorption might take place, it has been shown that one or more of the reactants undergoes chemisorption at the same temperature.

Also, the forces involved in physical adsorption are quite small compared to the heats and activation energies of chemical reactions. On this basis, physical adsorption would appear to play no part in the promotion of a catalytic reaction. Physical adsorption is, however, of interest in studying the fundamental nature of catalytic surfaces. As a result of such studies, Lennard-Jones (Ref.A-4) has shown theoretically, and experimental studies have since confirmed that a solid surface presents a periodic potential field for an atom or molecule approaching the surface. Furthermore, an adsorbed atom at a metal surface will perturb the periodic potential field (due to the regular lattice of the metal ions) in the neighborhood of the metal surface. This leads to a perturbation in the local energy level in the metal surface next to the adsorbed atom, and an electron in this level, under favorable conditions, will "exchange" with that in the adsorbed atom, leading to an essentially homopolar bond. Taylor (Ref.A-5) has, in similar fashion, referred to such points of maximum potential field perturbation as "active centers." Active centers are known to exist at lines of demarcation or discontinuity on the catalyst surfaces, and are thought to represent points of attachment for the "activated complex," (discussed in the following section) which

eventually decomposes into reaction products. On this basis, the rate of a chemical reaction may be a function of the degree of crystal deformation present in a catalyst. This hypothesis is supported by the fact that the manner of catalytic surface preparation is very important to highest catalyst activity and further by the fact that subjecting a catalyst to temperatures near the annealing temperature of the catalytic metal renders the catalyst virtually inactive.

Chemical Reaction at the Surface. Chemical reactions on the surface of a catalyst may occur by one or more of a number of mechanisms. From a very general point of view, however, the reactant(s), once adsorbed on the surface of the catalyst, undergo a combination to produce an "activated complex," or transition state. Marcelin Ref. A-6) first recognized the existence of the activated complex when he stated that "provided the chemical process does not disturb the equilibrium distribution of the molecules, in phase space, the rate of a process is given by the rate at which molecules cross a critical surface in phase space." Thus, for each process, there is an intermediate configuration situated near the highest point on the most favorable reaction path on the potential energy surface (i.e., the path requiring the least expenditure of energy). The word "near" is used advisedly, because a consideration of the potential energy surface for the reaction between a deuterium atom and a hydrogen molecule shows the D-H-H configuration (activated complex) to lie in a saddle at the top of the potential energy peak, as illustrated in Fig. A-1. In this instance, the position of the activated complex does not represent the minimum activation energy necessary for reaction. The activated complex D-H-H then requires additional energy for reaction. Slater (Ref.A-7)has discussed the manner in which the activated complex is converted into reaction products. The mathematical

form of the results of Slater's theory is not very concise, and for this reason the reader is referred to the original paper for the detailed theoretical equations.

The activated complex is similar to a normal stable molecule in every respect except one. The difference is that one of its vibrational degrees of freedom has been transformed into the translation along the reaction coordinate which results in destruction of the complex. Where the normal nonlinear molecule possesses $3n - 6$ (n = number of atoms) normal modes of vibration, the activated complex has only $3n - 7$. The specific effect of the transformation of a vibrational mode into a translational mode is to cause disintegration, since upon transformation, one of the bonds holding the complex together becomes merely the line of centers between separating fragments. The frequency at which the complex disintegrates may be expressed as

$$\nu = \frac{\overline{E}}{h} \tag{2}$$

Since the mode of decomposition is by hypothesis a thoroughly excited vibration at the temperature T, then $\overline{E} = \overline{kT}$, and

$$\nu = \frac{\overline{kT}}{h} \tag{3}$$

Intuitively, it is seen then that the rate of a chemical reaction occurring on a catalytic surface is proportional to the quantity $\overline{kT}/h$.

By definition, the function of a catalytic surface is to enhance the rate of the desired reaction. In this connection, a calculation can readily be made by making certain simple assumptions to show the ratio

of the rates of reaction of heterogeneous (catalytic) to homogeneous reactions. For a homogeneous (noncatalyzed) reaction between atoms A and B, the specific rate is given as (Ref. A-1).

$$k_{homo} = \frac{\bar{k}T}{h} \frac{Q^{\neq}}{Q_A Q_B} e^{-\frac{E_{homo}}{RT}} \tag{4}$$

where $Q^{\neq}$, Q_A, and Q_B are the partition functions for the activated complex AB, A, and B, respectively. The partition functions of the atoms are made up of the translational contributions only, so that

$$Q_A = \left[2\pi m_A \bar{k}T\right]^{3/2} / h^3 \tag{5}$$

$$Q_B = \left[2\pi m_B \bar{k}T\right]^{3/2} / h^3 \tag{6}$$

The partition function for the activated complex, however, is equal to the product of the translational and rotational contributions,

$$Q^{\neq} = \frac{\left[2\pi(m_A+m_B)\,\bar{k}T\right]^{3/2}}{h^3} \cdot \frac{8\pi^2 \sigma^2 \bar{k}T\, m_A m_B}{h^2 (m_A + m_B)} \tag{7}$$

Therefore, for the homogeneous reaction,

$$k_{homo} = \sigma^2\left[8\pi RT (M_A+M_B) M_A M_B\right]^{1/2} e^{-\frac{E_{homo}}{RT}} \tag{8}$$

where R and M are the products of Avogadro's number times $\bar{k}$ and m, respectively.

For the heterogeneous process,

$$k_{het} = c_s \frac{\overline{kT}}{h} \frac{Q^{\neq}}{Q_A Q_B Q_S} e^{-\frac{E_{het}}{RT}} \qquad (9)$$

The quantities $Q^{\neq}$ and Q_S cannot be evaluated, but since S is part of the surface it can have no translational and probably no rotational energy; hence, the only contribution to the partition function Q_S is vibrational, and is of the order of unity. Similarly, since the activated complex involves S, it will be fixed to the surface and subject to the same limitations as S. Since Q_S and $Q^{\neq}$ are of the order of unity, then $Q^{\neq}/Q_S$ will be essentially unity. Therefore, for the heterogeneous reaction,

$$k_{het} = c_s \frac{\overline{kT}}{h} \cdot \frac{1}{Q_A Q_B} e^{-\frac{E_{het}}{RT}} \qquad (10)$$

The relative rates of reaction are given by the relationship

$$\frac{k_{het}}{k_{homo}} = \frac{c_s}{Q^{\neq}} e^{\Delta E/RT} \qquad (11)$$

Since the translation partition function for unit volume for most molecules lies between 10^{24} and 10^{30}, 10^{27} may be assumed as an average value; and since for 1 cm^2 of surface, c_s can be taken as 10^{15} atoms/cm^2 then

$$\frac{k_{het}}{k_{homo}} = 10^{-12} e^{\Delta E/RT} \qquad (12)$$

On this basis, in order for a catalytic reaction to proceed (at 440 F) at a rate greater than that in the homogeneous case, either the catalytic surface must be increased, or the difference in activation energies must be greater than 28 kcal/mole. In actual catalytic process, the surface exposed to the gases is made as large as possible, and there is also a marked decrease in the activation energy. Typical values for ΔE range from 20 to 40 kcal/mole.

The foregoing has assumed that attaining the activated complex configuration guarantees reaction. This may not, necessarily, be so, and in such instances, a transmission coefficient $\varkappa$, which is numerically equal to unity or less, is added as a simple multiplier in Eq. 4 and 9, and carried through the mathematical development. In this instance, Eq. 12 becomes

$$\frac{k_{het}}{k_{homo}} = \left(\frac{\varkappa_{het}}{\varkappa_{homo}}\right) \tag{13}$$

It is noted that the transmission coefficients for the relative reactions may not be equal.

In considering the transmission coefficient, it is necessary to introduce the concept of the adiabatic course of reaction. For the electronic motion of an atomic system, for instance, in a system corresponding to such an elementary reaction as $D + H_2$, the quantities that determine the relative position of the atomic nuclei act as parameters. As the atoms approach each other, these parameters change, and since the heavy nuclei move much more slowly than the light electrons, it may be assumed that the electrons adapt themselves to new nuclear configurations and pressure almost exactly the character of motion they would have if the nuclei

remained in a given position for an infinitely long period of time. The adiabatic course of a reaction is based upon this assumption. If the assumption is valid, the representative point of the system moves on a potential surface corresponding to a given quantum state of the system. If the point reaches the top of the potential barrier, reaction necessarily occurs. Thus, for adiabatic processes, $\varkappa = 1.0$. Quantum mechanical treatment, however, shows that the assumption of adiabaticity of the elementary reaction may not be true. In fact, it is known that approximately 10 percent of reactions are nonadiabatic. The mathematics of the treatment, as developed by L. D. Landau (Ref. A-8) are not within the scope of this report, but the results illustrate that the process may be nonadiabatic if the total electron spin changes or if some other forbidden transition occurs. The theory of nonadiabatic processes shows that reaching the top of the energy barrier does not guarantee reaction, but that in most cases, the system returns to its original unreacted state. As a result, typical values for the transmission coefficient in nonadiabatic processes are of the order of 10^{-5}. This indicates that if the influence of a catalyst affects a reaction to the extent of changing the mechanism and shifts the reaction act from a nonadiabatic to an adiabatic process, Eq. 13 could be rewritten as

$$\frac{k_{het}}{k_{homo}} = 10^{-7} e^{\Delta E/RT}$$

On this basis, all other effects being equal, an adiabatic catalytic reaction occurring at 440 F (500 K) would proceed faster than the

nonadiabatic homogeneous reaction if the difference in activation energies exceeded 16 kcal/mole. This compares to the similar ΔE of 28 kcal/mole required for adiabatic processes, and could explain why catalytic reactions may occur at a much greater rate than would have been predicted on the basis of assumed activation energies.

NATURE OF THE CATALYST

On the basis of the general thermal, electrical, magnetic, and chemical properties of solid substances, solids may be empirically classified as (Ref. A-9).

1. Metals
2. Ionic crystals
3. Valence crystals
4. Semiconductors
5. Molecular crystals

There are, of course, transition regions between the various types, and actual solids often fall in these regions.

Molecular Crystals

Molecular crystals are unique in this classification in that they are not considered to be catalytic in their action. These molecular crystals are known to have only residual van der Waal's forces and can exert only

very weak forces of attraction. The possibility exists that irradiation in the ultraviolet region may produce metastable excited states sufficient to act as centers of catalytic activity. For this reason, limited study continues on the use of molecular crystals as catalysts.

Metals

Metals are characterized in terms of Pauling's formulation of the resonating-valence-bond treatment, in which the emphasis in terms of catalytic activity is placed on the existence of orbital functions for metallic bond formation. For the transition elements (Sc, Ti, V, etc.), hybridization of the available nine s, p, and d-type orbitals leads to three groups of orbitals: the "atomic" orbitals, principally of d character, the "bonding" orbitals of the "$d^{2.56}\ sp^{2.22}$" type which largely determine cohesion (valence orbitals), and the "metallic" orbitals, principally of the sp type. This model, which has justification in application (Ref. A-10, A-11) suggests that unfilled atomic orbitals provide residual valency in the bulk metal which results in the catalytic activity. The work of Schwab(Ref.A-10) has shown that as the "d character" (fraction of d-orbitals in shell) of a metal increases, the heat of chemisorption, and hence the catalytic activity, decreases. On this basis, it may be possible to predict catalytic activity from a knowledge of the structure of a metal atom. It had earlier been postulated(Ref.A-12) that lattice spacing controls catalytic activity. The observed effect of d-orbitals in controlling catalytic activity would seem to be a contradiction, except that the d character of a metal is known to control lattice spacing.

If d character controls the rate of a catalytic reaction, it would be expected that the order of activities would be

Rh > Pd > Pt > W > Ni > Fe

This expectation is generally borne out in fact, with the notable exceptions being tungsten and palladium. In general, tungsten is of higher activity than predicted, and palladium lower. No satisfactory explanation is given for this apparently diverse observation.

Ionic Crystals

Ionic crystals are characterized by good ionic conductivity at high temperatures, and by good cleavage. They are also distinguished by being made up of a combination of highly electropositive and highly electronegative elements. The surface of an ionic crystal, with its checkerboard of electron acceptors (cations) and centers of high electron density, may serve to bring about the incipient ionization of the activated complex on the surface.

From a quantum mechanics point of view, neglecting coulombic interactions, it could be concluded that the most important centers of catalytic activity would be the cations of the solids, since the atoms with their full electronic complement would not normally be expected to enter into chemical combination. Quantum mechanical exchange forces would then be associated almost entirely with the cations, which may utilize available p, d, or f orbitals of proper energy. This is generally true of most of the heavier metals and particularly of the transition elements with respect to the d-orbitals.

Valence Crystals

Valence crystals are distinguished by large cohesive energies, great hardness, and lack of conductivity. Typical of these substances are diamonds, boron, silicon, germanium, silicon carbide, and boron nitride.

Essentially, each of these substances represents very large inorganic polymers in which each atom exhibits its maximum valence, forming with adjacent atoms primarily covalent bonds. These so-called "insulators" are known to exhibit low catalytic activity, probably because of the unavailability of surface electrons for facilitating the formation of reaction complexes.

Semiconductors

Semiconductors are characterized as substances having an electrical conductivity intermediate between metals and insulating materials. In some instances, this behavior is exhibited by the substance in the pure state, where in others it may be induced by the presence of minute amounts of some impurity or impurities. From a band theory approach, conductivity in an impurity-type semiconductor may result from freeing an electron from a discrete level to an empty band, in which case conduction is by the electron itself, or from promotion of an electron from a filled band to a discrete level. In the latter case, conduction is by the "holes" left in the previously filled band. In a substance in the pure state, if a filled band and an empty band are sufficiently close together, there may be some threshold temperature level above which it may be possible to promote electrons from one band to the other. In this case, conduction is by the electron itself.

Pure metal semiconductors are not, in general, found to have catalytic activity as high as that of impurity semiconductors. Extensive study has been made of the catalytic activity of semiconductors (Ref. A-11, A-13, A-14, A-15) and it is generally believed that the activity of semiconducting materials is associated with the electron levels and lattice defects arising from the impurity centers.

CURRENT HYPOTHESES

The reaction of oxygen with hydrogen is thought to be initiated by the reaction

$$H_2 + O_2 \longrightarrow H + HO_2 \qquad (15)$$

and requires approximately 55 kcal/mole for initiation. The velocity for this reaction is such that, if the oxidation of hydrogen occurred solely by this mechanism, the reaction time might be several days. In reality, the reaction time is of the order of milliseconds; consequently the slow chain initiation reaction is considered to serve only as a trigger mechanism. The reaction then proceeds by means of the following steps:

$$H + O_2 \longrightarrow OH + O \qquad (16)$$

$$OH + H_2 \longrightarrow H_2O + H \qquad (17)$$

$$O + H_2 \longrightarrow OH + H \qquad (18)$$

The complete reaction scheme is then

$$H_2 + O_2 \longrightarrow H + HO_2 - 55 \text{ kcal} \quad \text{(chain initiation)} \qquad (15)$$

$$\left.\begin{array}{l} H + O_2 \longrightarrow OH + O \\ OH + H_2 \longrightarrow H_2O + H \\ O + H_2 \longrightarrow OH + H \end{array}\right\} \quad \text{(propogation of the branched chain)} \qquad \begin{array}{l} (16) \\ (17) \\ (18) \end{array}$$

$$OH + \text{wall} \longrightarrow \quad (19)$$

$$H + \text{wall} \longrightarrow \quad \text{(chain termination)} \quad (20)$$

$$O + \text{wall} \longrightarrow \quad (21)$$

From a catalytic standpoint, reaction 15 is considered to occur on the surface of the catalyst, the energy being supplied by the exothermic heat of chemical adsorption. The reaction products desorb and diffuse into bulk stream, where reactions 16 through 21 occur. It is intuitive that if reactions 19 through 21 proceed at a rate greater than that for reactions 16 through 18, the over-all reaction to produce water as a product results in quenching. Such quenching may be referred to as a gross wall effect. The wall effect can be largely diminished by reducing the amount of wall surface, or, in some instances, by increasing the catalytic surface, thereby increasing the rate of production of free radicals. From a very general standpoint, determined empirically, wall affects do not play a pronounced part in the reaction if the ratio of reactor-diameter/catalyst-pellet-diameter exceeds a value of approximately eight. Such a configuration also serves to minimize the effects of propellant channeling through the catalyst bed voids without contacting the catalyst.

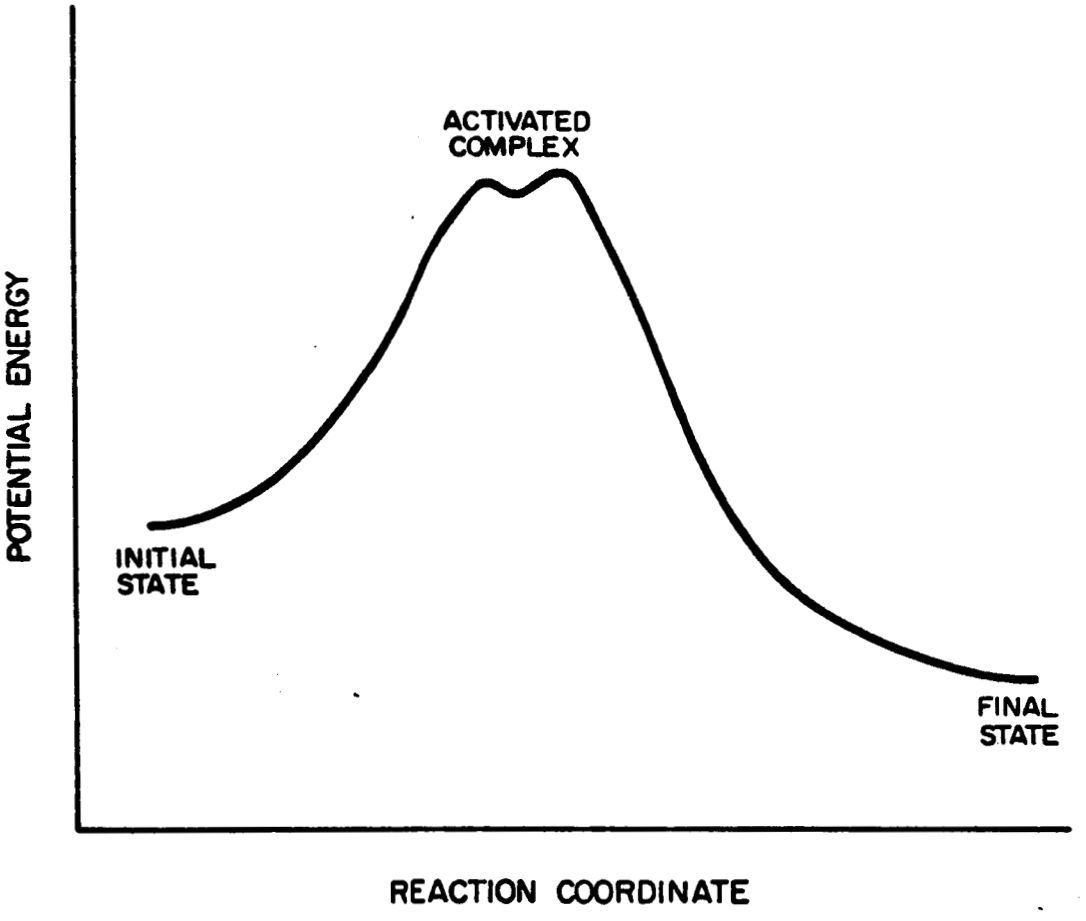

Figure A-1. Potential Energy Diagram Illustrating Relative Location of Activated Complex in Comparison to Initial and Final States of Reactants and Products.

REFERENCES

A-1. Glasstone, S.: Textbook of Physical Chemistry, D. Van Nostrand and Company, Inc., New York, 1946.

A-2. Langmuir, I.: JACS 38, 2221, 1916.

A-3. Roberts, J. K.: Proc. Royal Society, A152, 445, 1935.

A-4. Lennard-Jones, J. E.: Trans. Faraday Society, 28, 332, 1932.

A-5. Taylor, H. S.: Proc. Royal Society (London), A108, 105, 1925.

A-6. Marcelin, A.: Ann. Phys., 3, 158, 1915.

A-7. Slater, N. B.: Proc. Royal Society, A152, 224, 1953.

A-8. Landau, L. D.: Phys. Z. Sovietunion, 1. 88, 1932; 2, 46, 1932.

A-9. Sietz, F.: The Modern Theory of Solids, McGraw-Hill Book Company, New York, 1940.

A-10. Schwab, G. M.: Discussions of the Faraday Society, 8, 166, 1950.

A-11. Dowden, D. A. and P. W. Reynolds: Discussions of the Faraday Society, 8, 184, 1950.

A-12. Beeck, O.: Rev. Modern Physics,17, 61, 1945.

A-13. Garner, W. E. et al.: Proc. Royal Society (London), A211, 472, 1952.

A-14. Parravano, G.: JACS 75, 1452, 1953.

A-15. Huttig, G. F.: Discussions of the Faraday Society, 8, 215, 1950.

APPENDIX B

SUMMARY TRANSLATIONS FROM RUSSIAN LITERATURE

Boreskov, G. K., M. G. Slin'ko, A. G. Filippova, and R. N. Guryanova: Catalytic Activity of Metals of the Fourth Period in the Interaction of Hydrogen With Oxygen, Doklady Akademii Nauk SSSR 94, No. 4, 713-715, 1954.

Boreskov and coworkers studied the catalytic activity of metals of the Fourth Period (Ti, V, Cr, Mn, Fe, Co, Ni, Cu, Zn), with respect to the interaction of hydrogen with oxygen. The catalyst samples were unsupported discrete particles of pure metals, and were reduced in hydrogen at nominally 300 to 500 C prior to use. Analytical determinations were conducted at environmental temperatures from 135 to 302 C. The results of these tests are presented in Table B-1.

From the standpoint of activity, the results demonstrate dramatically that the metals that show potential for promoting the O_2/H_2 reaction are nickel and cobalt.

The program of evaluation was in all cases carried out with relatively low O_2/H_2 mixture ratios, all less than 0.325 by weight.

Boreskov, G. K., M. G. Slin'ko, and A. G. Filippova: Catalytic Activity of Nickel, Palladium, and Platinum in the Reaction of the Oxidation of Hydrogen, Doklady Akademii Nauk SSSR 92, No. 2, 353-355, 1953.

In this paper, the authors reported on analyses of the ability of the indicated metals to promote the O_2/H_2 reaction at low mixture ratios (near 0.33 and lower). Each of the catalytic metals were prepared in the form of a fine wire, nickel as an 0.5-millimeter-diameter wire, and palladium and platinum as 0.1-millimeter-diameter wires. The results are summarized in Table B-2.

The specific rate constant (k) indicated in the table is as used in the equation

$$W = k P_{O_2} S$$

where

W = rate of reaction, moles/hr

k = specific rate constant, cm/hr

P_{O_2} = oxygen content, moles/cu cm

S = actual surface of the catalyst, sq cm

TABLE B-1

SUMMARY RESULTS OF ACTIVITY MEASUREMENTS
FOR METALS OF THE FOURTH PERIOD

Metal	Specific Activity at					Activation Energy, cal/mole
	302 C	254 C	218 C	180 C	135 C	
V	1.24	0.87	- -	0.19	0.065	9,700
Cr	1.5	0.55	0.33	- -	- -	9,500
Mn	- -	2.0	- -	0.25	- -	12,800
Fe						
low 0_2	5.1	3.0	- -	1.9	- -	4,300
high 0_2	1.5	0.5	- -	0.15	0.44	10,000
Co						
low 0_2	85	67	- -	14.1	- -	7,400
high 0_2	- -	- -	- -	4.2	0.17	- -
Ni						
low 0_2	- -	62.6	- -	30.0	- -	5,300
high 0_2	- -	37.4	10.8	2.4	- -	14,000

TABLE B-2

SUMMARY RESULTS OF ACTIVITY MEASUREMENTS
FOR NICKEL, PALLADIUM, AND PLATINUM

Metal	$k \times 10^{-2}$, cm/hr at			Activation Energy, cal/mole
	180 C	140 C	100 C	
Nickel				
at MR < 0.15	12.1	- -	- -	
at MR > 0.15	0.82	0.12	- -	16,000
Palladium	62.5	16.6	4.4	11,200
Platinum	74.0	19.7	5.5	11,000

NOMENCLATURE

ΔG	=	surface free energy change, Btu/lb
ΔS	=	entropy change, Btu/lb-R
ΔH	=	enthalpy change, Btu/lb
ν	=	frequency, sec^{-1}
m	=	number of molecules
n	=	number of atoms
$\overline{E}$	=	decomposition energy (quantum)
h	=	Planck's constant, 6.624×10^{-27} erg sec
T	=	temperature, K
$\overline{k}$	=	Boltzmann constant = 1.380×10^{-16} erg/K
k_{homo}	=	reaction velocity constant for an uncatalyzed homogeneous reaction
$Q^{\neq}$	=	partition function for the activated complex AB
Q_A	=	partition function for the reactant A
Q_B	=	partition function for the reactant B
E_{homo}	=	activation energy for the uncatalyzed homogeneous reaction
R	=	gas constant = 1.987 cal/gm-mole K
M_A	=	molecular weight of A, gm/gm-mole
M_B	=	molecular weight of B, gm/gm-mole
σ	=	molecular collision diameter, cm
k_{het}	=	reaction velocity constant for the heterogeneous reaction
c_s	=	atoms/sq cm of surface
Q_s	=	partition function for the surface site
E_{het}	=	activation energy for the heterogeneous reaction
ΔE	=	$E_{homo} - E_{het}$
κ	=	transmission coefficient, dimensionless

TABLE 1

INVESTIGATION OF CATALYTIC IGNITION OF OXYGEN/HYDROGEN SYSTEMS

Code	Type	Substrate	Size and Shape	Manufacturer
DS	Palladium	Alumina	1/8-inch spheres	Engelhard Industries, Inc.
DSS	Palladium	Alumina	1/8-inch spheres	"
MFSS	Platinum-Rhodium	Alumina	1/8-, 1/4-inch spheres, cylinders	"
MFSA	Platinum-Rhodium-Lead	Alumina	1/8-inch spheres	"
G-43B	Platinum	Alumina	1/4-inch tablets	Girdler Chemical Company
G-46	Palladium	Alumina	3/16-inch tablets	"
G-55	Promoted Palladium	Alumina	1/8-inch tablets	"
G-58	Palladium	Alumina	3/16-inch tablets	"
G-68	Promoted Palladium	Alumina	1/8-inch tablets	"
C-54	Palladium	Alumina	3/16-inch spheres	Catalysts and Chemicals, Inc.
C-IV	Nickel	"Mineral Support"	1/8-inch tablets	Universal Oil Products
A-M	Platinum	Nickel-alloy	Robbon mat-plug	Catalytic Combustion Company
A-100S	Platinum	Alumina	1/8-inch cylinders	Houdry Process Corporation
A-200SR	Platinum	Alumina	3/16-inch cylinders	"

TABLE 1

(Continued)

Code	Type	Substrate	Size and Shape	Manufacturer
A-25Z	Chromia	Alumina	1/8-inch cylinders	Houdry Process Corp.
B-100S	Palladium	Alumina	1/8-inch cylinders	"
Pd-K	Palladium	Kaolin	0.15-inch spheres	"
SMR 55-1097-1	Platinum	Silica Gel	~1/16-inch granules	Davison Chemical Company
SMR 55-1097-2	Platinum	Alumina	1/8-inch tablets	"
SMR 55-1097-3	Platinum	Alumina	1/8-inch tablets	"
SMR 55-1097-4	Platinum	Silica Gel	1/8-inch tablets	"
8240-168	Noble Metal	Alumina	1/8-inch cylinders	Shell Development Company

TABLE 2

SPECTROGRAPHIC ANALYSIS OF CATALYSTS

Catalyst Metal	Composition, weight percent *				
	MFSS	MFSA	DS	DSS	A-200SR
Aluminum	48	52	47	48	52
Silicon	4.0	0.096	4.0	3.6	0.035
Palladium	0.001	nil	0.29	0.27	nil
Platinum	0.26	0.13	nil	nil	0.14
Rhodium	0.58	0.14	nil	nil	nil
Sodium	0.23	trace	0.92	0.61	trace
Calcium	0.027	0.001	0.023	0.021	0.003
Lead	nil	0.13	nil	nil	nil
Nickel	nil	nil	nil	nil	nil
Magnesium	nil	nil	nil	nil	nil

*The difference between the sum total percentages shown and 100, represent the amount of oxygen and trace impurities contained within the catalyst. This oxygen exists in the form of metal oxides (e.g., Al_2O_3, SiO_2 rather than Al or Si).

The underlined numbers represent items which contribute significantly to the performance of the catalyst.

TABLE 3

CATALYST SURFACE CHARACTERISTICS

Catalyst	Type	Surface Characteristic		
		Surface Area, m^2/gm	Pore Volume, ml/gm	Average Pore Diameter, Å
Engelhard Industries, Inc.				
DS	Pd	230	0.24	42
DSS	Pd	224	0.30	54
MFSS	Pt-Rh	251	0.28	44
MFSS*	Pt-Rh	191	0.21	44
MFSA	Pt-Rh-Pb	460	0.58	50
MFSA**	Pt-Rh-Pd	243	0.25	42
Houdry Process Corporation				
A-100S	Pt	120	0.13	43
A-220SR	Pt	238	0.32	53
Pd-K	Pd	141	0.18	51
Girdler Chemical Company				
G-55	Promoted Pd	288	0.38	52
G-58	Pd	10	0.01	4
G-68	Promoted Pd	290	0.36	49
G-68**	Promoted Pd	216	0.30	56
Universal Oil Products				
C-IV	Ni	189	0.14	29
Catalytic Combustion Company				
A-M	Pt	18	0.007	2
Davison Chemical Company				
SMR 55-1097-1	Pt	566	0.25	17.7
SMR 55-1097-4	Pt	542	0.22	16.2
Shell Development Company				
8240-168	Noble Metal	216	0.30	56

*Used
**Calcined

TABLE 4

RESULTS OF CATALYTIC ACTIVITY TESTS*

Catalyst	Pretreatment	Pre-environmental Temperature, F	Percent Conversion	Remarks
None	....	77	0	Blank
MFSA	None	77	95.7	
MFSA	None	-112	87.4	
MFSA	None	-300	63.7	
MFSA	3	77	97.0	
MFSA	3	-112	96.0	
MFSA	3	-300	78.3	
MFSS	None	77	91.7	1/8-inch spheres
MFSS	None	77	92.2	Repeat
MFSS	None	77	89.5	1/8-inch cylinders
MFSS	None	77	83.6	Used 1/8-inch spheres
MFSS	None	32	89.0	1/8-inch spheres
MFSS	None	-112	87.5	
MFSS	None	-300	24.2	

*O_2/H_2(wt) = 0.33; 2-minute H_2 lead; 5-gm catalyst; 10-minute run duration; maximum theoretical water = 0.396 gram; ambient gases

3 = Calcined in a muffle furnace for 2 hours at 1110 F

1 = Heated for 2 hours in hydrogen at 680 F

TABLE 4

(Continued)

Catalyst	Pretreatment	Pre-environmental Temperature, F	Percent Conversion	Remarks
MFSS	1	77	92.8	
MFSS	1	-112	76.2	1/8-inch spheres acti-
MFSS	1	-300	24.5	vated in situ
DSS	None	77	94.5	
DSS	None	77	91.8	Used sample
DSS	None	-112	92.7	
DSS	None	-300	22.7	
A-200SR	None	77	85.6	
A-200SR	None	-112	66.0	
A-200SR	None	-300	9.6	
DS	None	77	93.5	
DS	None	77	93.1	Used sample
DS	None	-112	86.3	
DS	None	-300	19.0	

1 = Heated for 2 hours in hydrogen at 680 F

TABLE 4

(Continued)

Catalyst	Pretreatment	Pre-environmental Temperature, F	Percent Conversion	Remarks
8240-168	None	77	89.5	
8240-168	None	-112	83.2	
8240-168	None	-300	28.3	
SMR 55-1097-1	None	77	99.9	
SMR 55-1097-1	None	-112	34.4	
SMR 55-1097-1	None	-300	12.2	
G-68	None	77	1.8	
G-68	2	77	67.0	
G-68	2	-112	19.8	
G-68	2	-300	3.3	
A-M	None	77	6.8	
A-M	1	77	6.8	Activated in situ
SMR 55-1097-4	None	77	8.8	
G-55	None	77	3.8	
G-55	2	77	5.6	

1 = Heated for 2 hours in hydrogen at 680 F

2 = Calcined in air for 2 hours at 680 F

TABLE 4

(Continued)

Catalyst	Pretreatment	Pre-environmental Temperature, F	Percent Conversion	Remarks
A-100S	None	77	3.3	
B-100S	None	77	2.7	
G-46	None	77	2.3	
A-25Z	None	77	2.3	
G-43B	None	77	2.0	
Pd-K	None	77	1.9	
C-54	None	77	0.9	
G-58	None	77	0.6	
SMR 55-1097-2	None	77	0.0	
SMR 55-1097-3	None	77	0.0	

TABLE 5

CATALYST CRUSH STRENGTH

Catalyst	Crush Strength, pounds		
	Spheres	Cylinders	
		Vertical	Horizontal
Engelhard Industries, Inc.			
DS			
Fresh	21		
Used	20		
DSS			
Fresh	26		
Used	12		
MFSS			
Fresh	27		
Calcined	23		
Sauna*	17		
MFSA			
Fresh	12		
Calcined	10		
Girdler Chemical Company			
G-43B		> 200	43
G-46		> 200	43
G-55			
Fresh		> 200	17
Calcined		73	20
G-58		> 200	112
G-68		> 200	20
Catalysts and Chemicals, Inc.			
C-54	52		
Universal Oil Products			
C-IV		20	8

*Catalyst previously subjected to thermal shock treatment, as described earlier.

TABLE 5
(Continued)

Catalyst	Crush Strength, pounds		
	Spheres	Cylinders	
		Vertical	Horizontal
Houdry Process Corporation			
A-100S		8	11
A-200SR			
Fresh		12	12
Calcined		11	13
B-100S		6	11
Pd-K	20		
Shell Development Company			
8240-168		36	19
Davison Chemical Company			
SMR 55-1097-1	10		
SMR 55-1097-2		88	14
SMR 55-1097-3		> 200	11
SMR 55-1097-4	9		

TABLE 6

THERMAL SHOCK RESISTANCE*

Catalyst	Form	Effect
Engelhard Industries, Inc.		
DS	1/8-inch spheres	None
DSS	1/8-inch spheres	None
MFSS	1/8-inch spheres	None
MFSS	1/8-inch cylinders	None
MFSS	1/4-inch spheres	About half shattered
MFSS	1/4-inch cylinders	A few pellets chipped
MFSA	1/8-inch spheres	None
Girdler Chemical Company		
G-43B	1/4-inch tablets	None
G-46	3/16-inch tablets	None
G-55	1/8-inch tablets	Turned nearly white
G-58	3/16-inch tablets	None
G-68	1/8-inch tablets	Turned black
Houdry Process Corporation		
A-100S	1/8-inch cylinders	None
A-200SR	3/16-inch cylinders	None
B-100S	1/8-inch cylinders	None
Pd-K	0.15-inch spheres	None
Catalysts and Chemicals, Inc.		
C-54	3/16-inch spheres	None
Universal Oil Products		
C-IV	1/8-inch tablets	None

*Catalyst samples immersed in liquid nitrogen, allowed to reach thermal equilibrium, placed in a muffle furnace at ~1825 F for 10 minutes, then returned to liquid nitrogen bath.

TABLE 7

EFFECT OF THE THERMAL SHOCK TREATMENT

ON CATALYTIC ACTIVITY

Catalyst	Percent Conversion					
	25 C		-80 C		-185 C	
	Untreated	Thermal Shock Treated	Untreated	Thermal Shock Treated	Untreated	Thermal Shock Treated
MFSA	95.7	94.5	87.4	64.2	63.7	17.7
MFSS	92.2	94.6	87.5	83.1	24.2	8.2
DSS	94.5	83.0	92.7	3.7	22.7	2.7
A-200SR	85.6	63.6	66.0	19.5	9.6	5.9

TABLE 8

EFFECT OF THE THERMAL SHOCK TREATMENT
ON SURFACE CHARACTERISTICS

Catalyst	Surface Area m^2/g		Pore Volume, ml/g		Average Pore Diameter, Å	
	Untreated	Thermal Shock Treated	Untreated	Thermal Shock Treated	Untreated	Thermal Shock Treated
MFSA	460	172	0.58	0.22	50	51
MFSS	255	264	0.28	0.49	44	59
DSS	224	241	0.30	0.40	54	50
A-200SR	238	142	0.32	0.22	53	62

TABLE 9

SUMMARY OF RESULTS WITH GASEOUS PROPELLANTS

Catalyst and Run No.	Environmental Temperature, F		Total Flowrate, lb/sec	Mixture Ratio, o/f	Chamber		Ignition Lag, milliseconds					
							Chamber Pressure			Chamber Temperature		
	Catalyst	Propellant			Temperature, F	Pressure, psig	First Indication	63.2 Percent of SS	90 Percent of SS	First Indication	62.3 Percent of SS	90 Percent of SS
MFSA-1	-250	-250	0.0125	1.05	1549	80	20	74	900	40	1270	3200
-2	-250	-250	0.0181	0.95	1466	122	20	980	1700	36		
-3	-250	-240	0.0228	0.93	1409	166	22			28		
-4	-250	-244	0.0295	0.92	1402	175	26			40		
-5	-250	-244	0.0288	0.99	cold	77	No ignition			No ignition		
-6	-250	-256	0.0065	0.91	1400	25	30	4200	6700	40	980	2100
-7	-250	-240	0.0287	0.94	1444	87	28			40		
-8	-250	-250	0.0195	0.65	cold	20	No ignition			No ignition		
-9	-250	-252	0.0124	0.98	1480	80	20			35		
-10	-250	-256	0.0095	1.21	1825	47	22	1870	3450	30	1400	2650
-11	-250	-180	0.0144	1.22	1862	78	20			35		
-12	-250	-60	0.0203	1.18	1779	130	18	88	2400	36	900	2800
-13	-250	-8	0.0295	1.15	1692	175	18			32		
-14	-250	-62	0.0327	1.22	1848	ND	28	700	1300	41	550	900
-15	-250	-48	0.0323	1.20	1848	116	34			40		
-16	-250	+4	0.0311	1.14	1665	101	30	1030	2200	34	600	1010
-17	-250	-252	0.0226	1.13	1656	53	26			36		
-18	-250	-258	0.0149	1.13	1652	32	20			41	800	1800
-19	-250	-205	0.0084	1.15	1710	ND	20	2800	4700	32		
-20	-250	-256	0.0149	1.13	1647	ND	22			36		
MFSS-1	-250	-245	0.0140	0.95	1488	76	20	73	2200	25	560	2000
-2	-250	-245	0.0173	1.03	1199t	76	20			28		
-3	-250	-245	0.0186	0.94	cold	45	No ignition			No ignition		
-4	-250	-247	0.0103	0.98	1523	58	20			35		
-5	-250	-247	0.0122	0.91	1207	55	24			30		
-6	-250	-250	0.0111	1.04	1532	58	20			30		
-7	-250	-256	0.0124	1.04	1603	ND	40	500	2200	85	1200	2800
-8	-250	-256	0.0176	1.05	1688	ND	20			30		
-9	-250	-253	0.0272	1.07	1688	90	22			30		
-10	-250	-248	0.0376	1.08	cold	25	No ignition			No ignition		
-11	-250	-250	0.0274	1.06	1674	ND	36	1300	2450	70	1200	2100
-12	-250	-248	0.0371	1.07	cold	ND	No ignition			No ignition		
-20	-250	-240	0.0253	0.86	1270	148	22			30		
-21	-250	-262	0.0050	0.86	1293	30	20	3600	10000	35	4000	10000
-22	-250	-252	0.0104	0.86	1270	ND	26	1450	3000	40	1200	3200
-23	-250	-252	0.0109	0.98	1440	ND	25	700	2050	30	520	1200
-24	-250	-252	0.0107	1.02	1580	ND	20			35		
-25	-250	-250	0.0145	1.02	1540	78	27			40		
-26	-250	-250	0.0170	1.02	1540	95	28			40		
-27	-266	-246	0.0170	1.02	1550	95	18			40		

ND—no data
t —transient
SS--steady state

TABLE 9
(Continued)

Catalyst and Run No.	Environmental Temperature, F		Total Flowrate, lb/sec	Mixture Ratio, o/f	Chamber		Ignition Lag, milliseconds					
							Chamber Pressure			Chamber Temperature		
	Catalyst	Propellant			Temperature, F	Pressure, psig	First Indication	63.2 Percent of SS	90 Percent of SS	First Indication	62.3 Percent of SS	90 Percent of SS
MFSS-28	-250	-250	0.0222	1.04	1630	128	19	800	1500	30	570	1600
-29	-250	-246	0.0285	1.06	500t	85t	18			40		
-30	-248	-250	0.0121	1.05	1558	90	18	1350	2200	65	1700	2300
-31	-250	-250	0.0118	1.11	1700	70	20			35		
-32	-260	-246	0.0116	1.0	1460	70	28			35		
-33	-250	-237	0.0077	0.93	cold	ND	No ignition			No ignition		
-34	-250	-240	0.0077	0.93	cold	ND	No ignition			No ignition		
-35	-250	-236	0.0120	1.03	1600	65	25			40		
DSS-1	-250	-250	0.0112	0.97	cold	36	No ignition			No ignition		
-2	-272	-256	0.0119	1.05	1720	45	18	1650	3700	70	2550	3700
-3	-278	-260	0.0159	1.04	cold	28	No ignition			No ignition		
-4	-250	-260	0.0119	1.05	cold	20	No ignition			No ignition		
-5	-250	-263	0.0123	1.05	1422	48	20			40		
-6	-280	-260	0.0183	1.06	cold	52	No ignition			No ignition		
-7	-250	-266	0.0187	1.01	cold	37	↓					
-8	-250	-250	0.0288	1.30	cold	25						
A-200SR-1	-250	-250	0.0109	1.03	cold	30						
-2	-250	-260	0.0137	1.25	cold	30						
-3	-250	-260	0.0137	1.28	cold	28						
-4	+71	-20	0.0135	1.29	300t	28t	200					
-5	-99	-25	0.0251	0.96	cold	37	No ignition					

ND--no data
t —transient
SS--steady state

TABLE 10

SUMMARY OF RESULTS WITH LIQUID PROPELLANTS

Run No.	Catalyst	Environmental Temperature, F			Total Flowrate, lb/sec	Mixture Ratio, o/f	Chamber		Ignition Lag, milliseconds			Remarks
		Catalyst Bed	Liquid Hydrogen	Liquid Oxygen			Temperature, F	Pressure, psig	First Indication	63.2 Percent of SS	90 Percent of SS	
1	MFSS	-420	-420	-293	0.242*	0.936*	2280*	75	35			LH_2 flow transient caused bed burnout
2	MFSS	-420	-420	-293	0.150*	0.83*	380*	70*	45			P_c spike blew out LH_2 manifold seals
3	MFSS	-427	-427	-291	0.200*	1.85*	----	----	45			P_c spike blew out catalyst bed
4	MFSS	-408	-408	-297	0.187	1.35	----	----	47			P_c spike
5	MFSS	-440	-440	-297	0.260	0.25	cold	0	No ignition			Mixture ratio too low**
6	MFSS	-415	-415	-297	0.223	1.12	cold	0	No ignition			Same catalyst as Run No. 51**
7	MFSS	-426	-426	-297	0.174	1.09	cold	0	No ignition			Same catalyst as Run No. 52**
8	MFSS	-421	-421	-297	0.097	0.865	cold	0	No ignition			Same catalyst as Run No. 53**
9	MFSA	-423	-423	-300	0.402*	3.40*	----	70	20			LH_2 flow transient caused bed burnout
10	MFSA	-426	-426	-300	0.380*	2.8*	2280*	62	20			Same as Run No. 55
11	MFSA	-426	-426	-300	0.295*	2.5*	2280*	40*	60			Same as Run No. 55
12	MFSA	-415	-415	-300	0.102	3.7*	2280*	40*	180			Same as Run No. 55
13	MFSA	-423	-423	-297	0.179	3.0*	2280*	117*	2408			P_c spiked to 117 psig
14	MFSA	-423	-423	-297	0.141	3.5*	***	64*	2184			LH_2 flow transient caused bed burnout
15	MFSA	-423	-423	-290	0.169	1.86*	cold	0	No ignition			
16	MFSA	-423	-423	-290	0.173	1.75*	cold	0	No ignition			
17	MFSA	-437	-437	-291	0.140	3.7*	cold	0	No ignition			LH_2 flow transient caused bed burnout
18	MFSS	-430	-430	-291	0.078	0.95		50*	1460			P_c spike blew out bed
19	MFSS	-430	-430	-291	0.091	0.72	***	380*	2775			P_c spiked to ~ 380 psig
20	MFSS	*	*	-291	0.166*	1.10*	cold	0	No ignition			LH_2 temperature unstable
21	MFSS	*	*	-291	0.105*	0.88*	cold	0	No ignition			LH_2 temperature unstable
22	MFSS	-430	-430	-291	*	*	cold	0	No ignition			LO_2 flowrate unstable

*Transient
**Catalyst probably contaminated by either wet or oily purge gas
***Thermocouple failure

TABLE 10

(Continued)

Run No.	Catalyst	Environmental Temperature, F			Total Flowrate, lb/sec	Mixture Ratio, o/f	Chamber		Ignition Lag, milliseconds			Remarks
		Catalyst Bed	Liquid Hydrogen	Liquid Oxygen			Temperature, F	Pressure, psig	First Indication	63.2 Percent of SS	90 Percent of SS	
23	MFSS	-430	-430	-291	0.343	1.54	2280*	60	53			P_c spiked to 80 psig, mixture ratio too high
24	MFSA	-430	-430	-298	0.346	1.51	***	650	55			P_c spiked to 650 psig
26	MFSS	-434	-434	-298	0.340	1.21	***	75	95	2000	2500	
27	MFSS	-430	-430	-298	0.350	1.21	***	80	44	1400	1900	Same catalyst bed
28	MFSS	-426	-426	-298	0.321	1.00	1460*	532	70	390	730	; P_c spiked to 532 psig
29	MFSS	-423	-423	-291	0.244	1.00	cold	0	No ignition			Unaware catalyst was lost on previous run
30	MFSA	-437	-437	-298	0.260*	1.13*	cold	0	No ignition			Catalyst probably iced over
31	MFSA	-430	-430	-298	0.251	0.66	----	57	No ignition			P_c spike
32	MFSA	-430	-430	-298	0.237	0.60	cold	0	No ignition			Mixture ratio too low
33	MFSA	-432	-432	-298	0.272	0.88	cold	0	No ignition			
25	MFSA	-427	-427	-298	0.340	1.15	***	390	140	1050	1900	
34	MFSA	-430	-430	-291	0.296	0.88	1200	75	35	1450	1750	
35	MFSA	-430	-430	-298	0.272	0.75	1100	85	40	1600	2200	Same catalyst bed
36	MFSA	-430	-430	-298	0.277	0.78	1150	72	150	1020	1900	; 96-psig P_c spike
37	DSS	-432	-432	-291	0.305	0.96	cold	0	No ignition			No ignition
38	DSS	-432	-432	-298	0.291	0.81	cold	0	No ignition			No ignition

*Transient

***Thermocouple failure

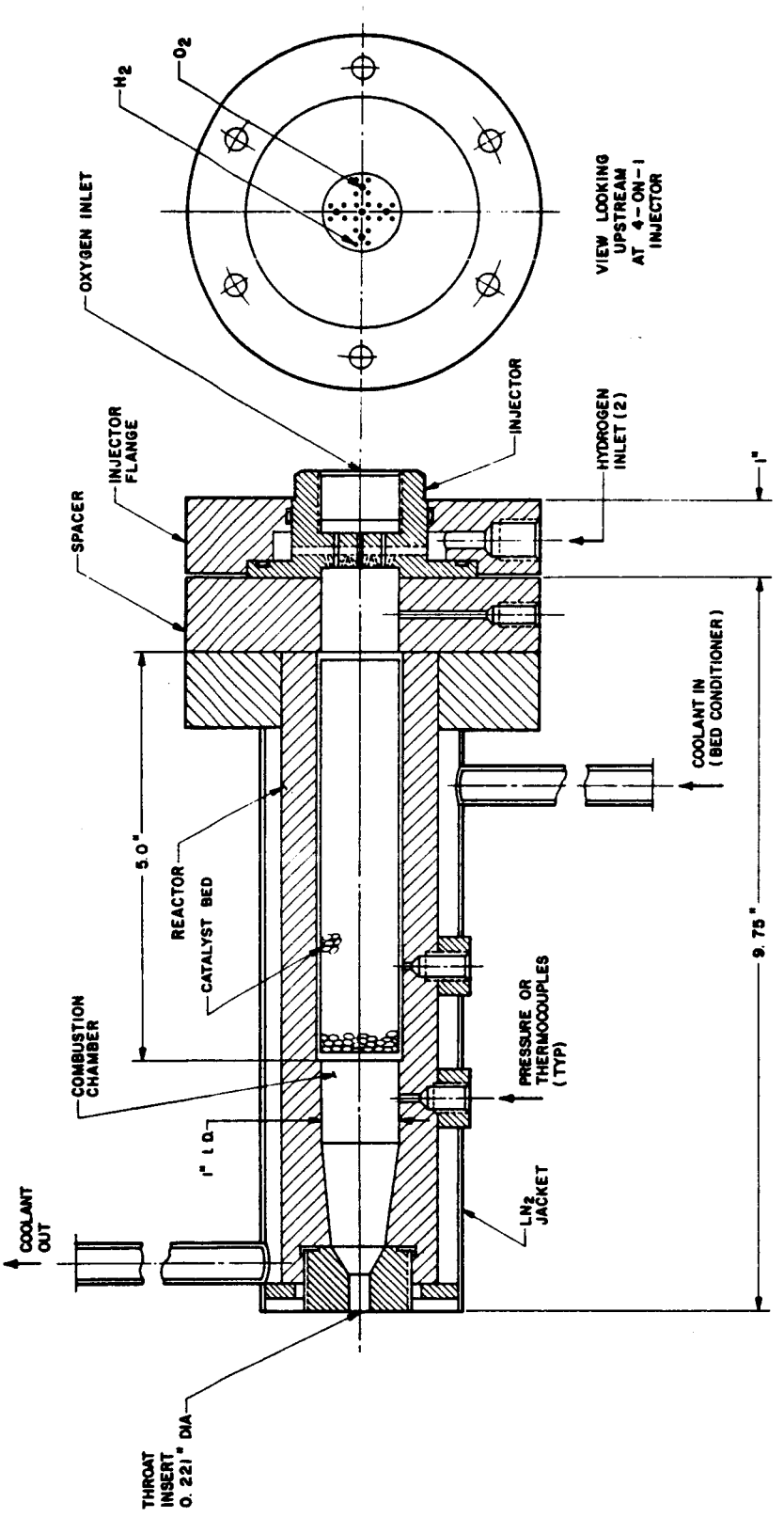

Figure 1. Schematic of Reactor Illustrating 4-on-1 Injection System and Component Parts of the Reaction Chamber

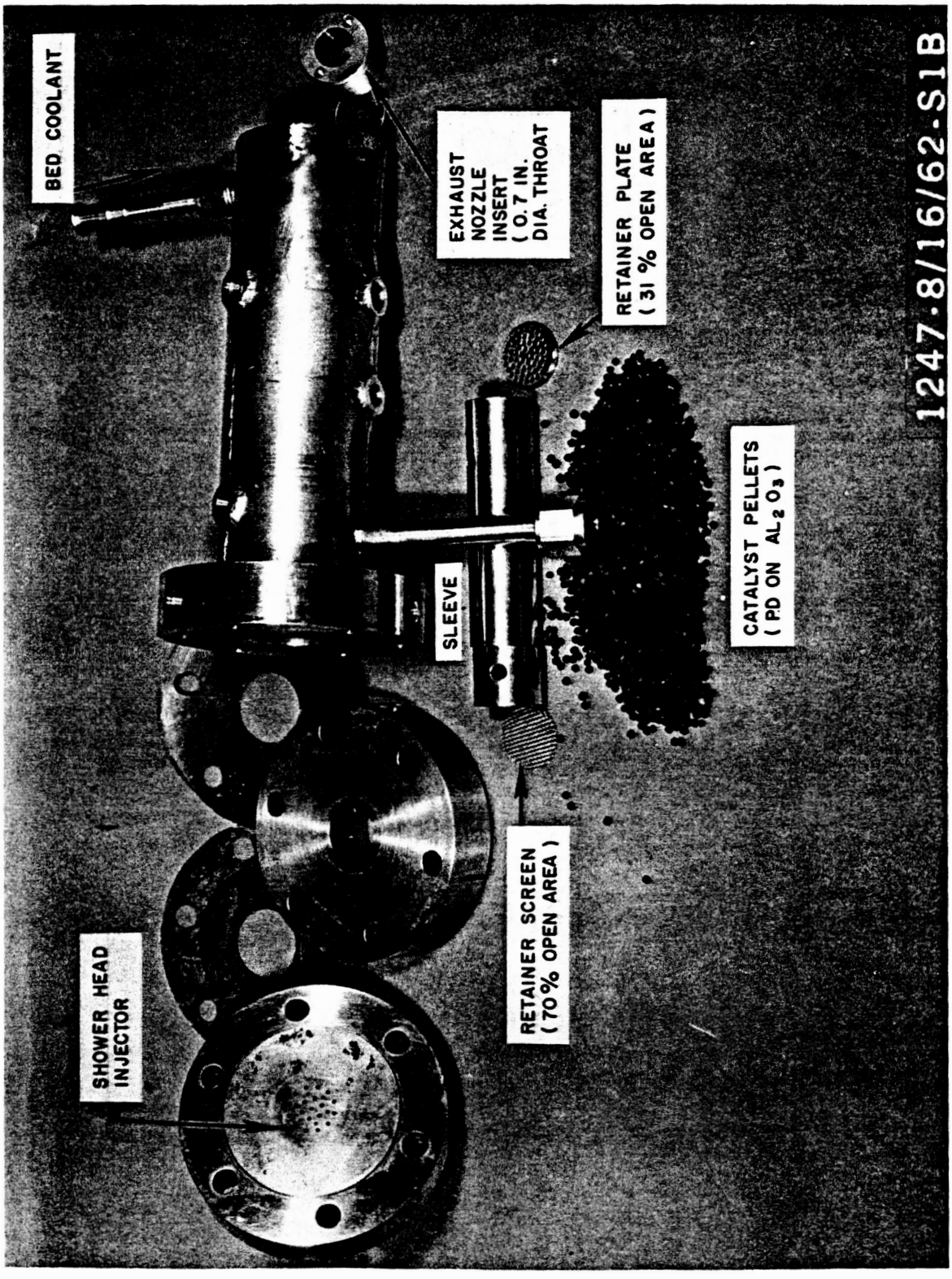

Figure 2. Photograph of 1-inch-Diameter Combustor Disassembled to Show Major Components - 5-inch Catalyst Bed Configuration.

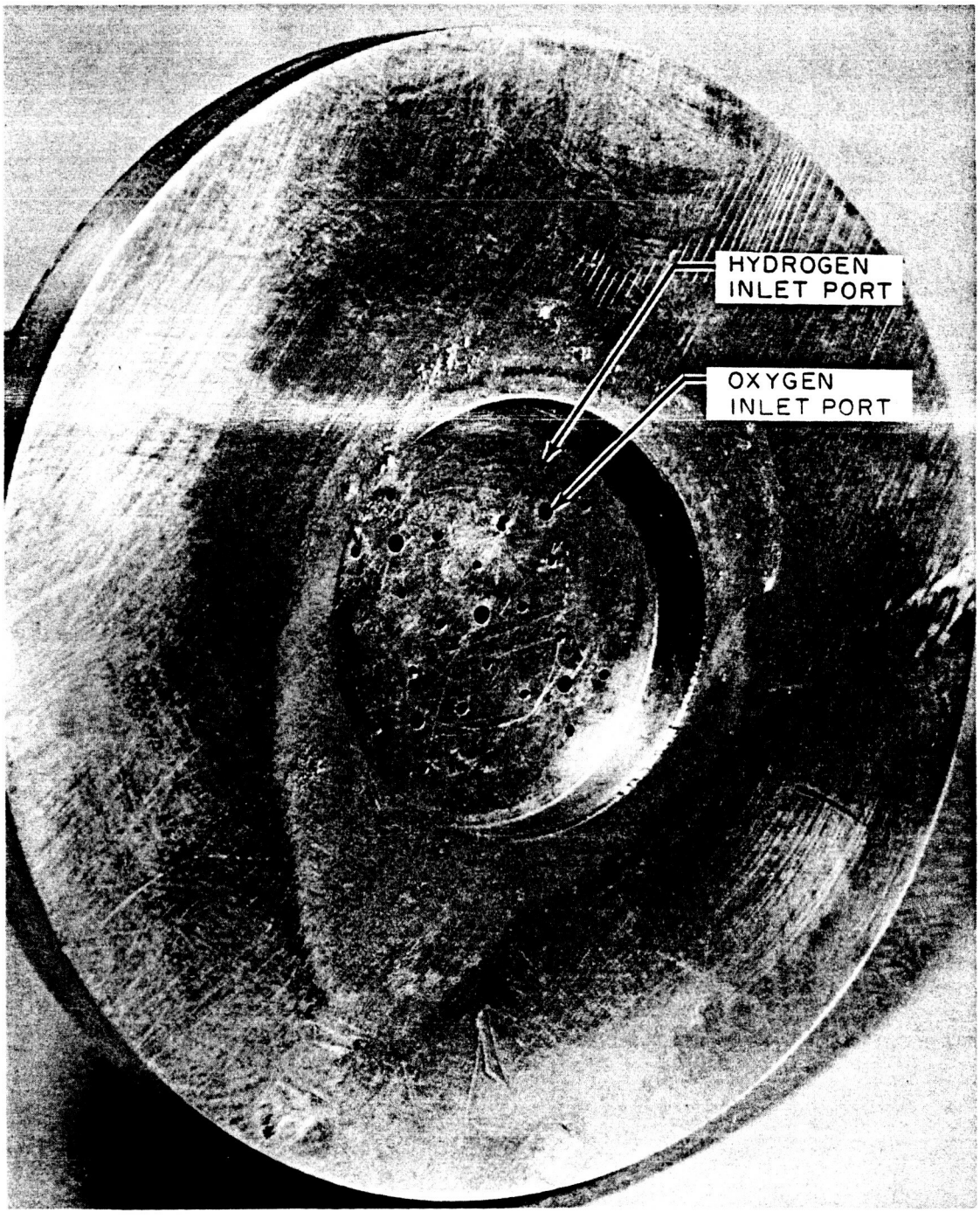

Figure 3. Illustration of 4-on-1 Injector Showing Relative Positions of Fuel and Oxidizer Injection Ports

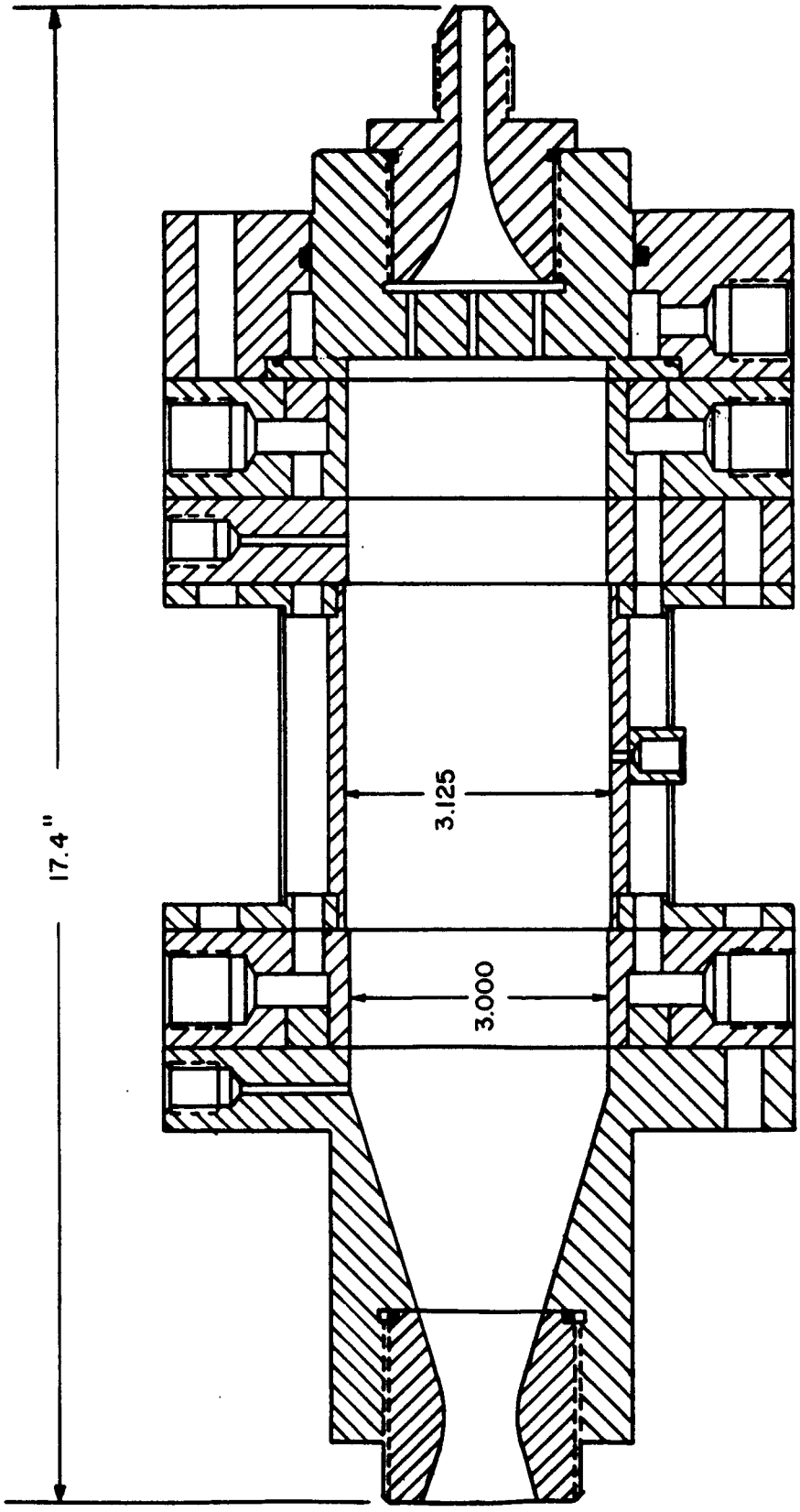

Figure 4. Schematic of Assembled Reactor

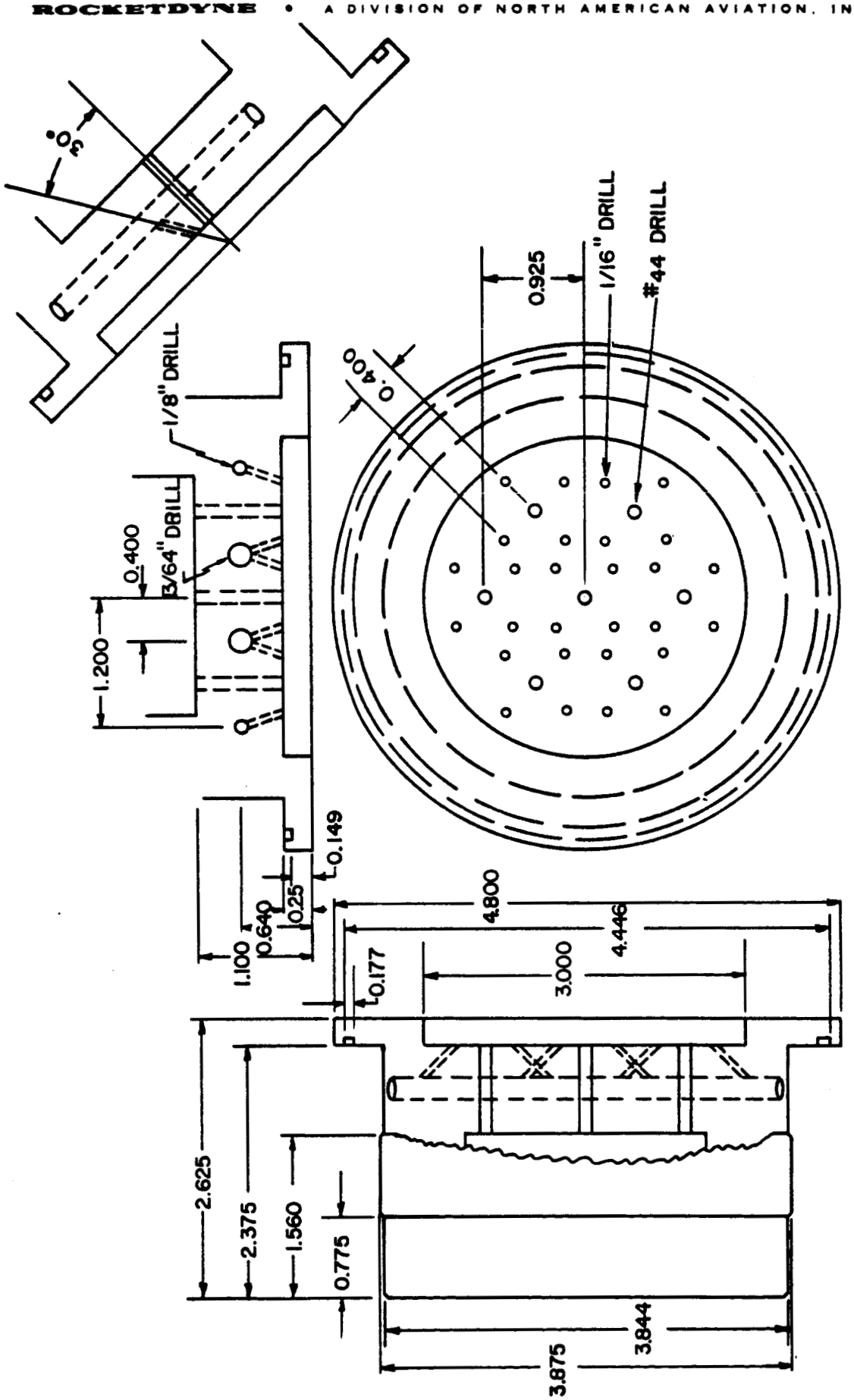

Figure 5. Injector Design Illustrating 7-element, 4-on-1 (H_2 on O_2) Impinging Stream Injector Pattern

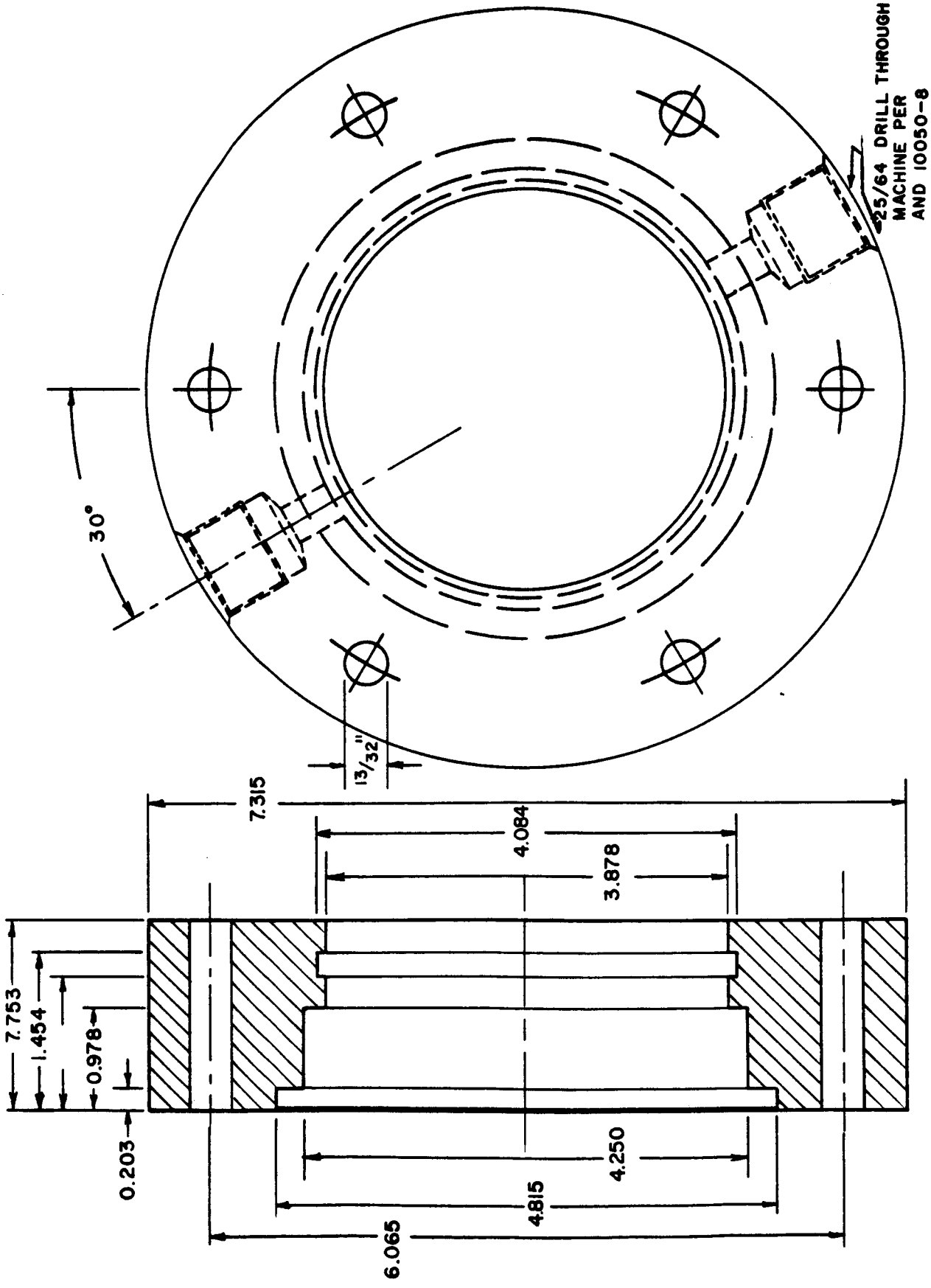

Figure 6, Injector Retainer Plate and Hydrogen Propellant Manifold

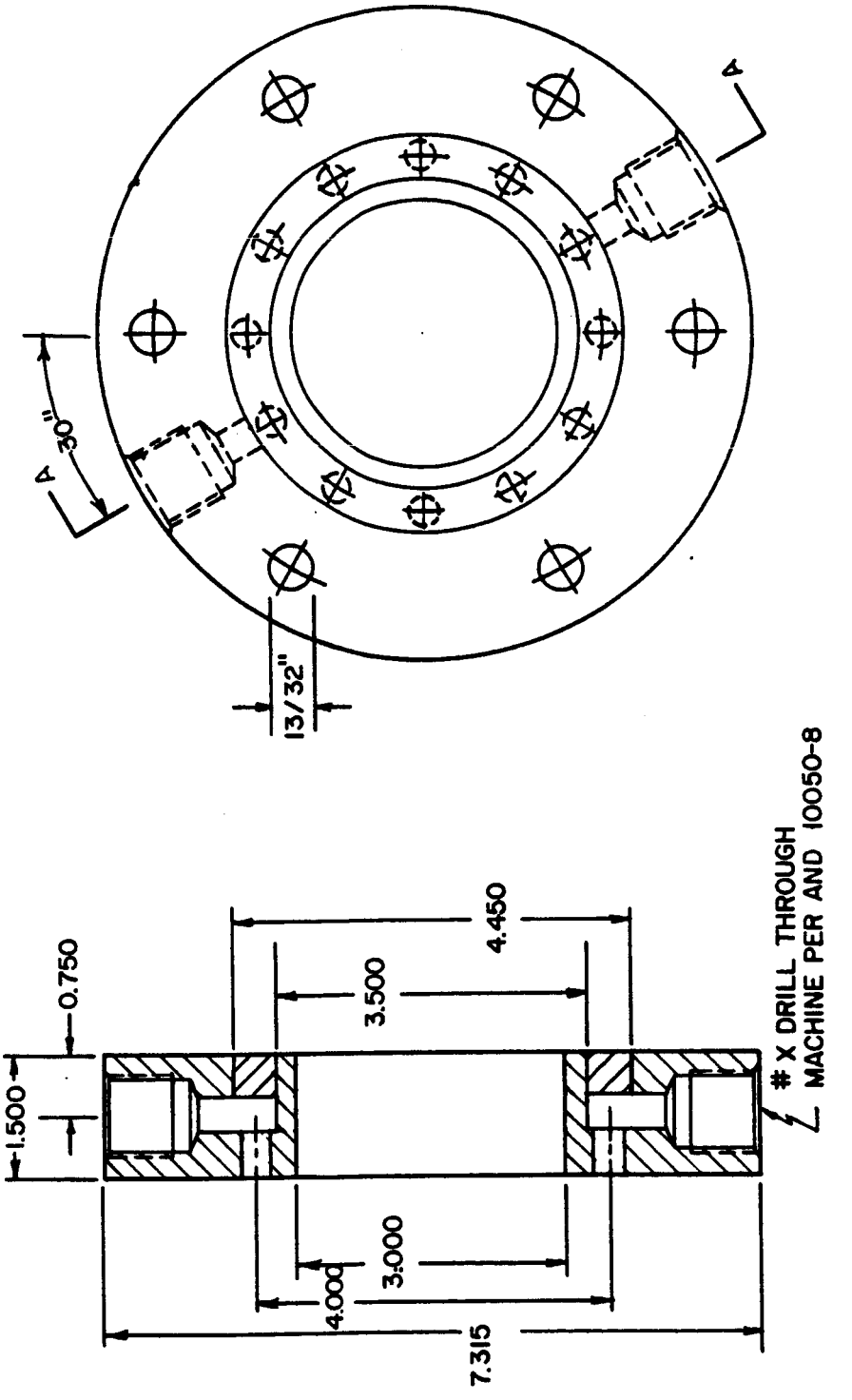

Figure 7. Catalyst Chamber Coolant Inlet Manifold

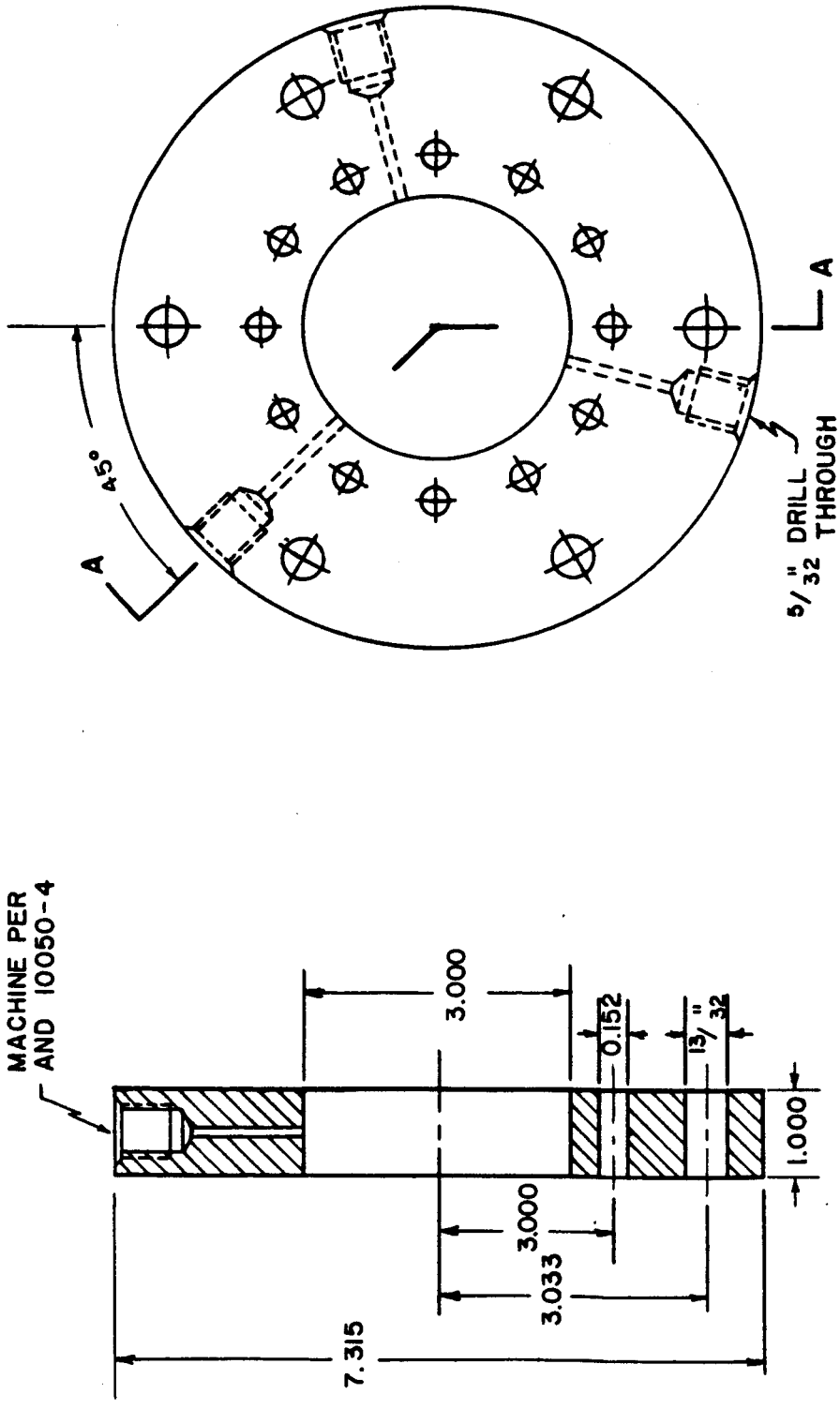

Figure 8. Adapter Plate for Temperature and Pressure Measurement Sensors

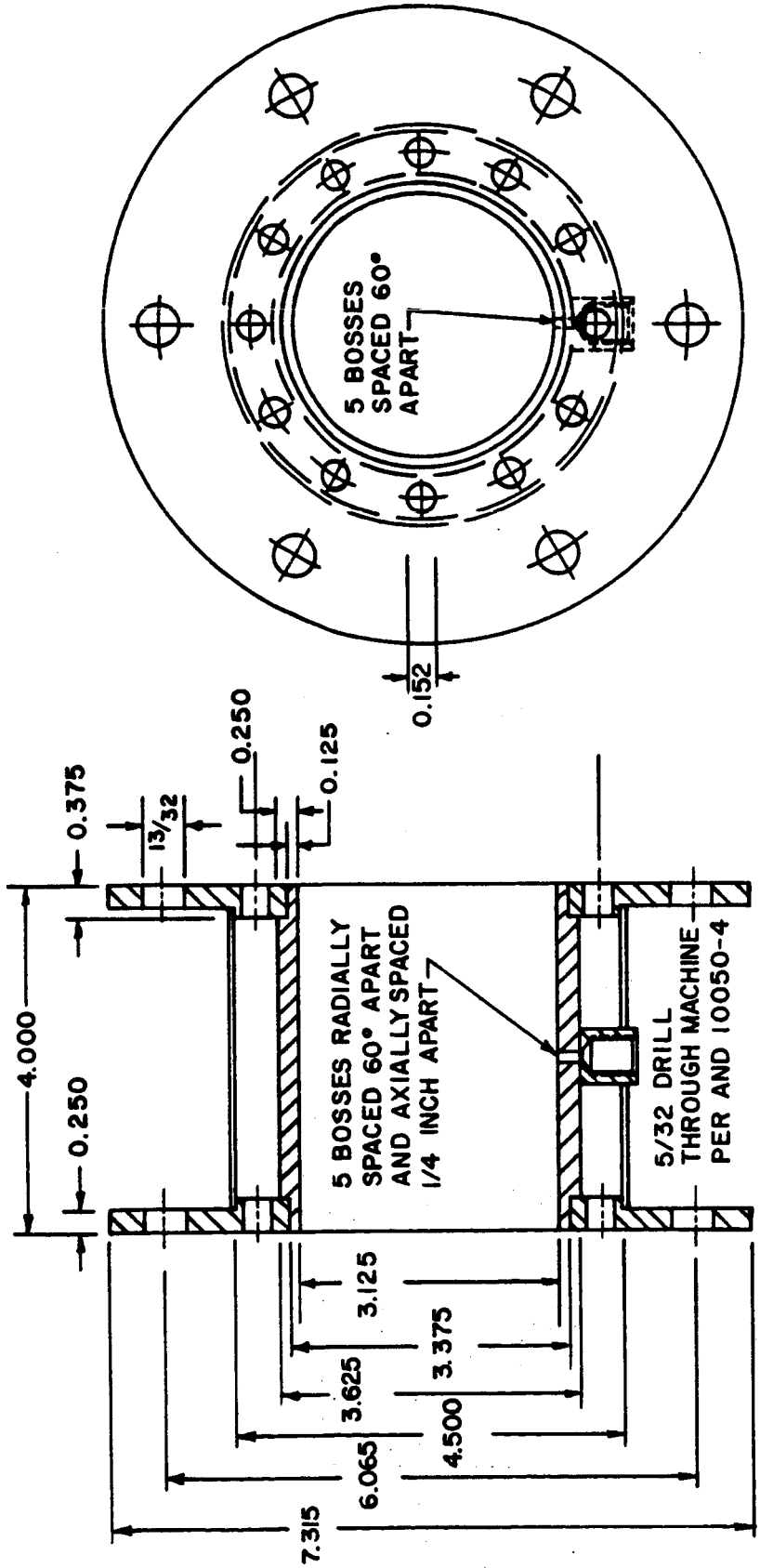

Figure 9. Catalyst Chamber Illustrating Coolant Jacket and Temperature Measurement Ports

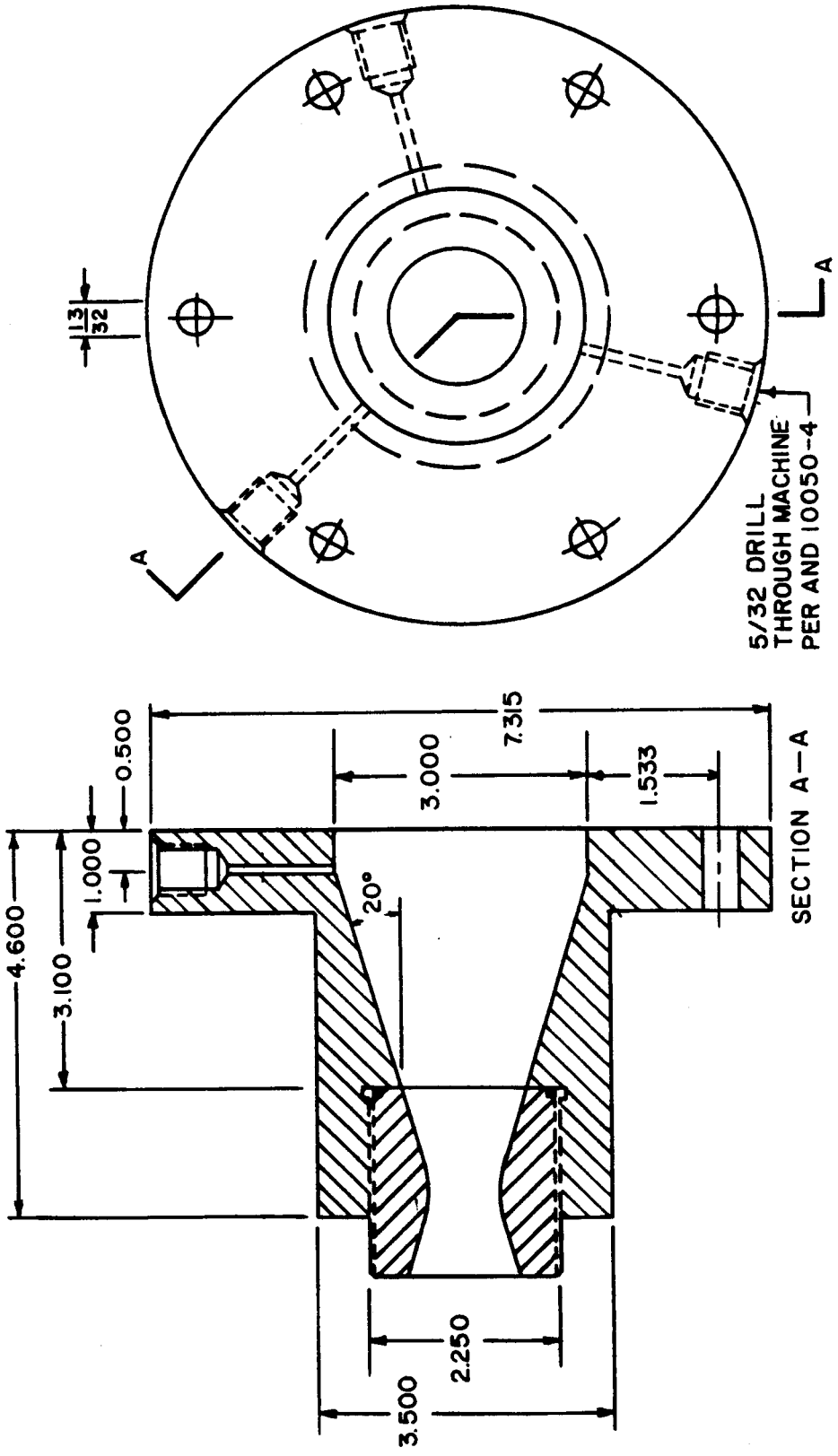

Figure 10. Exit Nozzle and Housing, and Temperature and Pressure Measurement Adapter

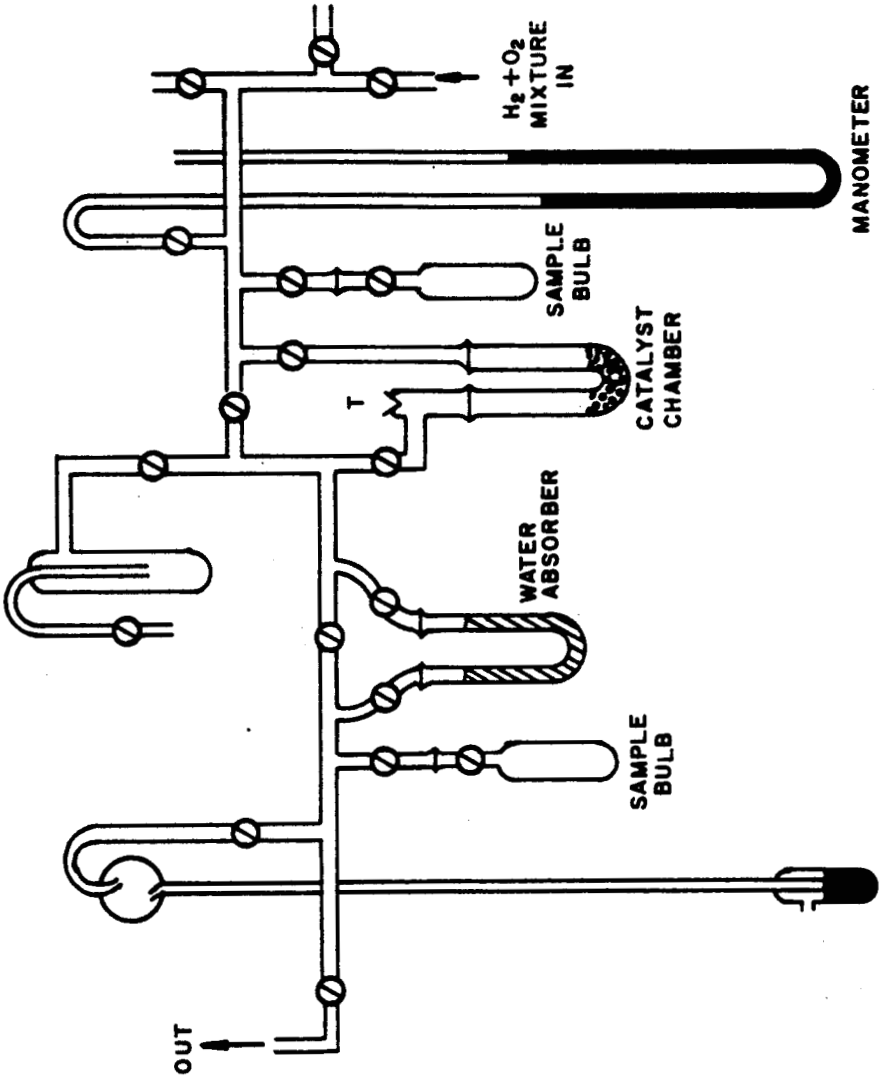

Figure 11. Schematic of Apparatus for Catalyst Activity Measurement

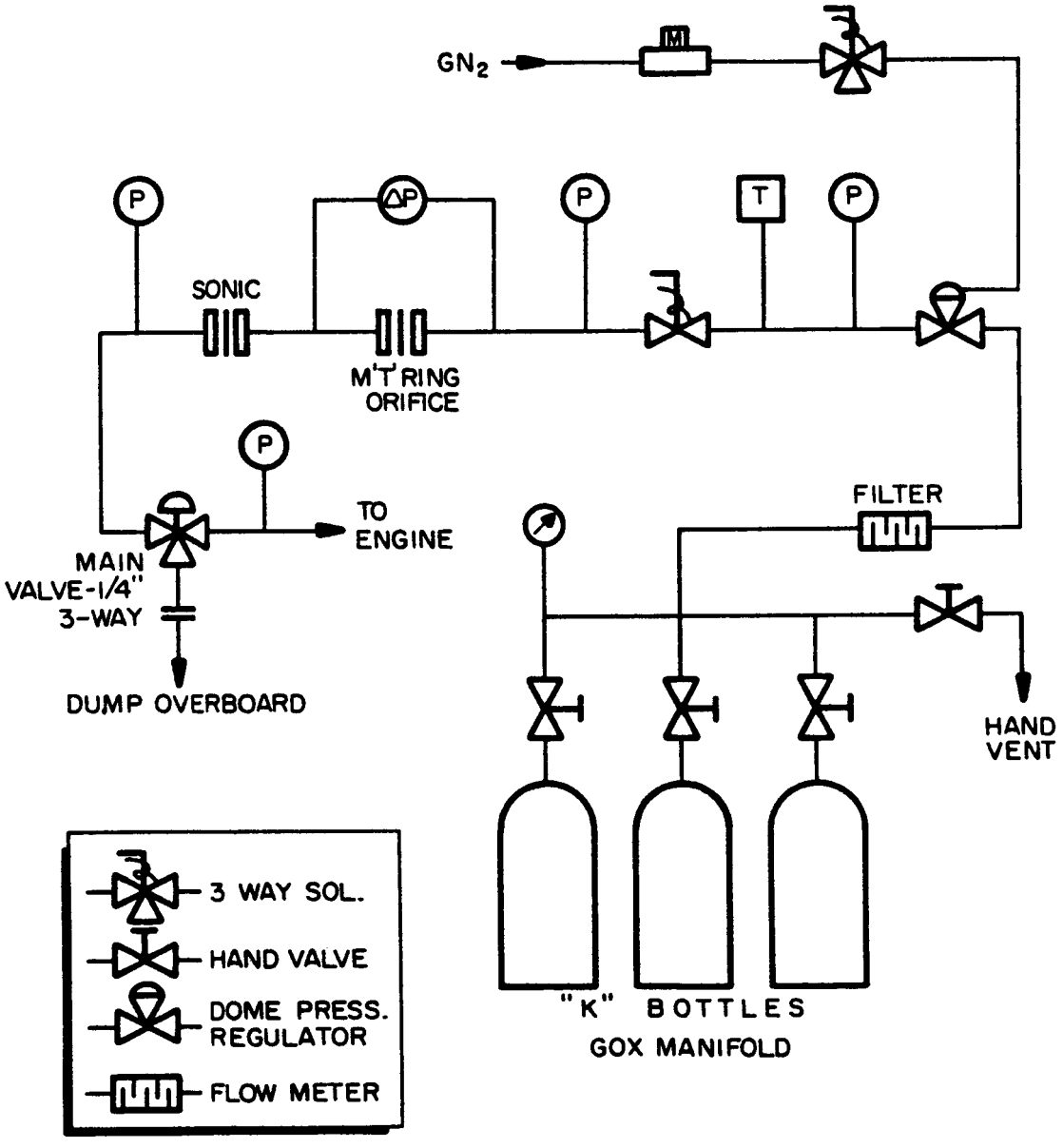

Figure 12. Schematic of Gaseous Oxygen Supply System

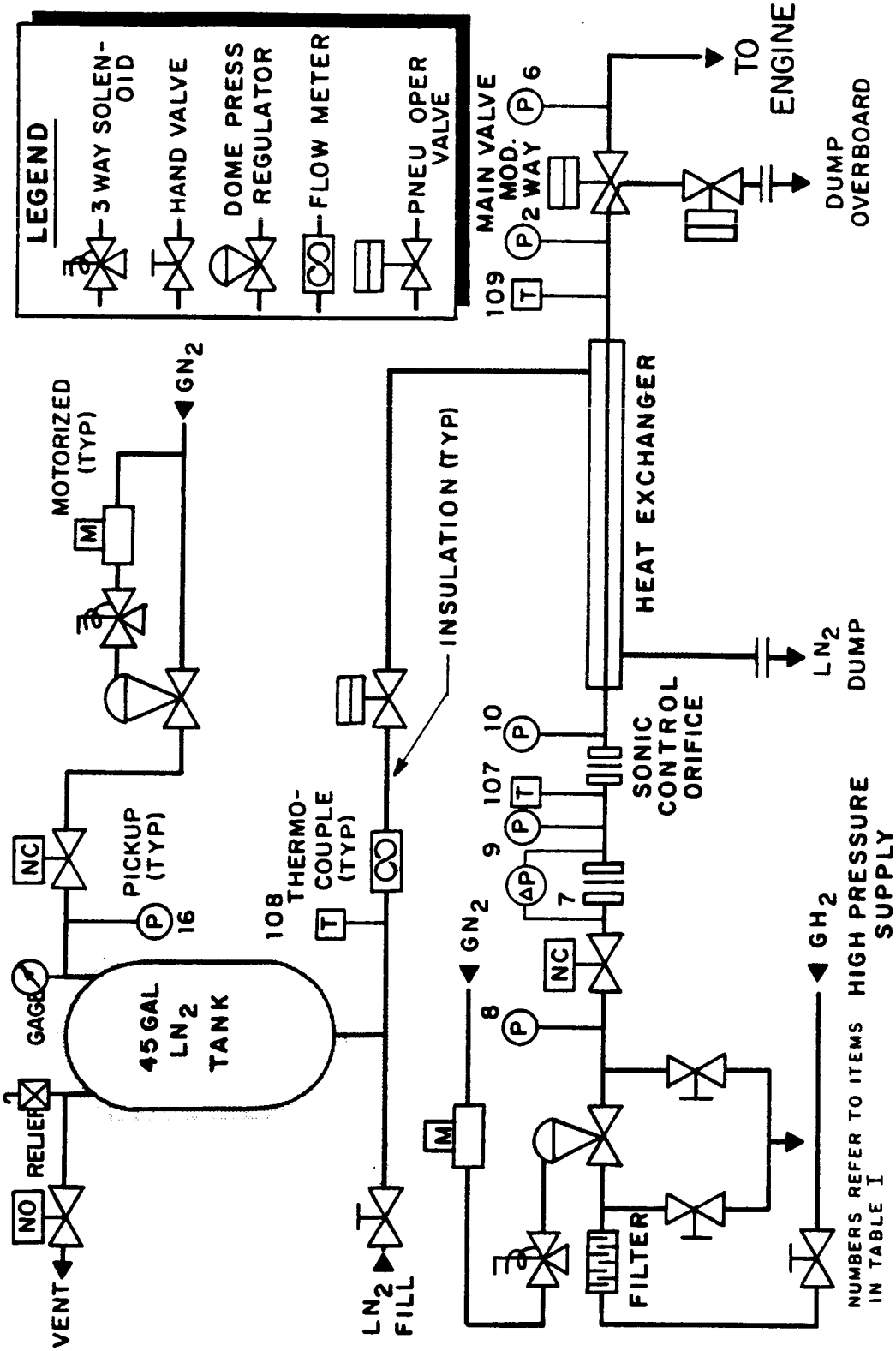

Figure 13. Plumbing Schematic of Modified Gaseous Hydrogen/Liquid Nitrogen Heat Exchanger System

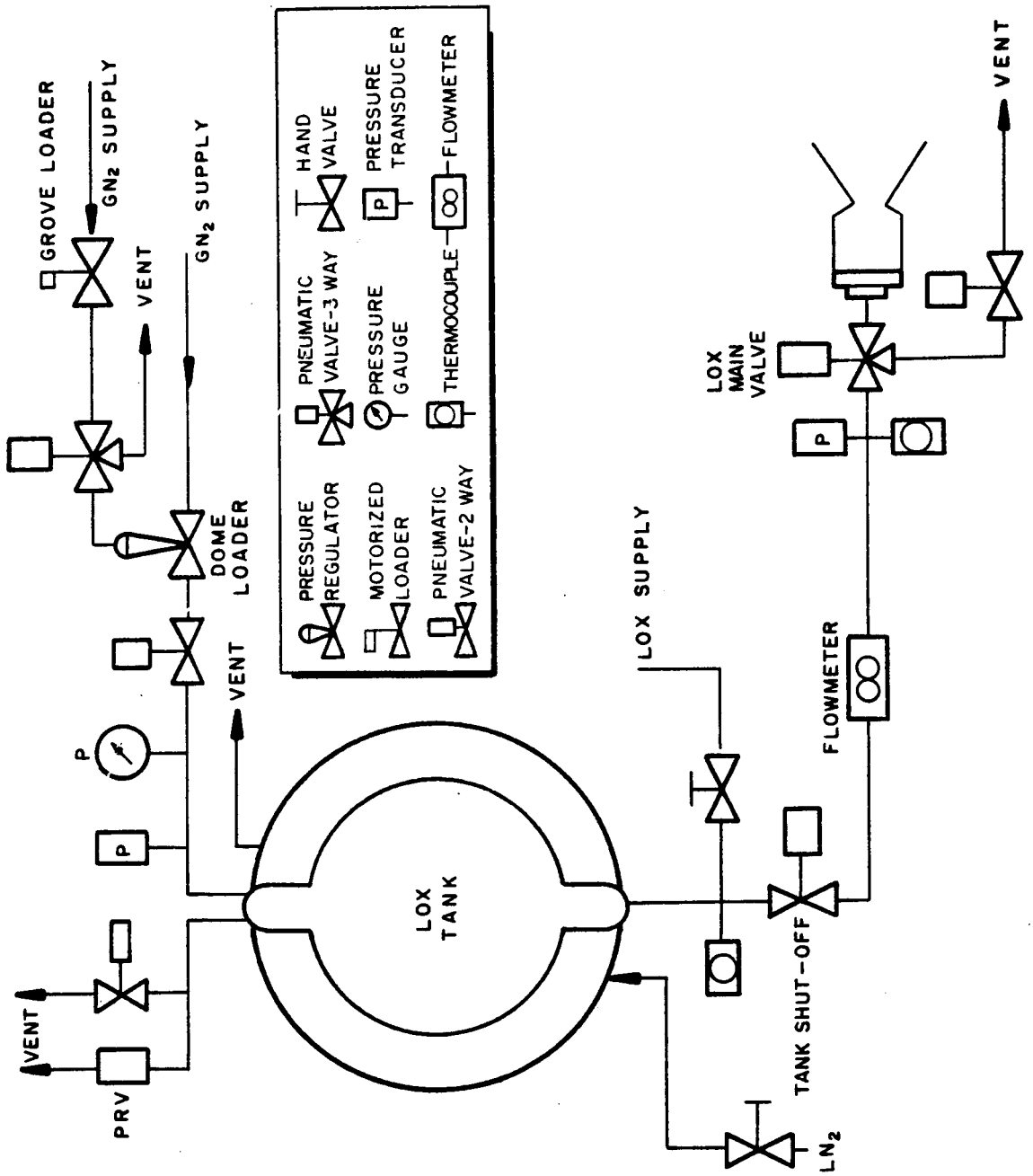

Figure 14. Schematic Representation of Liquid Oxygen System for Small Catalytic Igniter Studies

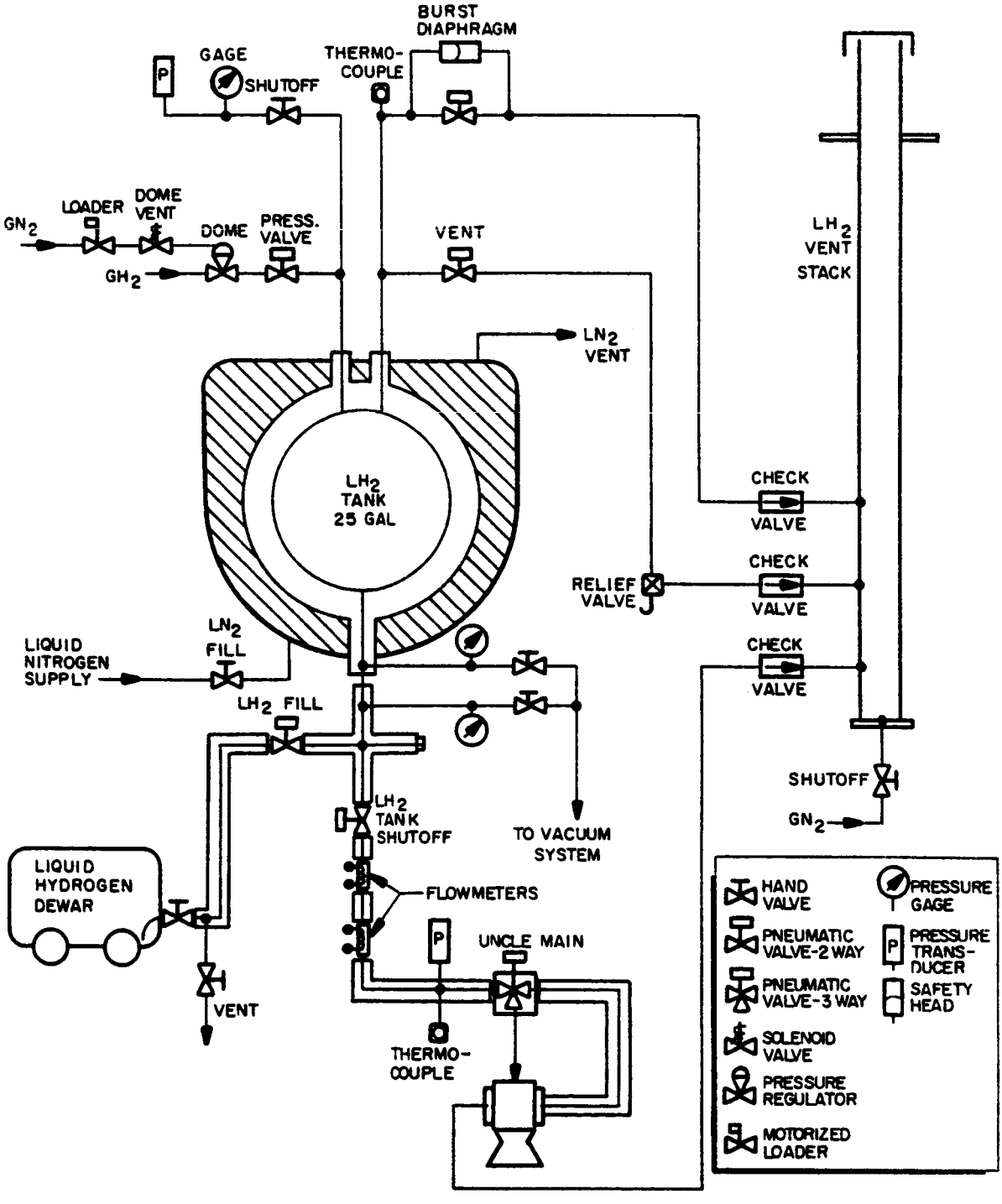

Figure 15. Schematic Representation of Liquid Hydrogen System for Small Igniter Evaluations

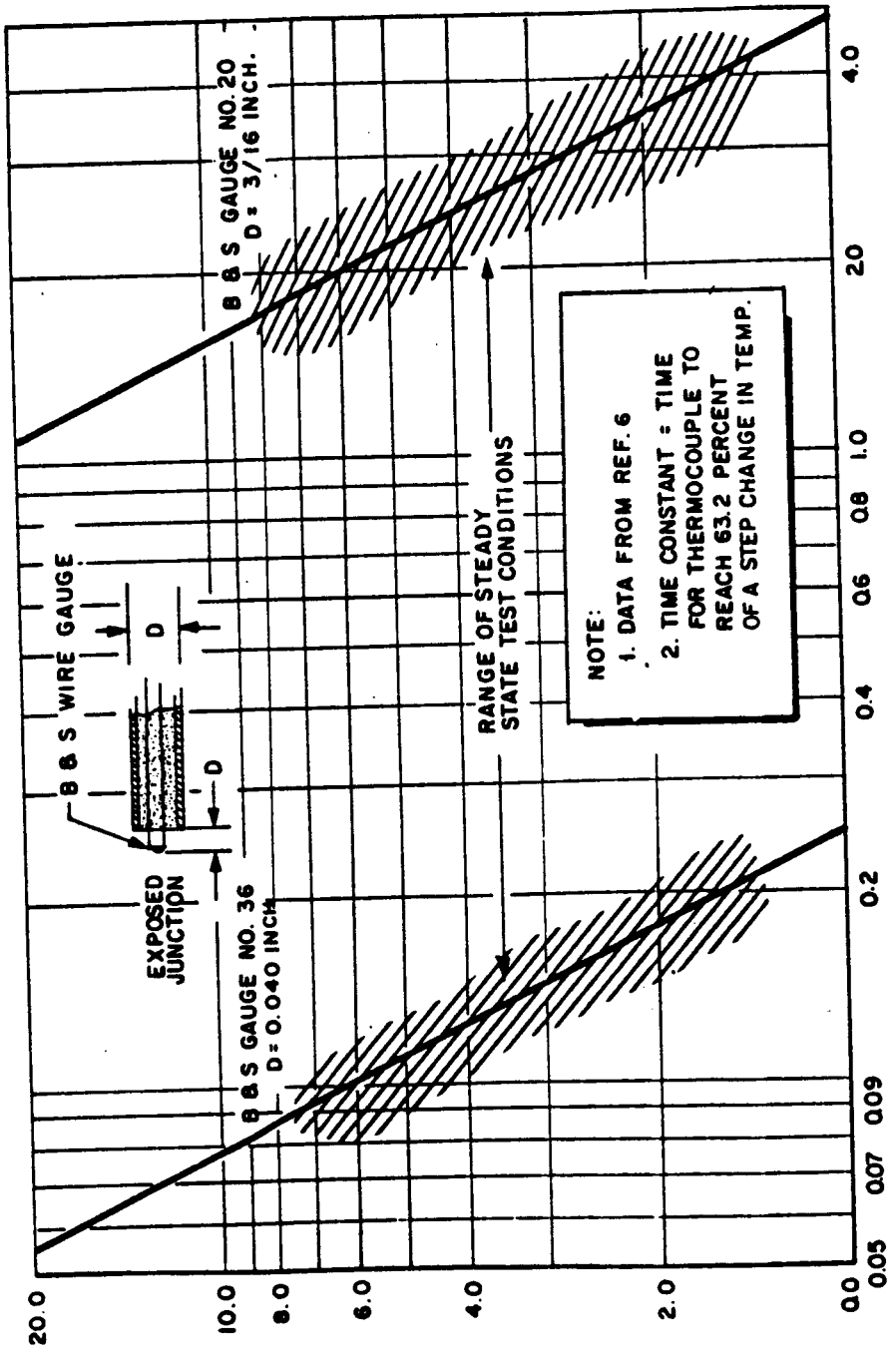

Figure 16. Approximate Time Constants for Exposed Junction Thermocouple in Moving Air

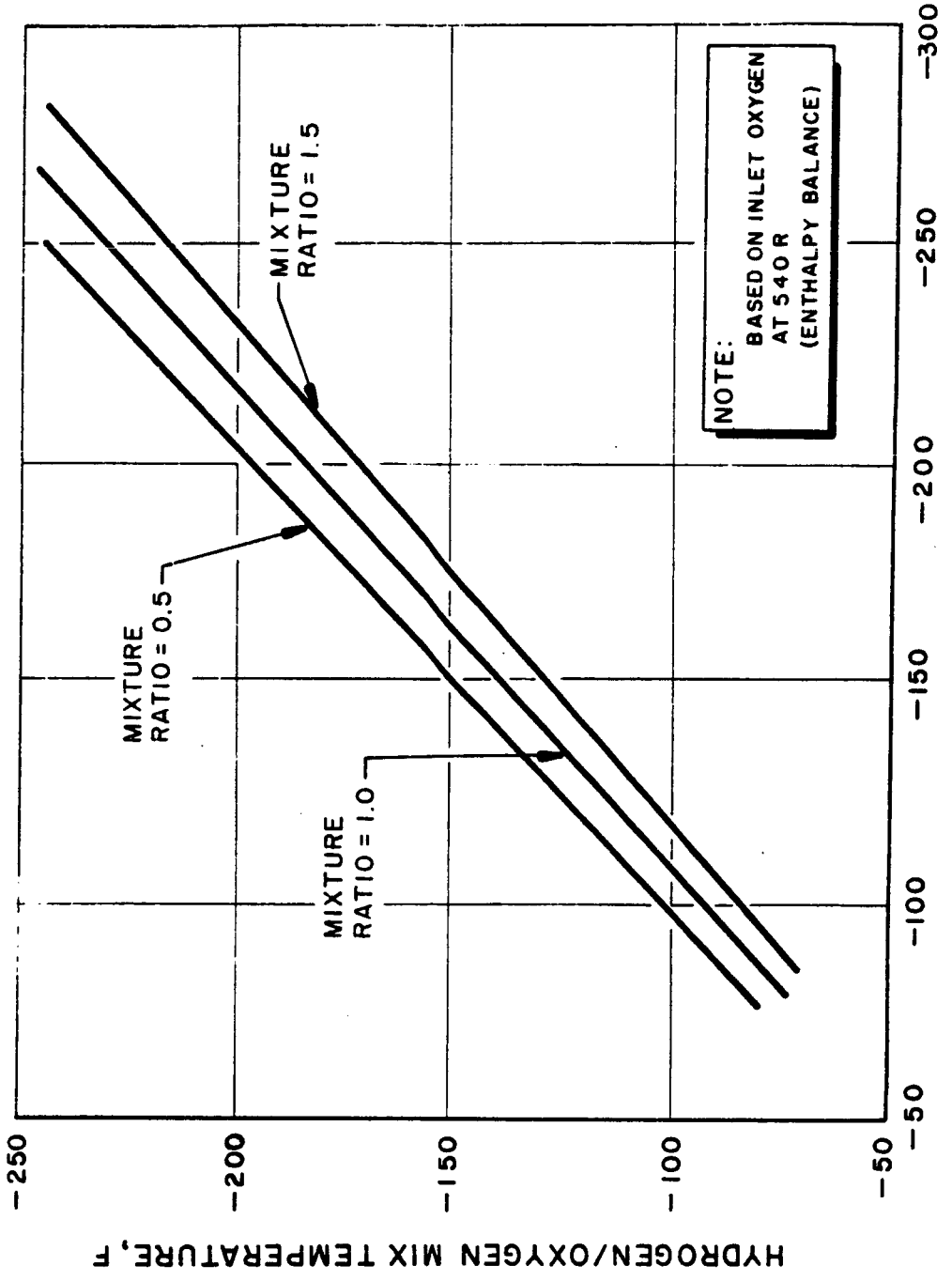

Figure 17. Theoretical Oxygen/Hydrogen Mixture Temperatures as a Function of Mixture Ratio and Hydrogen Inlet Temperature

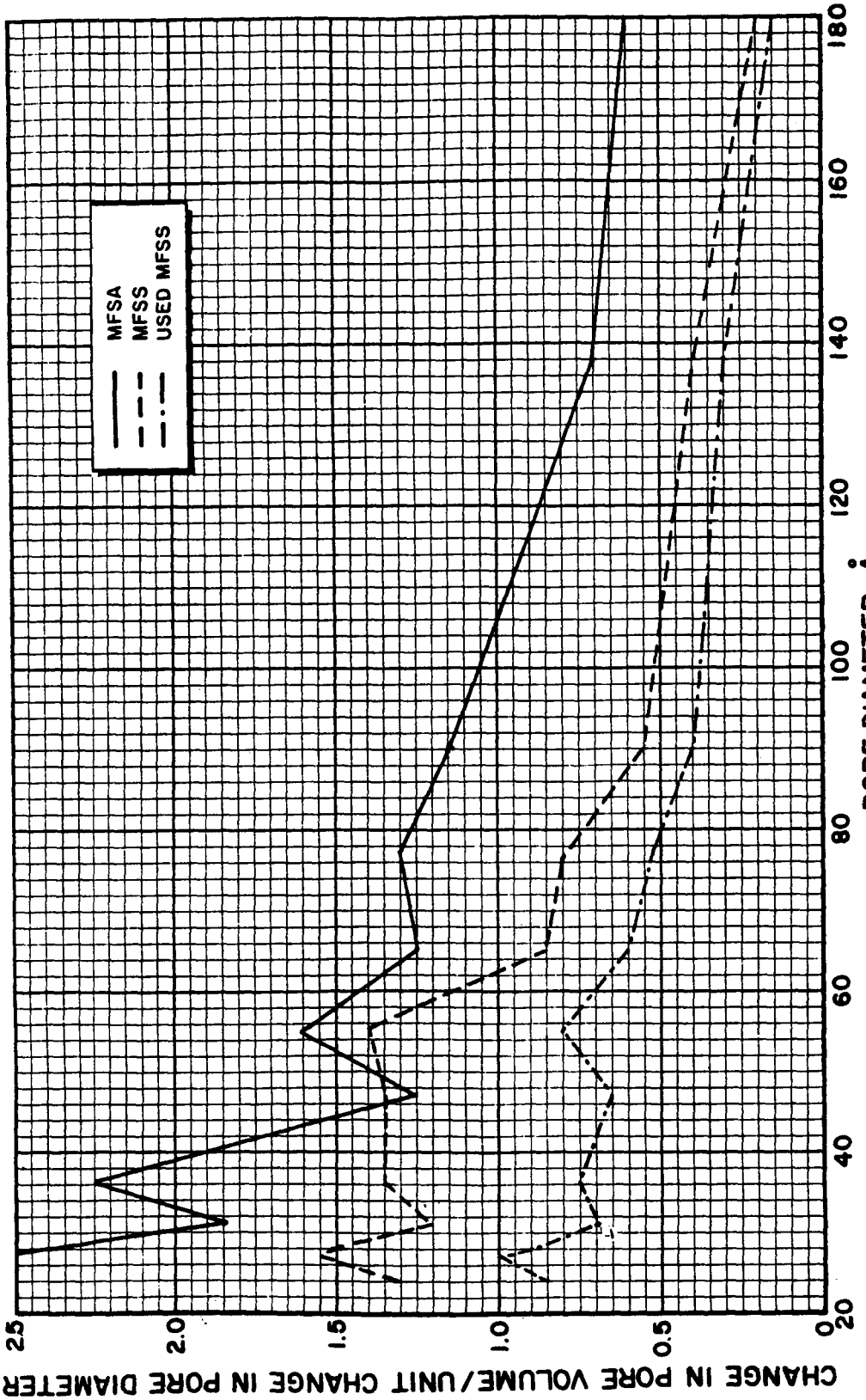

Figure 18. Comparative Pore Size Distribution for Engelhard MFSA, MFSS, and Used MFSS Catalysts Illustrating the Effect of Use on Catalyst Pore Size Distribution

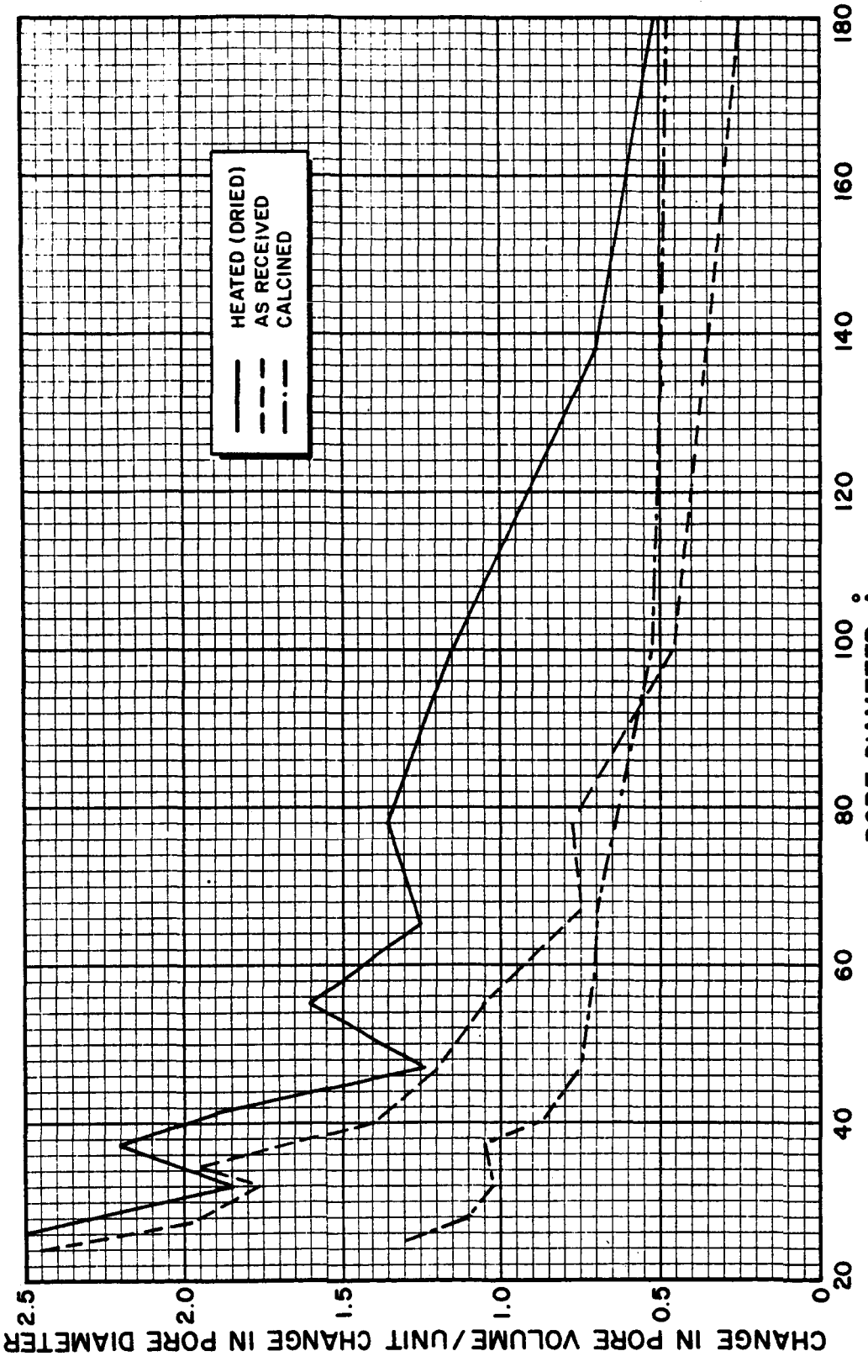

Figure 19. Comparative Pore Size Distribution Curves for the Englehard MFSA Catalyst Illustrating the Effects of Drying and Calcining on Pore Size Distribution

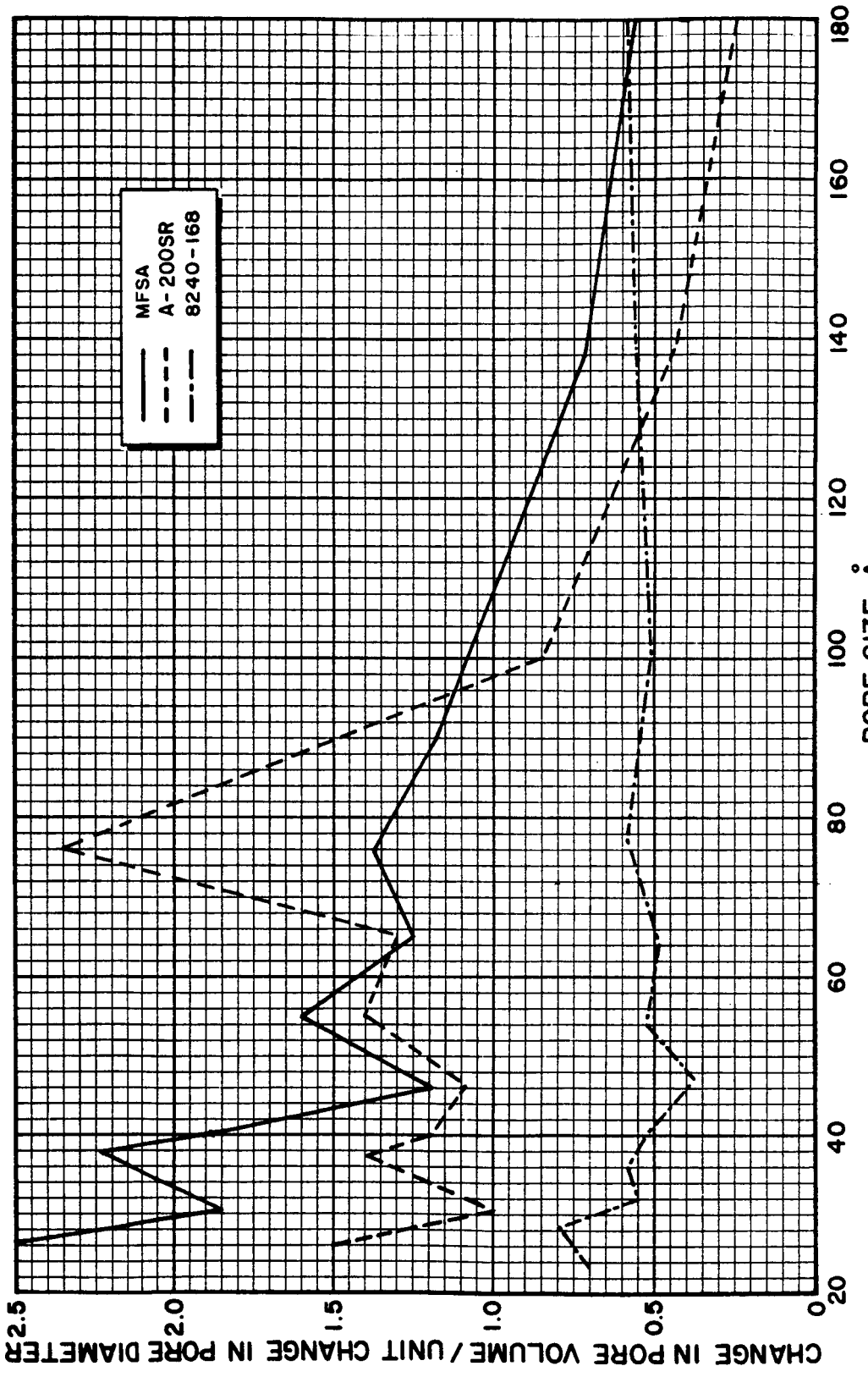

Figure 20. Pore Size Distribution Curves for Engelhard MFSA, Houdry A-200SR, and Shell 8240-168 Catalysts

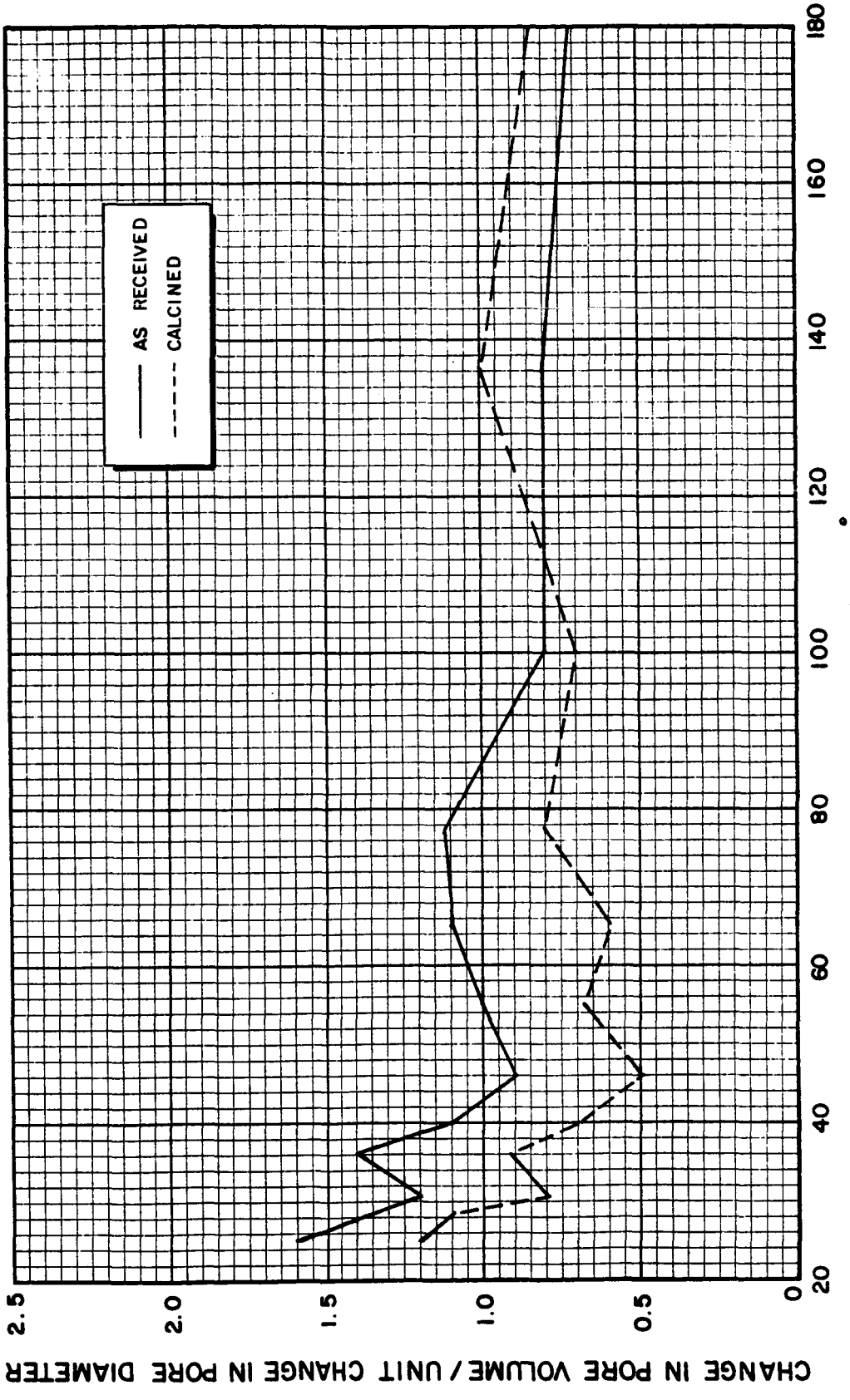

Figure 21. Pore Size Distribution Curves for Girdler G-68 Catalyst Illustrating the Effect of Calcining on Pore Size Distribution

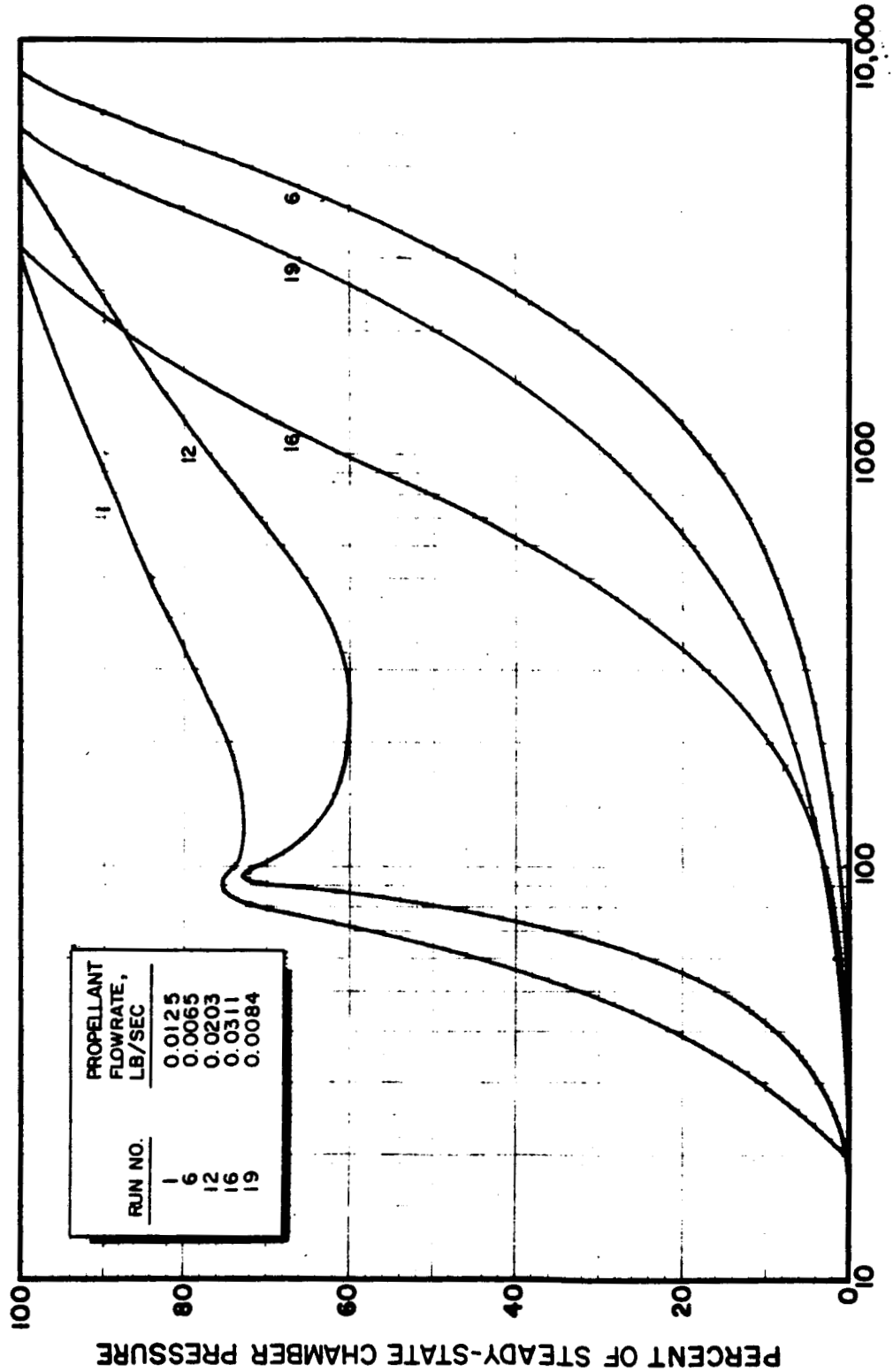

Figure 22. Representative Curves Depicting the Rate of Approach to Steady State Chamber Pressure for the Engelhard MFSA Catalyst With Gaseous Propellants. Illustrated are the Effects of Chamber Pressure Spiking Relative to Stable Ignition.

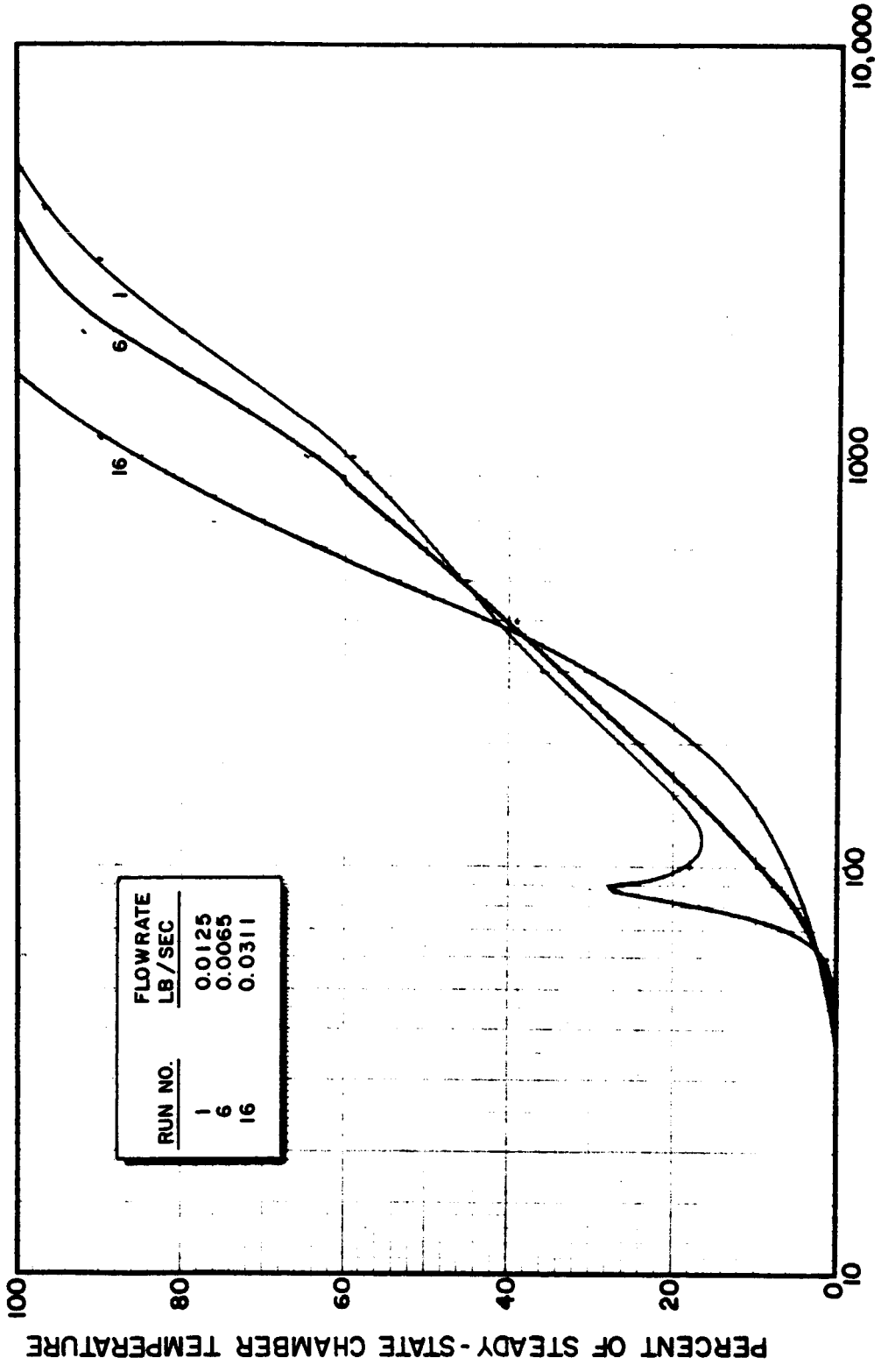

Figure 23. Typical Curves for the Rate of Approach to Steady State Chamber Temperature for the Engelhard MFSA Catalyst Illustrating the Effects of Chamber Temperature Spikes Relative to Stable Ignition with Gaseous Propellants

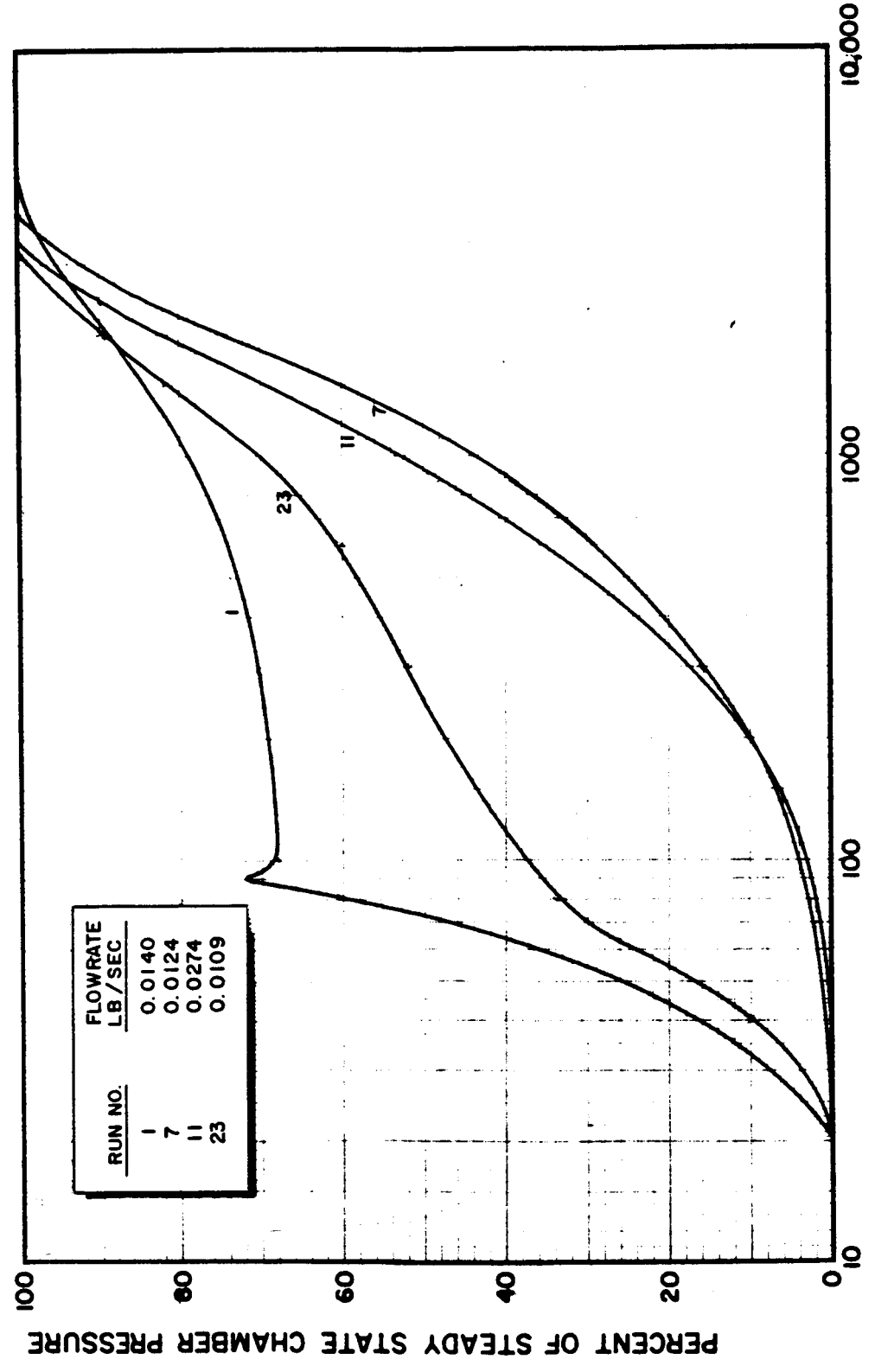

Figure 24. Typical Response Curves for the Engelhard MFSS Catalyst. Illustrated are the Effects of Chamber Pressure Spikes Relative to Stable Ignition, With Gaseous Propellants

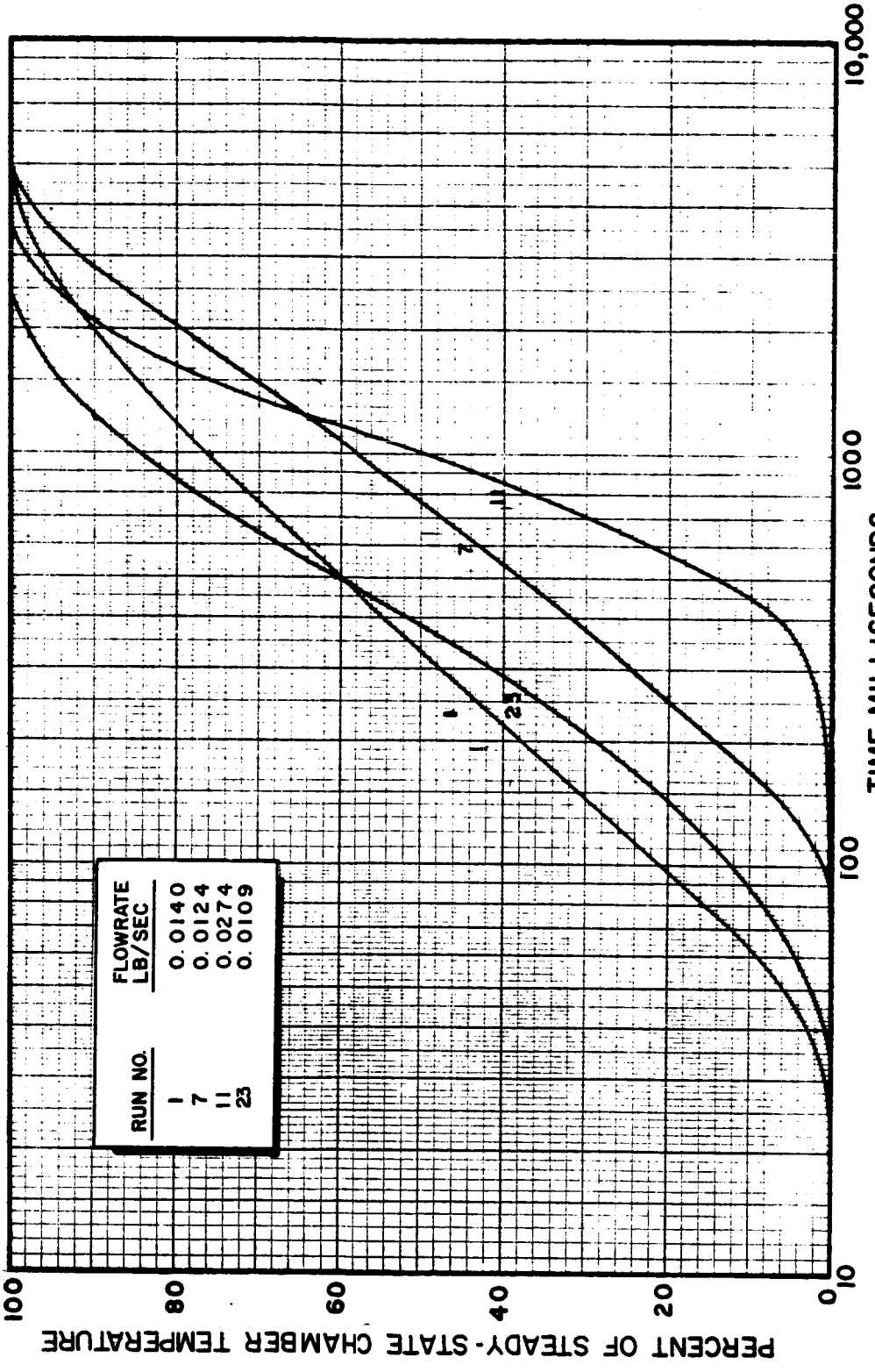

Figure 25. Typical Curves Presenting the Rate of Approach to Steady-State Chamber Temperature for the Engelhard MFSS Catalyst with the Gaseous O_2/H_2 System Illustrating the Effects of Flowrate on Rate of Approach to Equilibrium

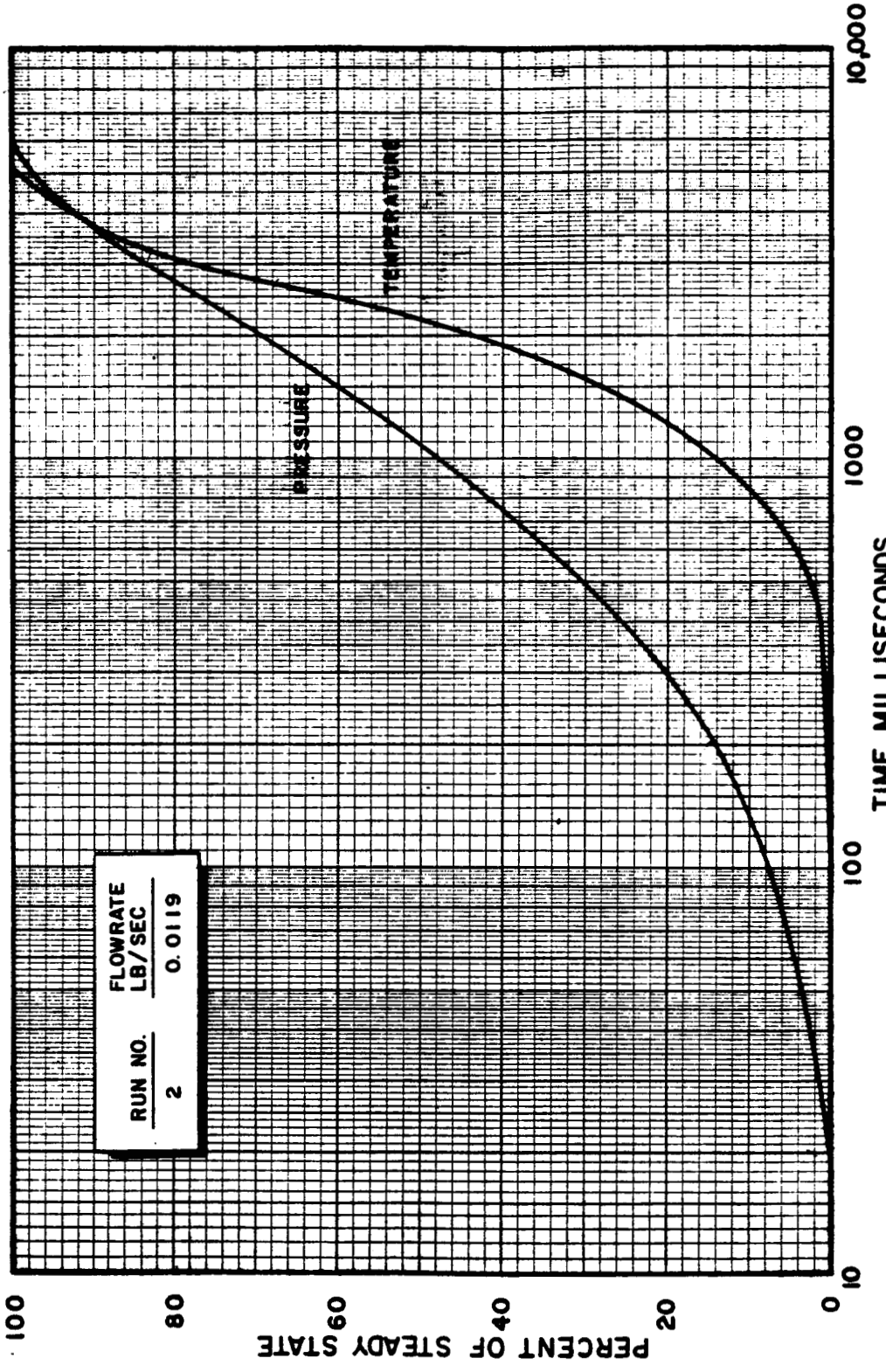

Figure 26. Typical Curves for the Relative Rates of Approach to Equilibrium Chamber Temperature and Pressure for the Engelhard DSS Catalyst using Gaseous Propellants

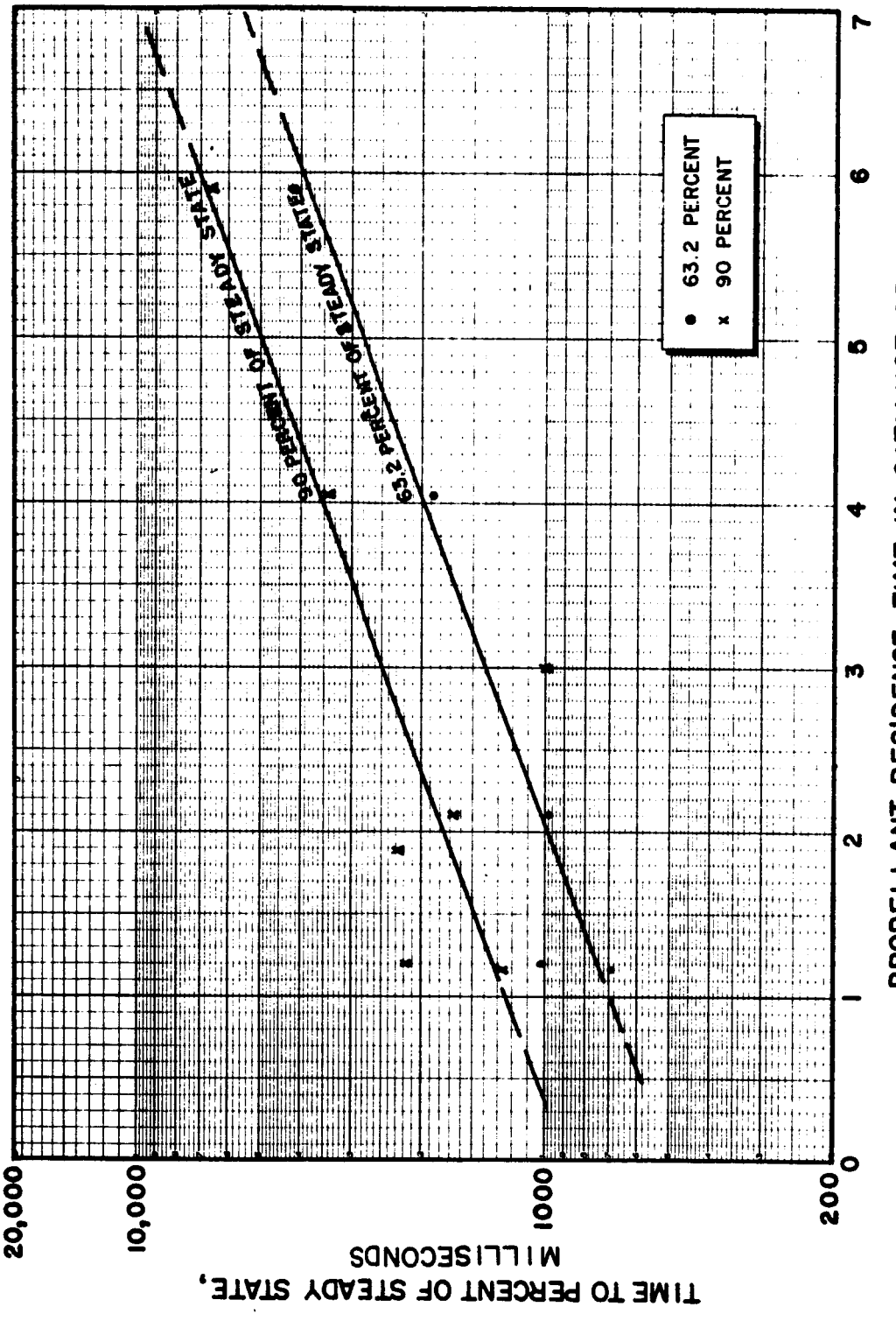

Figure 27. A Correlation of the Effect of Catalyst/Propellant Residence Time on the Rate of Approach to Steady State Chamber Pressure for the Engelhard MFSA Catalyst Using Gaseous Propellants

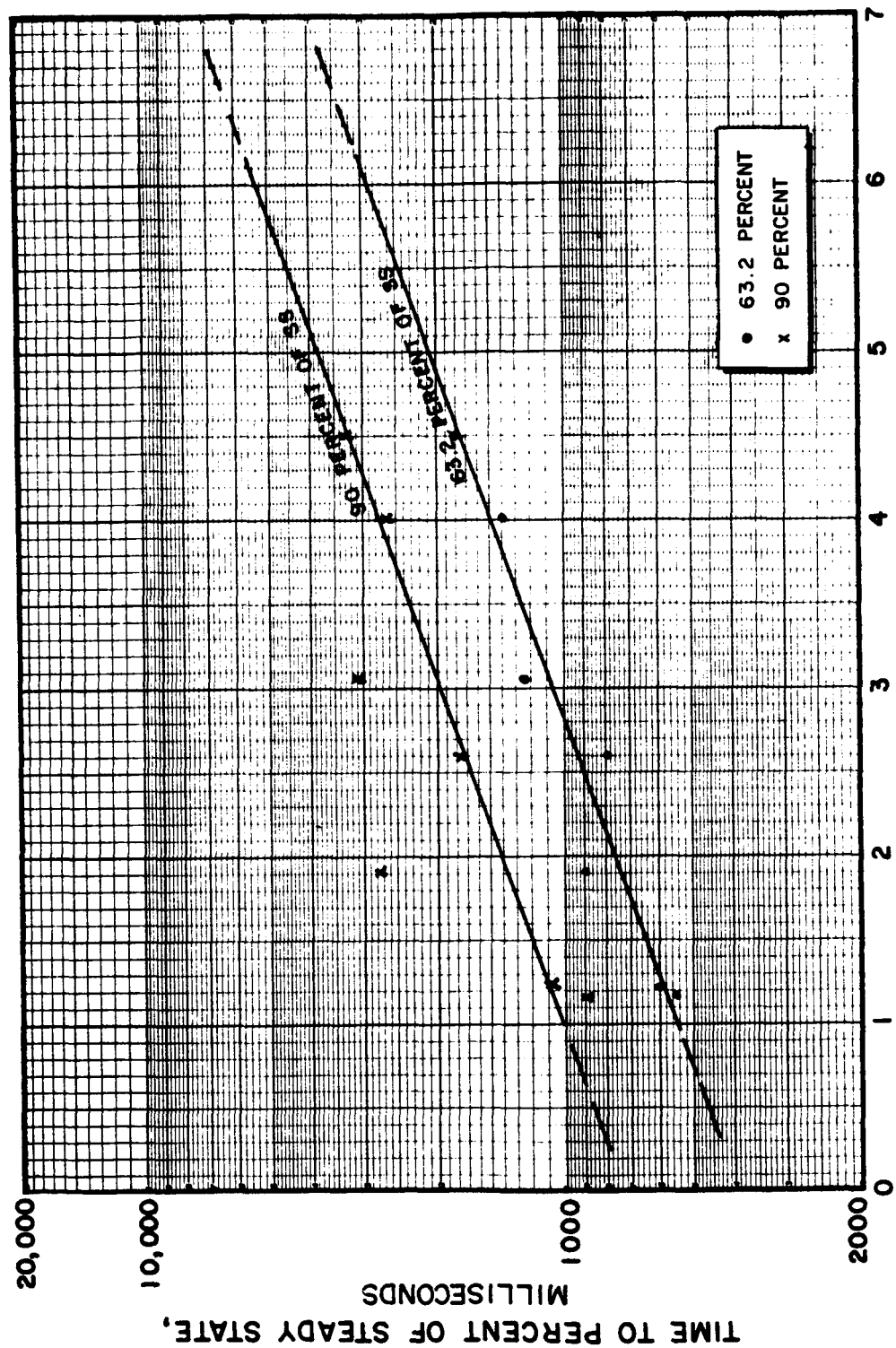

Figure 28. Correlation of the Effect of Propellant Residence Time in the Catalyst Bed on Rate of Approach to Steady-State Chamber Temperature for the Engelhard MFSA Catalyst Using Gaseous Propellants

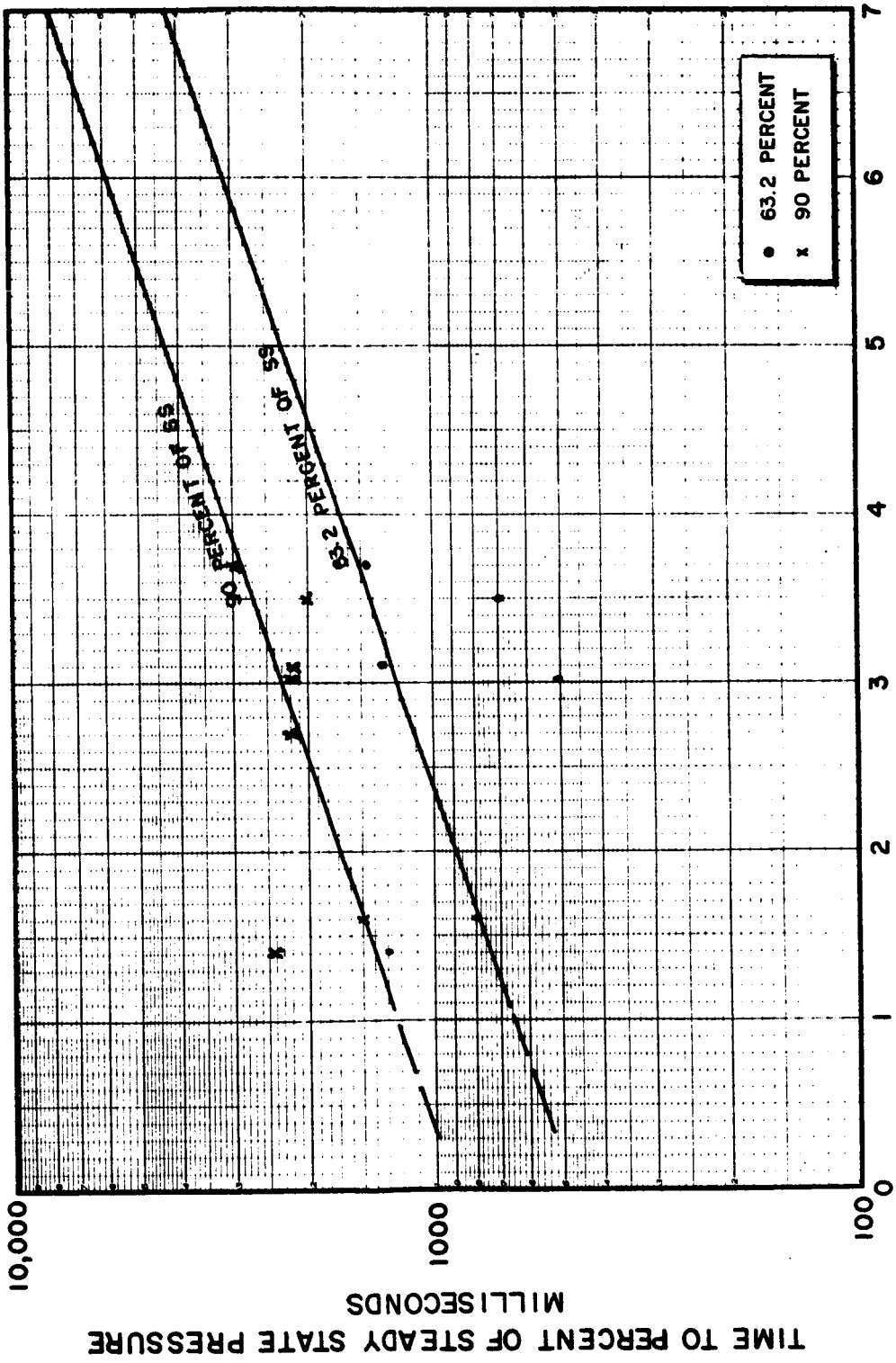

Figure 29. A Correlation of the Effect of Propellant Residence Time in the Catalyst Bed on the Rate of Approach to Steady State Chamber Pressure for the Engelhard MFSS Catalyst Using Gaseous Propellants

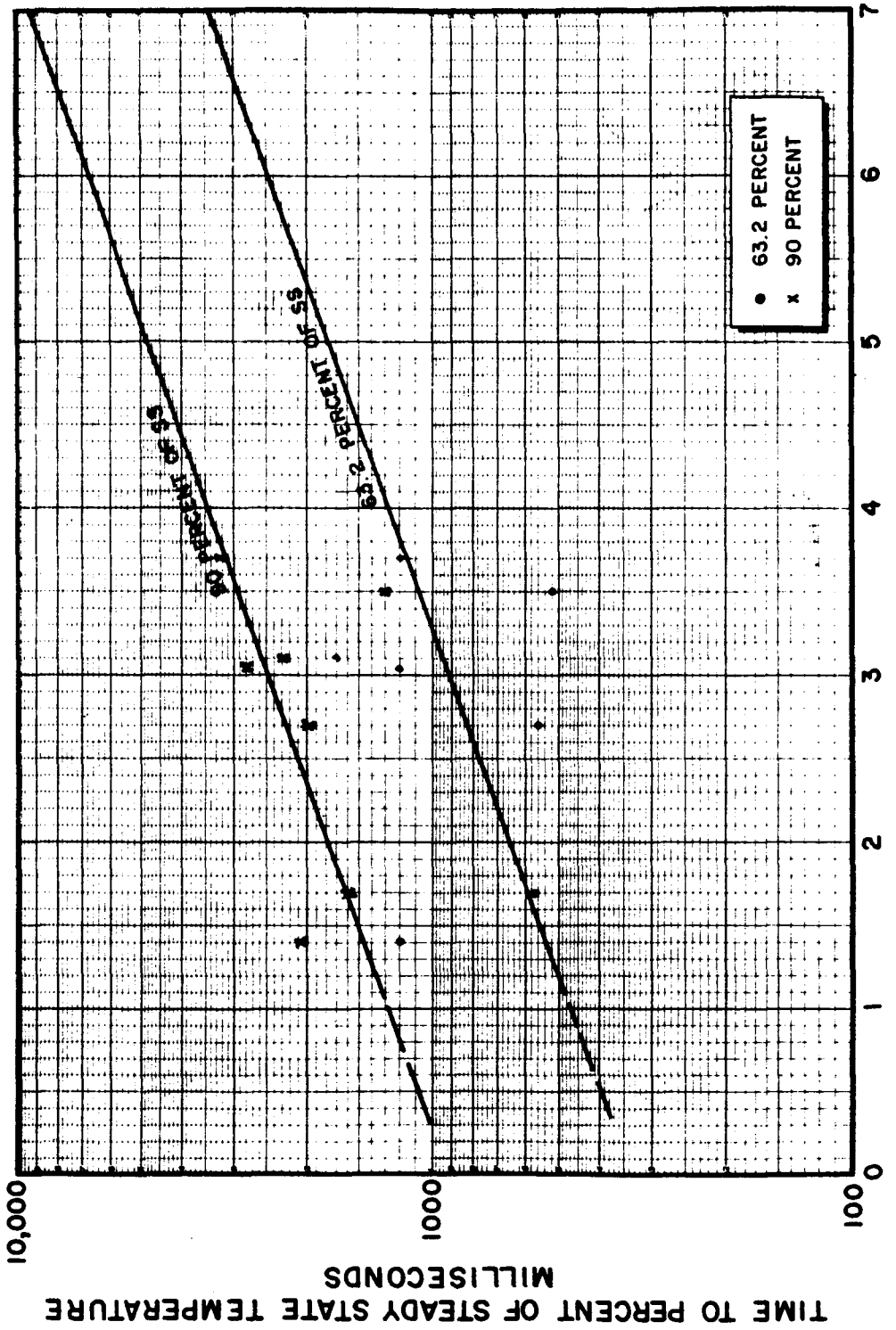

Figure 30. Correlation of the Effect of Catalyst/Propellant Contact Time on the Rate of Approach to Steady State Chamber Temperature for the Engelhard MFSS Catalyst Using Gaseous Propellants

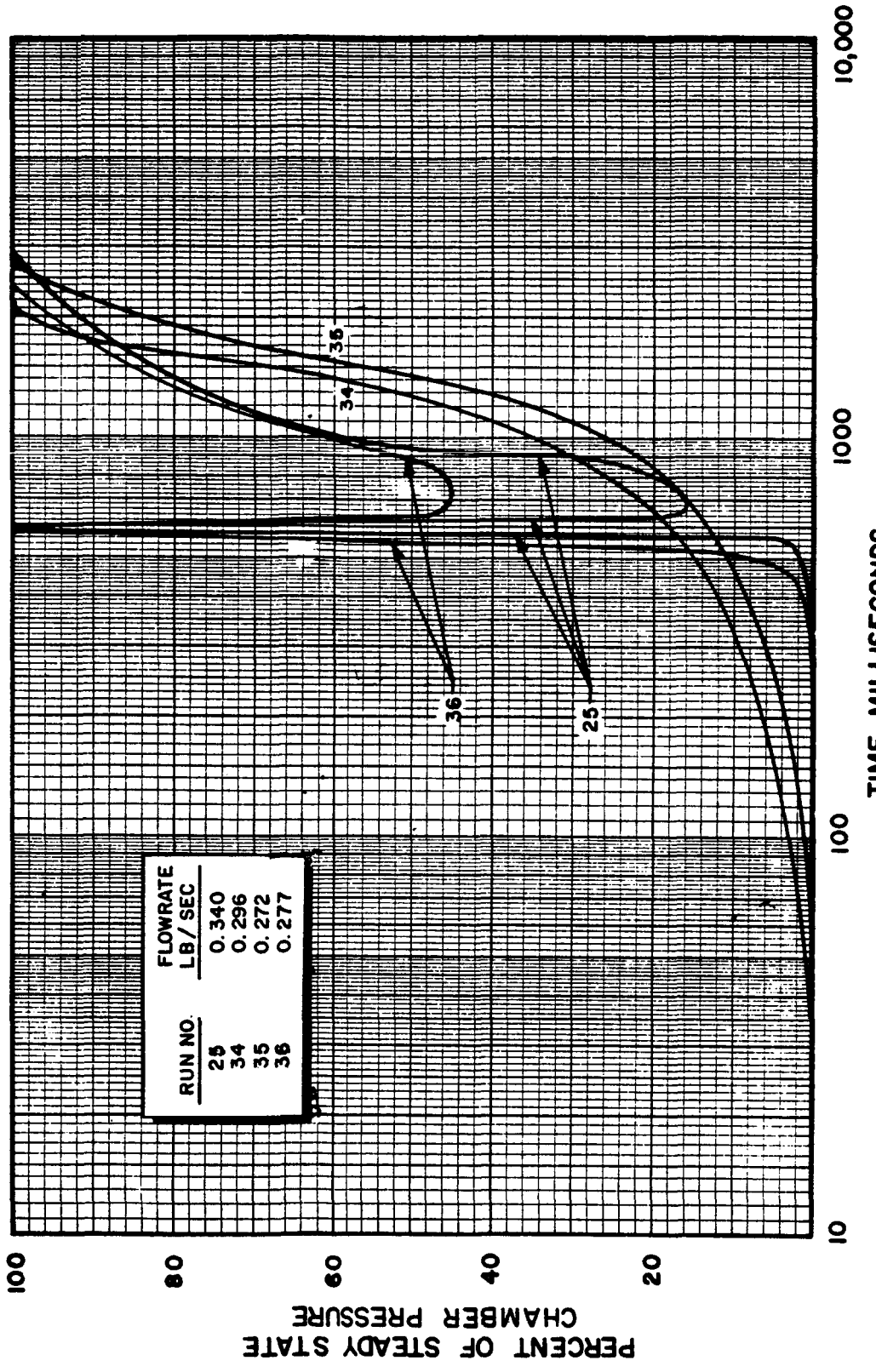

Figure 31. Typical Curves for the Rate of Approach to Steady-State Chamber Pressure for the Engelhard MFSA Catalyst Using Liquid Propellants. Illustrated are Comparative Effects of Spiking and Stable Ignition

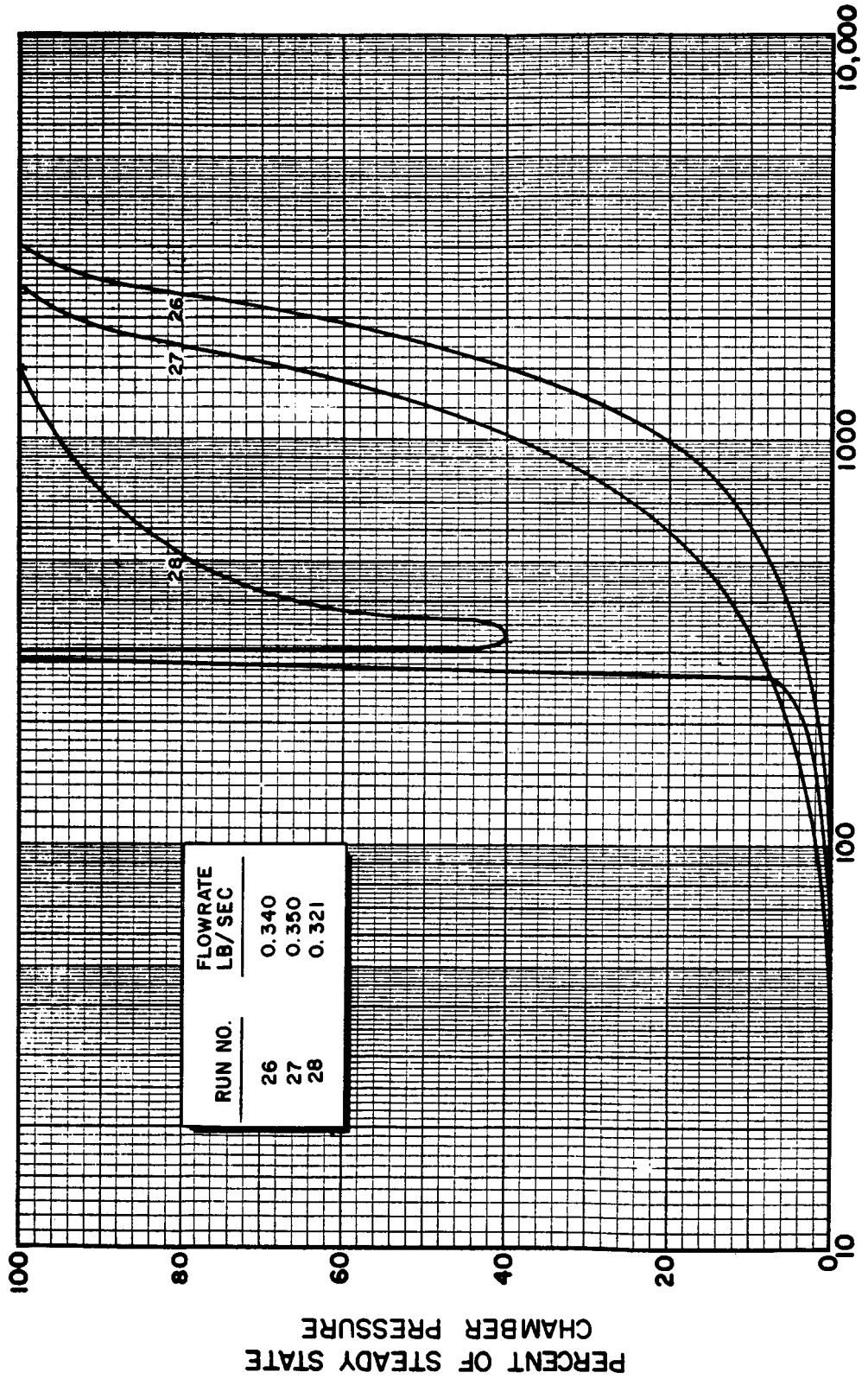

Figure 32. Typical Curves for the Rate of Approach to Equilibrium Chamber Pressure for the Engelhard MFSS Catalyst with Liquid Propellants Illustrating the Relative Effects of Spiking and Stable Ignition